computers

MDPI

Systematic Review

Agroclimatic Sensing, Communication, and Computational Systems-Based Methods and Technologies for Precision Irrigation Management: Current State and Prospects

Aminata Sarr [1,2], Abhilash K. Chandel [2,3,*], Lamine Diop [4], Yrébégnan Moussa Soro [1], Alain K. Tossa [5], Smrutilipi Hota [2] and Arunachalam Manimozhian [3]

[1] Laboratoire Energies Renouvelable et Efficacité Energétique, Institut International d'Ingénierie de l'Eau et de l'Environnement (2iE), Rue de la Science, Ouagadougou 01 BP 594, Burkina Faso; aminata.sarr@2ie-edu.org (A.S.); moussa.soro@2ie-edu.org (Y.M.S.)
[2] Tidewater Agricultural Research and Extension Center, Virginia Tech, 6321 Holland Rd, Suffolk, VA 23437, USA; smrutilipihota@vt.edu
[3] Biological Systems Engineering, Virginia Tech, 155 Ag-Quad Ln, Blacksburg, VA 24061, USA; arunam@vt.edu
[4] Laboratoire des Sciences Biologiques, Agronomique, Alimentaire et Modélisation des Systèmes Complexes (LABAAM), Unité de Formation et de Recherche des Sciences Agronomiques, de l'Aquaculture et des Technologies Alimentaires (UFR S2ATA), Gaston Berger University, Saint-Louis BP 234, Senegal; lamine.diop@ugb.edu.sn
[5] Laboratoire d'Energétique et de Mécanique Appliquée (LEMA), Ecole Polytechnique d'Abomey-Calavi, Cotonou 01 BP 2009, Benin; toskalain@gmail.com
* Correspondence: abhilashchandel@vt.edu

Abstract

Agriculture uses most of the world's fresh water. Given that the worldwide population is expanding at an alarming rate, more land cultivation is apparently in demand. As a result, much more water would be required to irrigate cultivable lands. However, fresh water is becoming scarce at a faster rate due to climate uncertainties and over-exploitation. Several controlled irrigation techniques, such as drip and sprinkler irrigation, have been introduced to safeguard water resources. However, these techniques do not readily meet crop water demands and often end up causing overapplication of water. Under these circumstances, smart precision irrigation is the best solution. Smart irrigation techniques facilitate delivery of water in an amount that is required by the crop as per site/location and temporal requirements. Several studies have been carried out in this area, and remarkable progress has been observed. These studies range from making use of in situ sophisticated sensors that are low-cost and consume minimum energy up to the use of small unmanned aerial systems (SUAS) and satellite imagery for irrigation management. This review summarizes research studies that highlight the components of developing and deploying various precision irrigation technologies, their benefits, and their limitations. Specifically, the scientific value of this study lies in outlining implications of using different sensors, parameters, and equipment, the agroclimatic models, communication technologies, artificial intelligence, and the energy sources to implement automated irrigation systems. A future scope of precision irrigation is also discussed in accordance with cost-effectiveness and sustainability. This study should also act as a referring guideline for new researchers as well as technology manufacturers who seek to design and develop a futuristic yet efficient irrigation system. Overall, this review is aimed at contributing to the understanding of automated irrigation systems for their effective deployment towards enhanced agricultural production, conserved water resources, and sustainable use of energy sources.

Check for updates

Academic Editor: Paolo Bellavista

Received: 6 January 2026
Revised: 3 February 2026
Accepted: 5 February 2026
Published: 23 February 2026

Copyright: © 2026 by the authors. Licensee MDPI, Basel, Switzerland. This article is an open access article distributed under the terms and conditions of the Creative Commons Attribution (CC BY) license.

Keywords: sustainable agriculture; precision irrigation; internet of things; agroclimatic sensors; remote sensing; energy efficiency

1. Introduction

Based on United Nations' forecasts, the world's population will rise from 8.5 billion in 2030 to 9.7 billion in 2050 [1]. More than half of this population increase will come from sub-Saharan African countries by 2050 [1,2]. Developing countries are the hardest hit, where rapid population growth can have negative consequences on efforts against poverty, hunger, and malnutrition [3]. About 75% of the population produces 80% of the food consumed in these countries and thereby derives their livelihoods from agriculture [4]. According to forecasts, global production needs to increase by 60% [5] and double in developing countries to meet the population's needs and the needs of their changing diets [4,6]. Nonetheless, to meet these increases, the entire globe will have to cope with the constraints of increased competition for access to water and energy as well as the impacts of climate uncertainty.

Water is the most important resource that drives agricultural production. However, the water–agriculture relationship is increasingly under threat due to the unavailability or inaccessibility of water resources [7,8]. This threat is further supplemented by the increasing population that, in most regions, also struggles to meet household water demands. For example, in sub-Saharan Africa, North Africa, and West Asia, the total annual renewable water resources per capita fell from 41% in 1997 to 32% in 2017 [9]. An imminent increase in groundwater withdrawals for households as well as agricultural consumption has been observed since the 1960s and has increased at double the rate of global demographic expansion over the past century [7,10]. In this period, more countries have crossed the water use limits beyond which supply services can no longer be assured [7]. This can be understood from the fact that the flows of several major rivers are now equivalent to just 5% of their previous water volumes, while many inland lakes and seas have shrunk in size, and wetlands in Europe and North America have half disappeared. Groundwater is being over-pumped beyond the natural replenishment rate of aquifers, resulting in increasing pollution and salinization in some coastal areas [11]. In this respect, the concern over water availability for agriculture takes on even greater importance in the regions that have already exhausted a large part of their renewable water resource potential, and rainfall deficits have risked agricultural production [11]. Such scarcity of water resources is a real constraint, which is expected to become even more pronounced by 2050 [12]. The decline in water resources is the result of several combined factors, namely climate uncertainty, global warming, drop in rainfall, increased frequency and intensity of extreme weather events, and the overexploitation of water resources [13–15].

Nevertheless, agriculture remains the focal point for enhanced water resource management [10]. There are several reasons for this. Firstly, agriculture remains the sector that consumes the most water, using on average over 70% of the world's fresh water and over 93% of fresh water in some developing countries [16]. In addition, over 90% of water use is non-renewable [7]. Secondly, there are agricultural practices capable of significantly increasing or reducing water demand and favoring water storage in the soil [10]. Worldwide, irrigation has doubled or tripled crop yields such that more than 40% of total agricultural produce comes from irrigated land. Yet irrigated land only accounts for around 20% of the world's cultivated land [9]. According to forecasts, irrigated agriculture will cover about 50–60% of additional food needs by 2050 [16,17], and water withdrawals could only rise by 10% if efficient irrigation is practiced. Conventional irrigated agriculture amounts to

water wastage and possibly deprives other sectors of need. Efficient irrigation management can minimize such wastage, boost productivity, and intensify sustainability, especially in arid and semi-arid zones where climate uncertainty threatens millions of farmers [11,18]. Efficient irrigation is possible through the following: innovative design methods when setting up water supply systems in farms, crop productivity and water use efficiency, translation from open-channel irrigation to micro irrigation (sprinkler and drips), irrigation scheduling by using agro-climatic and edaphic data, decision support systems based on sensors, communication technologies, and advanced control systems, among others [19,20]. Such methods can resolve constraints related to the difference between water supply and demand in agriculture [21,22].

Automated smart irrigation systems have garnered tremendous interest in the past decade for efficient irrigation management. As per Ighrakpata et al. [23], automated irrigation systems work based on data derived from continuous monitoring of soil water content to wirelessly trigger the opening of valves and release water in the amount required by crops. Khriji et al. [24] defined precision irrigation as the programming of water supply based on climatic data, crop water requirements, and soil water content, using monitoring and detection tools. Singh et al. [25] and Koech and Langat [26] perceive automation as a technique that uses machines, equipment, or systems whose operation requires no or minimal manual intervention. Rathika et al. [27] have divided automated irrigation systems into two categories: semi-automatic, in which irrigation periods and duration are controlled by the irrigator, and fully automatic, where sensors collect data and emit signals to automatically trigger irrigation mechanisms. Obaideen [28] further describes full automated irrigation systems as intelligent systems that enable more efficient use and sustainable management of water resources by applying only the quantities of water required by crops at the right time, determined by real-time monitoring systems. Wireless sensing, communication networks, and the Internet of Things (IoT) have become integral to fully automated irrigation systems. Here, soil, climate, and/or plant data form the basis of sensing, while communication between sensors and controllers is facilitated by Bluetooth, Zigbee, Wi-Fi, RF, or LoRaWAN systems [18,24,25,28]. Several research and development studies concerning automated irrigation systems have been conducted over the past decade [29–34].

In a nutshell, while numerous studies have investigated individual aspects of smart irrigation such as different sensor technologies, water use modeling, IoT-based platforms, remote sensing platforms, and machine learning applications, among others, for water-use optimization, there is a lack of integrative review that holistically examines their convergence, comparative effectiveness, and practical deployment challenges, including energy efficiency. This review addresses that gap by synthesizing interdisciplinary research across technological, agronomic, and sustainability perspectives, thereby providing a unified framework that highlights emerging trends, identifies unresolved issues, and outlines future research directions for advancing smart irrigation systems. Specifically in the context of precision irrigation, this review outlines the following: (i) the concept and evolution of automated irrigation, (ii) the parameters for determining crop water requirements, (iii) the in situ sensors, (iv) the use of remote sensing approaches, (v) the use of the Internet of Things, (vi) the emergence of artificial intelligence, (vii) energy utilization and efficiency, and (viii) a summary of the limitations of these systems and prospective methods that could further increase the efficiency of water use for crop irrigation.

This review provides structured and integrative synthesis of precision irrigation management technologies by organizing the evidence base across in situ sensing, remote sensing, IoT communication, and AI-enabled decision support. Unlike many existing reviews that focus primarily on single technical layers (e.g., sensor technologies, IoT plat-

forms, or machine learning models), this review brings all these components together within an end-to-end perspective of smart irrigation workflows. In particular, the review systematically traces the concept and evolution of automated irrigation and connects it to current agroclimatic sensing systems, satellite- and sUAS-based remote sensing approaches, cloud-based processing (e.g., Google Earth Engine), and computational intelligence techniques including fuzzy logic, machine learning, and deep learning. The review further consolidates energy efficiency considerations alongside system limitations and future opportunities in the context of industry 5.0, therefore offering a consolidated reference for both research development and practical system design in smart precision irrigation.

2. Review Methodology

A structured literature inclusion and exclusion design was developed to lay the foundation for this review paper to ensure that the selected studies were relevant, up to date, and of high quality for building the evidence base [35]. This design was carefully implemented to cover the breadth and depth of existing research in smart irrigation technologies and innovation while focusing on practical implementation capabilities. The full screening pipeline is outlined in Figure 1, and keyword/search formulation is summarized in Table 1.

Table 1. Keyword grouping by category to demonstrate selection of research studies using Boolean operators for development of this review paper.

Term 1 (Title-Abstract-Keywords) OR		**Term 2 (Title-Abstract-Keywords) OR**		**Term 3 (Title-Abstract-Keywords) OR**
Irrigation		IoT		Artificial intelligence
Irrigation system		Internet of Things		Fuzzy logic
Smart irrigation	AND	Wireless communication network	AND	Neural networks
Automatic irrigation		Sensor		Machine learning
Precision irrigation		Remote sensing		

- **Relevance**: This was the primary criterion where the studies that dealt with the topic of smart technologies for precision irrigation were identified. This identification was done using keywords such as automated irrigation, smart irrigation, precision irrigation, IoT, wireless communication network, artificial intelligence, machine learning (ML), fuzzy logic, neural networks, sensors for irrigation management, and remote sensing. Pertaining search strings were generated by combining the keywords and their synonyms to capture the broadest range of relevant studies. With the initial selection, articles containing at least one of the keywords were selected. The relevance of articles was confirmed by evaluating the study's research questions, objectives, methodology, and findings to see if those aligned with the theme of this review paper. In tandem, if the relevance criteria were not met, the studies were excluded. For example, the studies that focused on aspects of smart agriculture other than irrigation were excluded.
- **Database selection and retrieval strategy**: The first step of article inclusion and exclusion involved an extensive search process with Google Scholar, which served as the primary and broadest database, as it captures studies indexed across multiple major academic databases such as Elsevier (ScienceDirect), Springer, IEEE, MDPI, and Taylor & Francis. The search was conducted for studies published during 2015–2025, with

selected foundational studies included when necessary. The Google Scholar search using the Boolean search string compiled from Table 1 returned 17,700 records. Since Google Scholar does not support bulk exporting of all search results, 567 potentially relevant studies were selected for export and screening by manually reviewing the title, abstract, document type, language, and topical relevance in the search results.

-- Search String: Google Scholar
(Irrigation OR "Irrigation system" OR "Smart irrigation" OR "Automatic irrigation" OR "Precision irrigation") AND ("IoT" OR "Internet of Things" OR "Wireless communication network" OR "Sensor" OR "Remote sensing") AND ("Artificial intelligence" OR "Fuzzy logic" OR "Neural networks" OR "Machine learning") AND ("Precision Agriculture")

- **Duplicate removal**: All the initially selected papers from Google Scholar were compiled in the Zotero software that allowed for the identification and removal of duplicates before proceeding to the initial screening. As a result, 106 duplicate records were removed, yielding 461 unique studies for initial screening.
- **Initial screening**: After duplicate removal, the remaining 461 records were screened in stages using the title, abstract, and introduction to confirm alignment with smart/precision irrigation management systems (Figure 1). During this stage, off-topic records (n = 18) were excluded based on title-level screening. Further screening of abstracts and introductions resulted in the exclusion of irrelevant studies (n = 50), particularly those related to smart agriculture domains not connected to irrigation decision-making, such as groundwater recharge monitoring, generic crop growth monitoring, and plant disease monitoring without irrigation relevance (Figure 1).
- **Quality control**: At the initial screening stage, quality control was also addressed to eliminate gray literature that could include possible bias in the review. This was done by prioritizing peer-reviewed journal publications and by checking the credibility of journal/publisher information before inclusion. For the papers published in other journals, a thorough reading of the abstract, introduction, and methodology was conducted. In addition, the title, journal, authors and their affiliations, and year of publication were carefully checked before elimination.
- **Practical implementation and evidence**: To comprehensively provide a full overview of the state of the art, studies that scoped for practical implementations with evidence of their findings were included. This includes articles that describe deployment of sensors, smart irrigation prototypes, operation and/or information, water requirement estimation models, AI models, communication systems, and energy sources for real-world agricultural irrigation management. Evidence of findings in real situations was crucial, as it demonstrates feasibility, effectiveness, and potential impact of the developed technologies and methods. This evidence pertained to studies that focused on case studies, and field/experimental trials were included. Selected studies were assessed on these aspects, and the ones that did not meet these criteria were excluded.
- **Methodological depth and rigor**: The methodological depth and rigor of a study was another essential criterion for article inclusion and exclusion in this review. To conform with these criteria, the robustness of research design, data collection, analysis, validation, and interpretation methods in each identified study were assessed. Studies that deployed well-established standard methodologies, sufficiently sized and diversified datasets, and thorough validation that provided reliable and generalizable findings were included, and the remaining were excluded from further analysis.

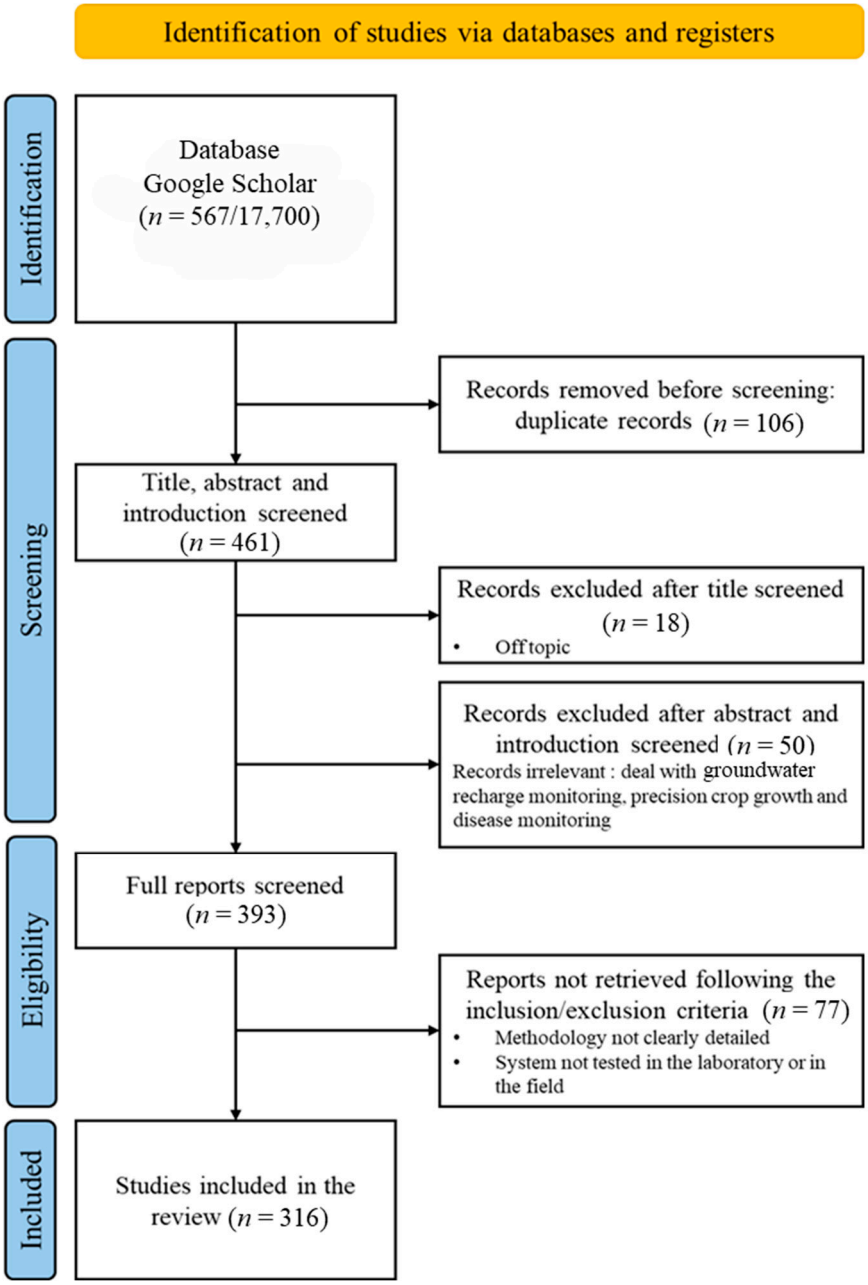


Figure 1. The PRISMA inclusion–exclusion flowchart showing filtration of studies for developing this review paper.

- **Knowledge contribution**: It is important to select studies that contribute significantly to the field of smart irrigation. Therefore, papers that introduced novel sensors, techniques, models, analytical frameworks, computation and communication technologies, and energy sources, as well as those providing comprehensive reviews or meta-analyses of existing research, were included after in-depth evaluation. Studies that identified and addressed key challenges, gaps, and future directions in smart irrigation were also included, while the studies that did not make an advancing contribution to the field were excluded. These were the articles that reiterated well-known findings but did not offer new insights, failed to address challenges, lacked in originality of approaches, or did not provide a comprehensive review or contextualization of their findings to the broader field area.
- **Historical and foundational work**: While this review primarily focused on a decadal evaluation and recent advancements in smart irrigation technologies, foundational

studies published before 2015 were also included that provided basic knowledge and theoretical underpinnings essential for understanding current developments. Foundational works from as far back as 1967 were also considered, particularly if key concepts, methods, or technologies significantly influenced subsequent research.

- **Language and accessibility**: To ensure that this review would serve the global audience, only the studies published in English were included. This was essential to maintain consistency and comprehensibility across the breadth of review. The criteria were further facilitated by also selecting studies that are published in open-access journals or repositories for a wider outreach to researchers and practitioners in the field.
- **Risk of bias and study quality consideration:** A structured quality appraisal was applied during full-text screening. Studies were assessed for completeness in system description, methodological transparency, adequacy of experimental design, data quality, presence of evaluation evidence in field and laboratory setting, reporting of performance metrics, and clarity of limitations and uncertainty.
- **Eligibility criteria**: After the initial screening, full texts of the shortlisted studies (n = 393) were examined in detail to confirm relevance, methodological rigor, and contribution to the field by applying the complete inclusion and exclusion criteria described above. Reports not retrieved or not meeting the inclusion/exclusion criteria were excluded (n = 77). Studies were also excluded when the methodology was insufficiently described, the system lacked evaluation evidence in laboratory or field conditions, or the work did not support irrigation decision-making.
- **Included studies for evidence synthesis**: As a result of the complete screening and eligibility assessment process, 316 peer-reviewed publications were finally chosen to be included in development of this review paper (Figure 1). The major advantage of this process is that it ensures a rigorous and systematic approach for selecting relevant literature to provide a comprehensive overview of recent developments and future directions in smart irrigation under the realm of precision agriculture.

Overall, this screening process ensured a rigorous, traceable, and systematic selection of relevant evidence, thereby strengthening the quality and reliability of the final evidence base used in this review.

3. Automated Irrigation: Concept and Evolution

The automated irrigation system focuses on providing sufficient water supply for crop growth in all seasons, even during the physical absence of a farmer, thus enabling the maintenance of an adequate water level on-site through regular monitoring of soil moisture levels [36]. Automated irrigation approaches also rely on measurements of volumetric water content, crop temperature, and weather data [28,37]. Another definition from the perspective of wireless communication networks states that an automated irrigation system integrates numerous sensor nodes equipped with radio transceivers that detect, monitor, and analyze environmental conditions, communicate with each other, are connected to a main site via a gateway, and are powered by an energy source to actuate crop water application [38].

Automated irrigation techniques have been used for quite some time now and have undergone significant changes over the years. A timeline of key milestones from 1967 to the present is summarized in Figure 2. It was first developed and implemented in 1967 for surface irrigation, where the objective was to reduce the amount of labor. In that system, floats were used to trigger pre-set timers, which in turn triggered the closure of dam gates once irrigation was complete [39]. Then, in 1971, automatic irrigation was implemented with furrow irrigation [40]. The system was later refined in 1978, where control systems with valves and automated controls for pipes were developed to conserve water used for

irrigation [41]. In 1984, more precision to automatic control systems for drip irrigation were added by actuating irrigation based on root-zone soil moisture levels measured by electronic soil moisture sensors [42]. Further in 1996, Evett et al. [43] developed an automatic irrigation control system based on canopy temperature thresholds. This was also the decade where several studies on automated field irrigation were pursued, and several sophisticated technologies have been developed and integrated since then [44–48]. Starting in 2001, studies began to emerge on the integration of solar energy to optimize automated irrigation systems [48,49]. During the same period, and continuing to the present day, several studies have been conducted to optimize irrigation and conserve water resources through the automation of precision irrigation systems, namely drip irrigation systems, sprinkler irrigation systems, center pivot systems, and, thanks to the use of IoT, wireless communication networks, ML, and artificial intelligence [50–57]. These technologies have become increasingly important in irrigation automation over the years.

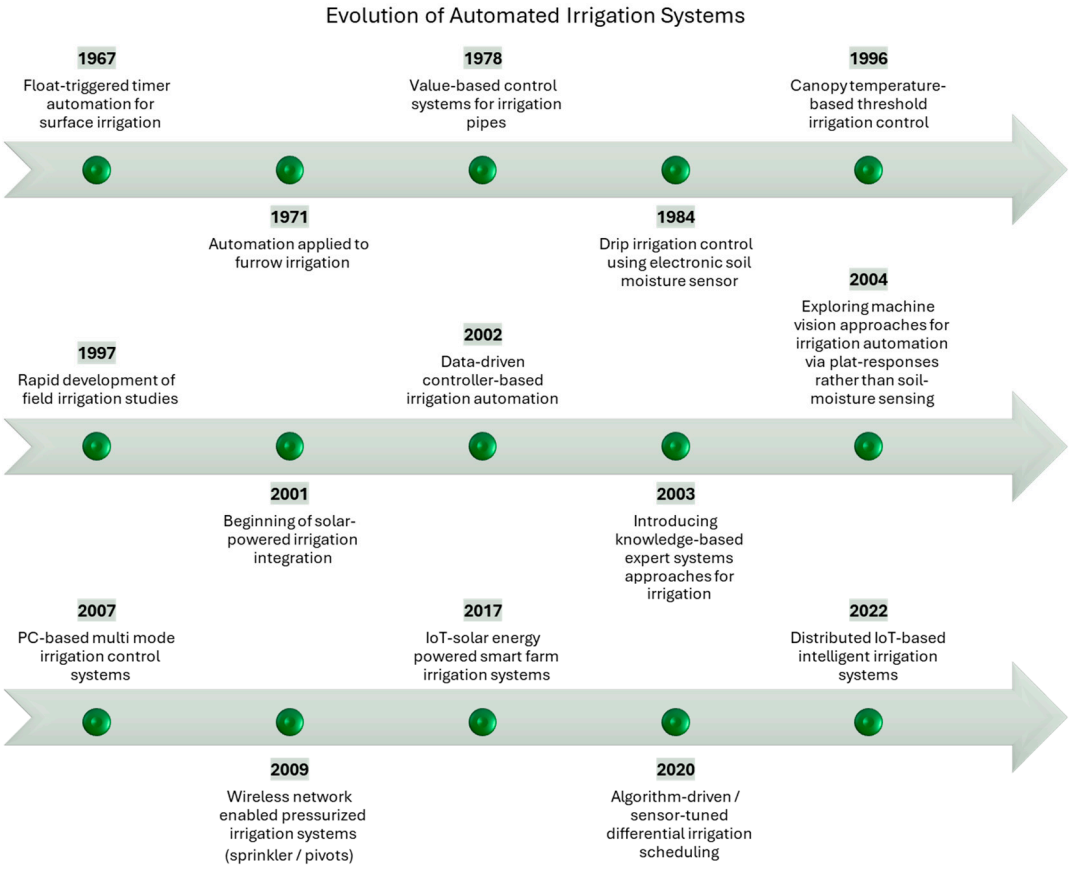


Figure 2. Timeline of key milestones in the evolution of automated irrigation systems from early control mechanisms (1967) to modern IoT- and AI-enabled precision irrigation.

As per the developments so far, smart irrigation systems typically consist of a data acquisition network of sensors, wireless communication hardware, microcontrollers and data processing units, and an irrigation actuation unit. Although the combination of these components varies depending upon the need and irrigation systems, most systems follow a similar configuration. A detailed summary of utilized smart irrigation systems with combinations of different components is provided in Appendix A (Table A1, [58–77]).

Through Table A1, it is observed that smart irrigation systems have mostly relied on using low-cost sensors, namely DS18B20 (±5%), DHT11 (±2 °C and ±5%RH), and DHT22 (±2–5% RH and ±0.5 °C); resistive sensors, such as YL-69 and FS-28 [60,67,68,72]; and low-cost capacitive sensors, namely V1.2 and V2.0 [65,69,75,76]. Moreover, Saputri et al. [77]

showed a bias of −0.9 °C when using DS18B20 and −0.2% for DHT22. Concerning low-cost sensors, Chikankar et al. [58] used LM-35 (±0.8 °C) and SY-HS-220 (± 5%) sensors to collect temperature and humidity, respectively. In such low-cost systems, NodeMCU has been widely used for data handling and processing [62,65,67,68,70,72,74,76,77]. In addition, most systems are powered by solar photovoltaic panels and energy storage batteries [62,77]. These systems have been tested in laboratory and in the field. Some authors have tested the systems to verify that the system works well without assessing their impact on water resources and crop yields [60,62,67,68,71,76]. Nevertheless, assessing impacts on water conservation and crop yields would enable a better evaluation of system performance. Other authors have tested the systems and reported measurable improvements in water saving and water yield performance [63,66,70].

Osroosh et al. [59] developed a system using the IRT/c.2 infrared thermometers and the CR10(X) datalogger (Campbell Scientific, Logan, UT, USA) with 900 MHz spread-spectrum radio for data handling and processing. This system is more expensive than those developed or evaluated in previous studies. However, it enabled the recording of a low water deficit with a $p < 0.05$ compared to the well-trusted but expensive neutron probe method. In addition, Domínguez-Niño et al. [64] implemented an irrigation system using VP3 (METER Group) temperature and 10HS (METER Group) soil moisture sensors and the CR800 data logger (Campbell Scientific, Logan, UT, USA). Although more expensive than earlier reported low-cost systems, it enabled water savings of 24% compared to unregulated uniform rate irrigation of small apple trees.

Results show a positive effect of smart irrigation on water saving, with an improvement between 11 and 42% (Figure 3) compared to the classical system. The forest plot presents the reported water savings (%) at a 95% confidence interval from seven studies, indicating considerable variability in water-saving potential. Barkunan et al. [63] report the highest central estimate of water savings, around 40%, with a wide confidence interval extending roughly from 20% to nearly 80%, suggesting both substantial potential and uncertainty. Similarly, Kumar et al. [73] and Prasad et al. [75] report central values close to 40%, but with slightly narrower confidence intervals, indicating more consistent findings. Studies by Domínguez-Niño et al. [64], Shufian et al. [65], and Zhang et al. [69] show moderate water savings between 25% and 31%, again with variable ranges reflecting study-specific differences. The smallest water savings are reported by Kumar et al. [70], with estimated savings around 10–20% and a relatively narrow confidence interval, indicating more precise but lower effectiveness.

Most of the developed systems have not been field-tested to evaluate their performance under real-world conditions, and laboratory tests alone are insufficient to confirm system robustness. Therefore, long-term field evaluation is necessary to confirm performance under practical variability. Furthermore, apart from Saputri et al. [77], most authors did not perform bias testing to verify proper functioning of sensors in field conditions. Several studies also did not quantify system impacts in terms of water savings and crop yield outcomes, which limits assessments of their true effectiveness. Some authors did not specify the exact soil moisture sensor used [31,58,61,62,71,74], while others relied on V2.0, FC-28, V1.2, and YL-69 sensors, which have corrosion-related limitations that may affect operational reliability. In addition, studies such as, Chikankar et al. [58], Rawal [60], Barkunan et al. [63], Domínguez-Niño et al. [64], and Saputri et al. [77] did not report the energy sources, despite growing trend towards solar-powered energy systems. Most of these studies did not carry out an economic feasibility analysis, which may hinder reproducibility and adoption in resource-limited farming contexts.

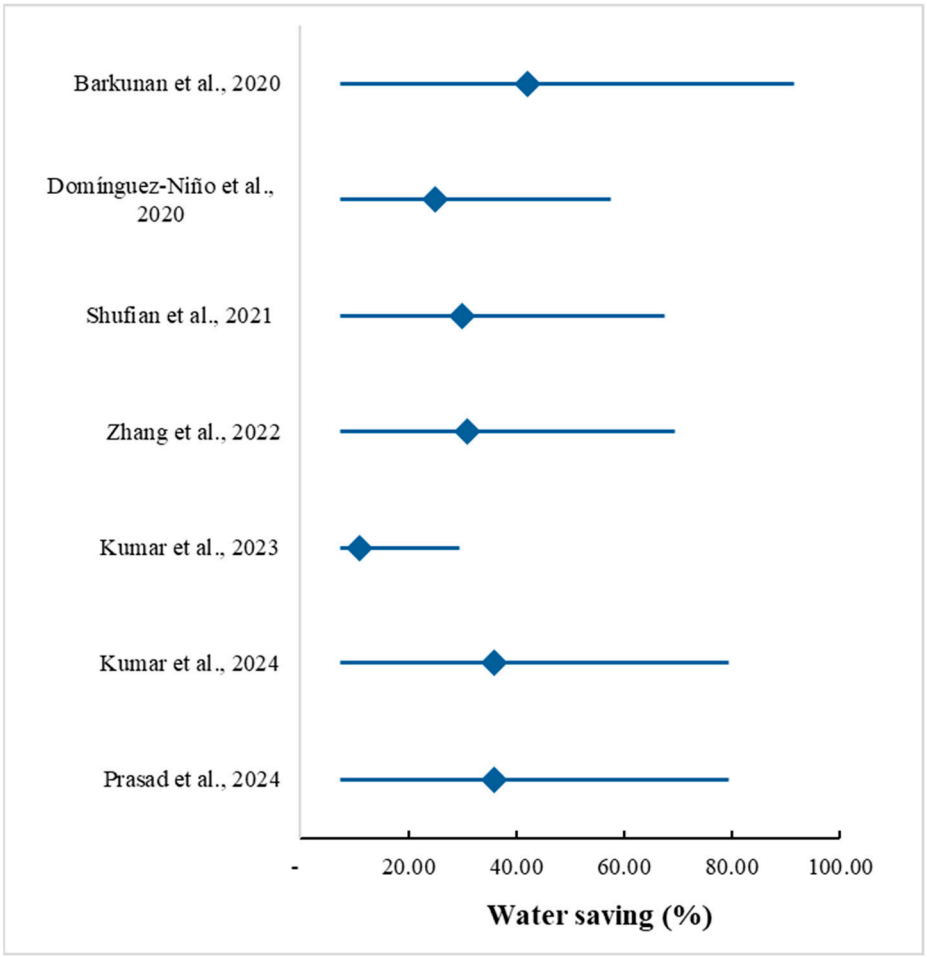


Figure 3. Forest plot of water savings in developed systems [63–65,69,70,73,75]. Square symbols indicate mean water savings.

Therefore, a practical economic feasibility assessment should consider the cost associated with (i) system hardware (sensor, controller, loggers, and actuation units), (ii) installation and calibration, (iii) operation and maintenance, (iv) communication and data handling requirements, and (v) energy sources and data storing components. In addition, long-term endurance of the system also depends on recurring costs such as sensor replacement, corrosion-related repairs, battery degradation, and maintenance. Therefore, further research should include standardized cost benefit analysis and adoption assessment by transparently reporting payback period, return on investment, and affordability under different farm scales and agroclimatic conditions. Such economic evaluation is essential to improve reproducibility and support broader deployment of smart irrigation systems in real-world agricultural environments.

4. Key Parameters for Determining Crop Water Requirements

Water requirement represents the quantity of water that needs to be applied to crops to optimize crop growth [78]. Several parameters are used to calculate irrigation water requirements: crop evapotranspiration or actual ET (ETa), soil moisture, precipitation, and leaching water requirements. Thus, the irrigation water requirements can be calculated through the soil water balance, which are the driving principles behind the estimation of crop water requirements. The soil water consists of an assessment of the inflow and outflow of water in the root zone of the crops over a given period (Figure 4).

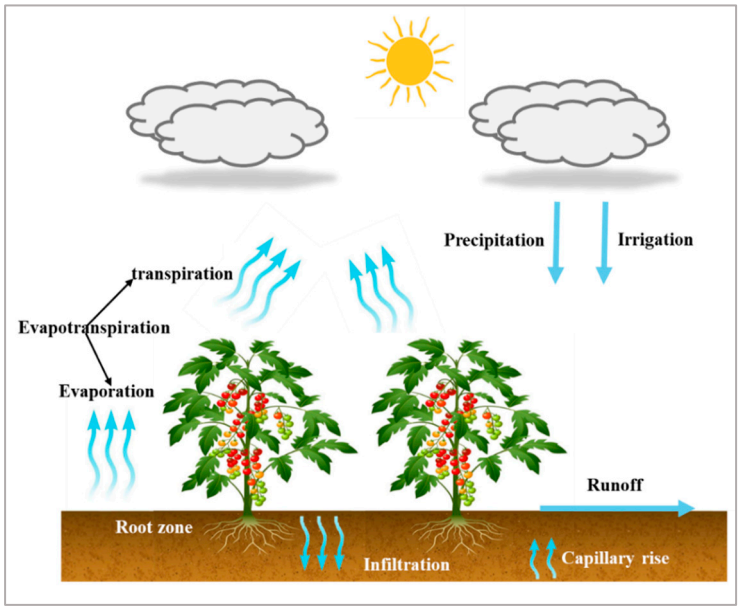


Figure 4. Water cycle shows incoming and outgoing water components to/from the soil.

Therefore, using a soil–water balance approach, irrigation depth can be calculated using Equation (1) [79–81].

$$I = P + CR - D - R + \Delta S - ET_a, \quad (1)$$

where ET_a is the actual evapotranspiration, P is the precipitation (mm), I is the irrigation depth in last 24 h (mm), CR is the capillary rise from the groundwater table (mm), D is the deep percolation (mm), R is the surface runoff (mm), and ΔS is the soil water storage variation in the plant rooting depth (mm).

Irrigation water requirements can be calculated more precisely as the net irrigation requirement (NIR) based on ET_a and leaching water requirements (LR) in areas where higher soil salinity is a constraint.

$$NIR = ET_a + LR \quad (2)$$

Crop ET_a is calculated by multiplying the reference ET (ET_o) with the crop coefficients (K_c) in equation 3 or by multiplying the reference ET (ET_o) with the sum of the basal crop coefficient (K_{cb}) and soil evaporation coefficient (K_e) as in Equation (4) [82]. K_c or K_{cb} are the standard crop coefficients tabulated in the irrigation and drainage paper 56 that are used as is or after specific adjustments for localized conditions.

$$ET_a = ET_o \times K_c \quad (3)$$

$$ET_a = ET_o \times (K_{cb} + K_e) \quad (4)$$

Reference ET (ET_o) is a standard water loss from the hypothetical crop surface (well-watered shortgrass) representing the atmospheric demand for water. This can be calculated using the most-adopted Penman–Monteith Equation ([82–85], Equation (5)).

$$ET_o = \frac{0.408 \times \Delta \times (R_n - G) + \gamma \times \frac{900}{T+273} \times u_2 \times (e_s - e_a)}{\Delta + \gamma \times (1 + 0.34 \times u_2)} \quad (5)$$

where ET_o is the reference ET (mm/day), R_n is the net radiation at the crop surface ($MJ/m^2/d$), G is the soil heat flux density ($MJ/m^2/d$), T is the mean daily air temperature

at 2 m height (°C), u_2 is the wind speed at 2 m height (m/s), e_s is the saturation vapor pressure (kPa), e_a is the actual vapor pressure (kPa), Δ is the slope of the vapor pressure curve (kPa/°C), and γ is the psychrometric constant (kPa/°C).

In addition, according to McShane et al. [86] and Senay et al. [87], surface energy balance approaches have also been one of the most effective methods for estimating actual ET from the difference between net surface radiation and losses due to sensible and ground heat fluxes (Figure 5).

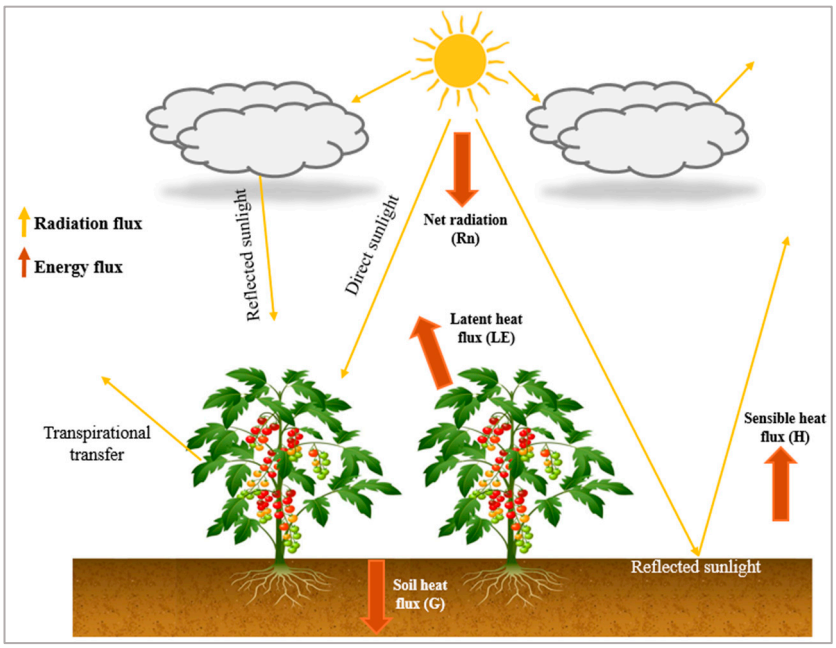


Figure 5. Energy balance diagram showing components of energies interacting with the land surface and resulting in evapotranspiration.

Crop ET_a from energy balance models (Equation (9)) can also be used to compute monthly, seasonal, and annual crop water requirements.

$$ET_a = ET_oF \times ET_o \quad (6)$$

$$ET_oF = \frac{ET_{inst}}{ET_{o,h}} \quad (7)$$

$$ET_{inst} = 3600\frac{\lambda ET}{l} \quad (8)$$

$$\lambda ET = R_n - G - H \quad (9)$$

where G is the soil heat flux (W/m^2), H is the sensible heat flux (W/m^2), R_n is the net radiation (W/m^2), λET is the latent heat flux (W/m^2), ET_{inst} is the instantaneous ET, ET_o is the reference evapotranspiration, and ET_oF is the daily ET as a fraction of reference ET [88].

ET_a is also calculated using the method developed by Nisa et al. [89]. This method uses the Bowen ratio, which is based on the energy balance equation where temperature and humidity gradients are used to estimate latent heat flux (or ET).

$$ET_{a_Bowen} = \frac{1}{\lambda \times \rho_w} \times \left(\frac{R_n - G}{1 + \left(\gamma \times \left(\frac{\Delta T}{\Delta e} \right) \right)} \right) \quad (10)$$

where R_n is the net radiation (W/m^2), G is the ground heat flux (W/m^2), γ is the psychometric constant, ΔT and Δe are the temperature and humidity difference between surface and height, ρ_w is the water density, and λ is the latent heat of vaporization.

The FAO Penman–Monteith method is the most used method to determine the actual crop water requirements of ET_a but requires a large amount of meteorological data, which often limits its use in data-sparse regions [90,91]. In addition, Ragab et al. [92] have shown that estimating ET using the crop-coefficient method leads to an overestimation of crop water requirements. The authors compared ET_a obtained using the crop coefficient with measurements taken using the eddy covariance and Scintillometer methods in Bologna, Italy, during the 2014 and 2015 growing seasons. Crop rotation was carried out with winter wheat, sorghum, sunflower, maize, processing tomato, and orchards. The results showed that ET_a obtained using eddy covariance techniques represented 45% of that of the crop coefficient, while that measured by the Scintillometer represented 35% of K_c-based ET_a. In addition, Dingre and Gorantiwar [93] compared sugarcane crop coefficients obtained from field water balance measurements with those reported by FAO-56 in the semi-arid conditions of India in 2015 and 2016. The results showed that the crop coefficients obtained using the FAO-56 method were higher than those measured by 25.5% during the tillering stage, 4% during rapid growth, and 20.4% at maturity. To solve these problems, models for estimating ET_a based on energy balance are being increasingly used. Madugundu et al. [94] showed that using the METRIC, i.e., Mapping ET at High Resolution with Internalized Calibration, a single-source energy balance model, provided an accurate estimate of the ET_a of an alfalfa field in Saudi Arabia, with RMSE values of 0.13 and 4.15 mm/day. Nevertheless, it caused a 6.6% overestimation of hourly ET and a 4.2% underestimation of daily ET_a compared to the eddy covariance method. According to the author, its performance may be reduced in partial canopy conditions. Nisa et al. [89] also showed that the METRIC method can produce a reasonable estimation of ET with an RMSE of 1.2 mm/day, whereas Venancio et al. [95] showed that the energy balance method slightly underestimated ET compared to the crop-coefficient method for the soybean crop.

Other methods of estimating ET_a are used, namely the Bowen ratio (BR) method. Thus, Xiong et al. [96] compared the calibrated and uncalibrated surface renewal (SR) model with the Bowen ratio (BR) model to estimate ET_a. To evaluate the performance of these methods, an experiment was conducted in a vineyard near the city of Yinchuang in northwestern China, where the climate is temperate continental. The experiment was performed between 2017 and 2019. Comparison of the BR method with the uncalibrated SR method yielded a coefficient of determination of 0.83, a mean absolute error of 0.41 mm/day, and an RMSE of 0.57 mm/day. Comparing the BR method with the calibrated SR method can yield a mean absolute error ranging from 0.38 to 0.39 mm/day and an RMSE ranging from 0.52 mm/day to 0.51 mm/day. Irmak [97] showed that the FAO56 method overestimates ET_a based on the field studies conducted during the 2005 and 2006 growing seasons in Nebraska, USA with overestimation of 15% in 2005 and 10.3% in 2006.

Ding et al. [98] also estimated ET_a from cabbage cultivation using the eddy covariance method over two growing periods in Wuwei City in northwest of China: 17 April to 1 July (first period) and 1 August to 16 October 2020 (second period), with errors of 17–19%. Such errors are mostly because eddy covariance methods suffer from non-closure of energy balance, leading to under- or overestimations [99,100]. A study by Gokool et al. [101] evaluated the use of the METRIC energy balance model to quantify water use by M. oleifera in a semi-arid region in Limpopo Province of South Africa from November 2022 to May 2023 and recorded a root mean square error of 2.03 mm/day and a mean absolute error of 1.63 mm/d with R^2 of 0.24. This suggests appropriate region-specific calibration of energy balance for arid, semi-arid, rainfed, or irrigated conditions.

The weighing lysimeter estimates crop ET_a through a very precise soil–water balance approach with the change in weight of the plant, soil, and water, which is interpreted as the water lost through soil evaporation and plant transpiration [102]. Kebede et al. [103] custom-designed a simple weighing lysimeter for measuring water requirements and crop coefficients of shallow-rooted crops in the Southeast Shoa Zone of Oromia regional state in Ethiopia. This system was reported to have linearity errors between 0.03 and 0.04 kg in the first two years of evaluations (2023 and 2024). Liu et al. [104] compared the lysimeter and eddy covariance methods for measuring ET from rice fields in wet and dry conditions during late 2016 and early 2017 rice seasons in Jiangxi Province in China, showing a linear agreement post-closure of energy balance of eddy covariance. Nonetheless, the use of the lysimeter can be limited by its high initial, installation, and maintenance costs, and the measurements are representative of a very small area, not the entire crop field or larger area [105]. Table A2 summarizes the ET_a estimation models used for different crops and under different climatic conditions and their comparison with standard eddy covariance, FAO-56, and/or lysimeter methods [89,94,95,106–112].

The FAO Penman–Monteith method requires a lot of data, which can limit its use in remote areas where data are not available. As for the METRIC method, its performance can be reduced when coverage is low. METRIC uses "hot" and "cold" anchor pixels in the image for built-in calibration of sensible heat flux, reducing dependence for external meteorological data and contributing to reducing bias across regions. The eddy covariance method may require specific adjustments for each region's energy balance in arid, semi-arid, rainy, or irrigated conditions. Lysimeters are expensive to install, and the values they provide may be specific to the area concerned and not representative of a large plot. The Operational Simplified Surface Energy Balance (SSEBop) method overestimates potential evapotranspiration during cloudy weather. This method provides poor data quality in arid and semi-arid areas, as it requires high NDVI pixels for calibration, which are often unavailable in these areas. It is highly dependent on the land surface temperature (LST) derived from satellites, and its accuracy is related to the weather data quality used to calculate ET_r. The Surface Energy Balance System (SEBS) is limited by its single-layer assumption, which can cause constraints on its use in dry and vegetated areas. These results are more effective in non-cloudy conditions. The QWaterModel can be operated with UAS, satellites, and portable thermal cameras to suit both field and regional scales. It is sensitive to errors in thermal band calibration, atmospheric correction, or emissivity assumptions, which have a direct influence on ET. The model provides better performance in high-density and tall crops. The Surface Energy Balance Algorithm for Land (SEBAL) can lead to errors for heterogeneous surfaces where land cover is mixed, with some areas of bare soil and others covered with vegetation. This model only needs air temperature, solar radiation, and wind speed as weather data in comparison with the Penman–Monteith method. It is also very sensitive to these weather data and to LST from satellites. The Atmosphere-Land Exchange Inverse (ALEXI)/Disaggregation (DisALEXI) method is limited by the low resolution of thermal satellite images. It uses a two-source energy balance framework and provides a better representation of heterogeneous surfaces than single-source models such as SEBAL or METRIC. The Priestley Taylor Jet Propulsion Laboratory (PT-JPL) method can also lead to underestimation or overestimation of ET_a in heterogeneous areas or under water stress conditions. It is dependent on satellite-derived LAI, NDVI, and fraction of photosynthetically active radiation absorbed (fPAR). The Satellite Irrigation Management Support (SIMS) method can overestimate ET_a in cases of irrigation deficit and underestimate evaporation in bare soils. The modified Priestley-Taylor (MPT) method can also be less accurate in heterogeneous surface areas due to its dependency on relatively uniform properties of vegetation cover and surface. However, this model provides more accurate

data at the local level where data can be adjusted. The CropSyst-W model is limited by a lack of detail for certain crops and growth patterns, providing poor data for certain crops such as lettuce, escarole, and some winter cereals. It also requires detailed and consistent field data for accurate validation and struggles to handle high spatial and temporal variability, requiring adaptation to specific locations and cropping systems.

Irrigation water contains dissolved salts that can deposit in the root zone of the crop, and as ET occurs, the soil water evaporates but leaves behind the salts. As such salts keep on accumulating, it can become difficult for the roots to access water, resulting in reduced crop growth and eventually yields. To mitigate such situations, an extra amount of irrigation water can be applied to eliminate salt buildup in the crop root zone. This excess water is called the LR that can be calculated using different parameters, as in Equation (11).

$$\mathrm{LR} = \frac{\mathrm{DP}}{\mathrm{AW}} = \frac{\mathrm{EC_w}}{5 \times \mathrm{EC_t} - \mathrm{EC_w}} = \frac{\mathrm{V_{dw}}}{\mathrm{V_{inf}}} = \frac{\mathrm{EC_{iw}}}{\mathrm{EC_{dw}}} \tag{11}$$

where DP is the deep percolation (mm); AW is the applied water (mm) [113]; EC_w is the salinity of the applied irrigation water (dS/m); EC_t is the threshold salinity, which is the average soil salinity that can be tolerated by the crop (dS/m) [114,115]; V_{dw} is the volume of drainage water (mm); V_{inf} is the infiltrating irrigation water (mm); EC_{iw} is the electrical conductivity of the irrigation water (dS/m); and EC_{dw} is the electrical conductivity of the drainage water (dS/m) [115]. Assuming that irrigation is conducted at a uniform rate, if the irrigation efficiency, i.e., the ratio or water in the root zone to the applied water, is greater than (1-LR), then LR should be used along with actual ET and runoff from applied water (D_r) to calculate the amount of irrigation water (IR_n) needed to be applied (Equation (12)). Otherwise, if the irrigation efficiency is lower than (1-LR), then the leaching water requirements are already satisfied.

$$\mathrm{IR}_n = \frac{\mathrm{ET_a} - D_\mathrm{r}}{1 - \mathrm{LR}} \tag{12}$$

5. In Situ Sensor-Based Precision Irrigation

Use of sensors has been prevalent to determine the amount of water to be applied through automated irrigation systems. Studies so far have either used single-parameter measuring sensors such as those measuring soil moisture, air temperature, or humidity, among others, or their combinations (Table A1). Such studies have been summarized in this section.

5.1. Soil Moisture Sensors

Soil moisture is a key variable governing irrigation management and crop water use efficiency. Moisture sensors are broadly classified as resistive or capacitive, with advancements in reflectometry-based and neutron probe technologies. These sensors estimate volumetric water content (VWC), which is compared against field capacity or the permanent wilting point to determine irrigation needs. When soil moisture falls below a crop-specific threshold (e.g., 65% of field capacity), irrigation is triggered to restore optimal levels. VWC data also supports soil–water balance modeling and forecasting of irrigation requirements using ET values derived from weather data. Modern systems integrate these processes within IoT-based platforms that automate measurement, computation, and actuation for real-time irrigation control (Table A1). The following sections discuss the principles, performance, and applications of various soil moisture sensors in precision irrigation.

Resistive sensors such as FC-28, YL69, and granular matrix sensors estimate soil moisture by measuring resistance variations as current passes through the soil. Lower resistance indicates higher moisture levels. Studies by Jain [116] and Ramli and Jabbar [67] utilized the

FC-28 sensor (operating at 5 V and outputting 0–4.2 V) for volumetric water content (VWC) measurement, while YL69 was used to record surrounding humidity levels [60,69,117]. The granular matrix sensor, operating across 0–200 kPa, offers high sensitivity and ease of use but suffers from low accuracy, slow response, and poor performance in coarse-textured or shallow soils [118].

Capacitive sensors, including 10HS, SEN0308, V2.0, ECH2O, TEROS, GS1, WaterScout SM100, and CropX, measure the soil's dielectric constant, which varies with water content. Domínguez-Niño et al. [64] used the 10HS sensor (Meter Group, Pullman, WA, USA) to measure VWC via capacitance. The sensor's larger volume of influence (1 L) compared to EC-5 and EC-20 (0.3 L) minimizes noise due to soil heterogeneity [119–121] and comes with low power requirements (3–15 V DC, 12–15 mA) and output voltages of 300–1250 mV [119,120,122]. Similar sensors—EC-10, EC-20, TEROS 10–54—measure soil moisture, electrical conductivity, and temperature at multiple depths [123–125]. The SEN0308 sensor [126] and its variants (V1.2, V2.0) [66,70] with improved sealing and corrosion resistance, operate at 3.3–5.5 V DC with ±2% accuracy.

Reflectometry-based sensors, including TDR315, GS1, WaterScout SM100, CS625, CS655, CS616, CS650, and HydraProbe2, employ high-frequency electromagnetic pulses to estimate VWC from dielectric permittivity. The TDR315 operates at 3.5 GHz, measuring reflection times to derive moisture content [127–130]; TDR310 adds an integrated thermistor for ±0.3 °C temperature accuracy [131,132]. The GS1 (Campbell Scientific, Logan, UT, USA) uses 70 MHz oscillating waves to measure VWC (0–57%) with ±0.03 m^3/m^3 accuracy for EC < 10 dS/m [128,133]. WaterScout SM100 operates at 80 MHz with ±3% accuracy for EC < 8 mS/cm [128,134,135], while CropX applies amplitude-domain reflectometry with ±3% moisture and ±0.5 °C temperature precision [136]. HydraProbe2 measures true relative permittivity with ±2.5% accuracy [137–139], whereas CS655 and CS650 employ transmission line oscillation (TLO) for ±1–3% precision under specific calibration [127,128]. The neutron probe, such as the CPN 503 Elite HYDROPROBE, measures soil moisture through neutron thermalization, offering high accuracy (precision 0.24% at 24% VWC) but requiring strict radioactive source handling [140,141].

Numerous studies have implemented these sensors in automated irrigation systems, achieving significant gains in water use efficiency and yield. FC-28 and YL69 sensors have been used for threshold-based control [142,143], while granular matrix sensors demonstrated limited suitability due to slow response [144]. 10HS integration improved water use efficiency up to 1.92 kg/m^3 [145,146]; SEN0308 and V2.0 enabled 11% water savings and 12.05% yield increase [70,126]. Other studies employed EC-20 [147], TEROS 12 [148], TDR315 [149], WaterScout SM100 [150], and CS625/CS616 [151,152] for precise irrigation scheduling and soil water monitoring.

In summary, resistive sensors are cost-effective but limited by environmental sensitivity, while capacitive and reflectometry-based systems deliver greater accuracy, stability, and integrability with IoT-based irrigation frameworks. Future developments should emphasize multi-sensor fusion, adaptive calibration, and cloud-based data integration to enhance cross-soil and cross-climate reliability. The performance levels of soil sensors, such as the range of measured values, accuracy, and power required for sensor operation, are shown in Figure 6.

Figure 7 illustrates the variability in key sensor performance parameters including soil moisture, temperature, electrical conductivity (EC), and energy consumption across the smart irrigation system. Overall, soil moisture measurements ranged from 0 to 100%, temperature from –50 °C to 70 °C, EC from 0 to 25 dS/m, and operating voltage from 2 to 24 V. To evaluate overall temperature performance, the maximum readings from all sensors were consolidated into a single dataset. Figure 7a shows a median maximum

temperature of 60 °C with an interquartile range (IQR) of 60–70 °C. A few outliers correspond to sporadic high-temperature peaks likely caused by extreme weather events. The mean maximum temperature (Figure 7b) was 65.0 ± 3.42 °C, with error bars reflecting measurement uncertainty. For soil moisture, the median maximum value was 80% (IQR: 61–100%), and the mean maximum was 80.0 ± 6.84%. Maximum EC values exhibited a median of 8 dS/m (IQR: 5.5–17.5 dS/m) with an overall mean of 13.0 ± 2.9 dS/m. Voltage measurements showed a median maximum of 15 V (IQR: 5–15 V) and an average of 12.5 ± 1.73 V. Minimum values for soil moisture and EC were consistently zero. The median minimum temperature was –40 °C, with extreme cases reaching –50 °C, and an overall average of –40.0 ± 8.18 °C. The median minimum voltage was 3 V (IQR: 2.5–4.5 V). These results collectively highlight the operational stability and measurement range of sensors used in automated irrigation systems, confirming their adaptability across diverse soil and climatic conditions.

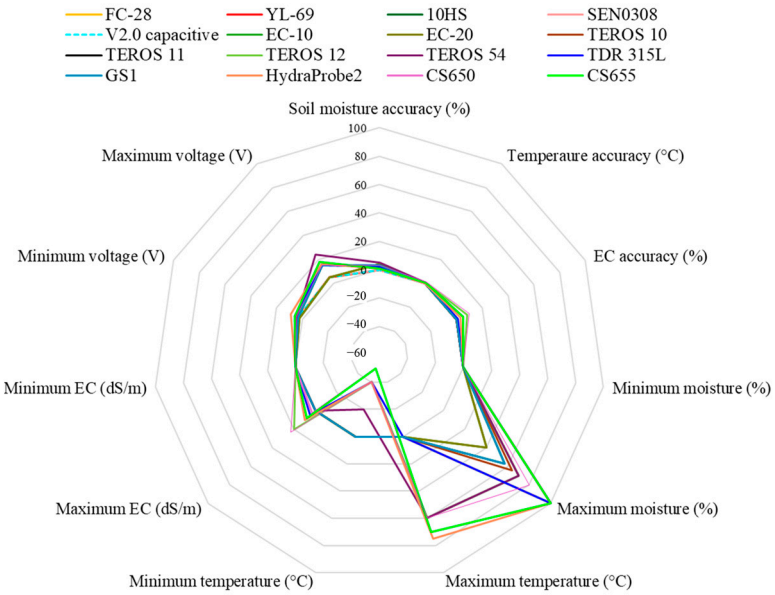


Figure 6. Performance of soil sensors widely used in research studies for addressing irrigation management.

Resistive sensors determine soil moisture by measuring electrical resistance between two metal probes; resistance decreases as soil moisture increases. While inexpensive and easy to deploy, they are prone to corrosion, short lifespan, and accuracy degradation, with readings often influenced by soil type and salinity. In contrast, capacitive sensors measure variations in the soil's dielectric permittivity, offering greater durability, stability, and resistance to salinity, though at higher cost and calibration complexity. Nandi and Shrestha [153] compared four sensor categories—low-cost resistive (FC-28), low-cost capacitive (V1.2), intermediate-cost capacitive (VH400), and high-end (Decagon 5TM)—across fine, medium, and coarse soils. The 5TM and VH400 sensors demonstrated superior accuracy ($R^2 \approx 1.0$; RMSE $\leq$ 1.8), while low-cost sensors exhibited higher deviations (R^2 = 0.92–0.99; RMSE = 1.88–4.79). Capacitive sensors consistently outperformed resistive ones across soil textures, particularly in coarse soils. Subsequent studies confirmed the versatility of capacitive sensors such as SEN0193 and 5TE in loamy silt and coarse soils [154,155]. Furthermore, the TEROS series (TEROS 10, 11, 12, 54) showed exceptional long-term reliability, maintaining accurate performance for over 10 years of continuous use [156]. In addition, these technologies may face cybersecurity vulnerabilities, especially when integrated within IoT-based irrigation networks. Implementing robust encryption and device-specific identifiers is critical to ensure data integrity and protect against unau-

thorized access. Based on the overall assessment, capacitive sensors outperform resistive types in accuracy, stability, and longevity. Their ability to also simultaneously measure multiple parameters, i.e., soil moisture, temperature, and electrical conductivity, further enhance their utility for precision irrigation. Thus, advanced sensors such as the 5TM and TEROS 12 are recommended for reliable, multi-parameter soil monitoring in smart irrigation systems.

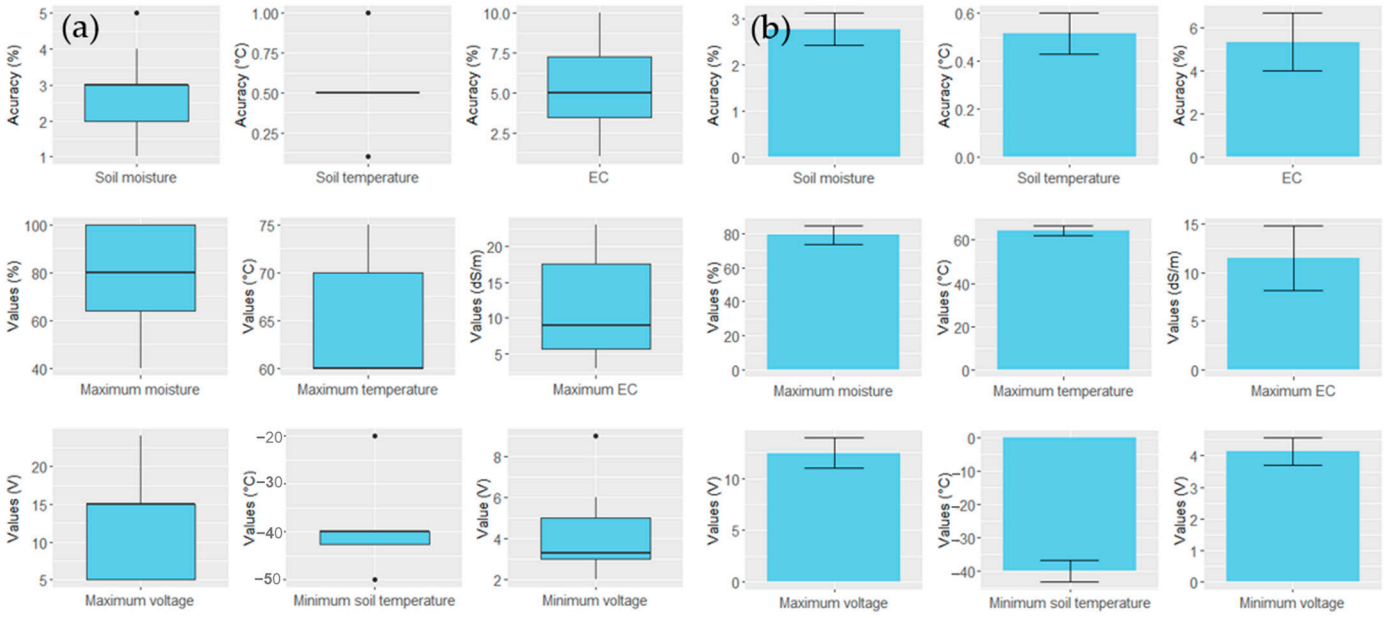


Figure 7. (**a**) Variation in measured soil parameters and power requirements and (**b**) pertaining errors in measurements from different types of soil sensors.

5.2. In Situ Weather Sensors

Weather sensing plays a pivotal role in crop management, particularly for optimizing irrigation scheduling. Key meteorological variables include solar radiation, wind speed, relative humidity, and air temperature, which collectively influence crop evapotranspiration (ET). These parameters are measured through either individual weather sensors or integrated all-in-one stations, enabling the estimation of reference ET (ET_o) and subsequent calculation of actual ET using standard or crop-specific coefficients. The use, configuration, and performance of such weather sensing systems are discussed in this section.

5.2.1. Sensors for Individual Weather Parameter Measurements

Pyranometers are critical for quantifying incident solar radiation, the primary energy source driving ET and overall plant water dynamics. The SP-110 pyranometer (Apogee Instruments, Logan, UT, USA) is among the most widely used devices for this purpose [157]. It measures total incoming shortwave radiation across the solar spectrum using a silicon photovoltaic detector housed in a cosine-corrected head, ensuring accurate angular response and consistent energy flux estimation. For wind measurements, the 034B wind sensor is a standard choice, featuring an aluminum wind vane and precision potentiometer for reliable and continuous long-term operation even under extreme environmental conditions [157]. It measures wind speed and direction within the ranges of 0–75 m s^{-1} and 0–360°, respectively [158].

The SY-HS-220 capacitive humidity sensor is commonly used for monitoring relative humidity [117]. It outputs voltage proportional to ambient humidity, which is subsequently converted and conditioned to provide accurate readings (±5%) [159–161]. In combination,

these weather sensing units enable computation of the Crop Water Stress Index (CWSI), supporting data-driven irrigation scheduling and water-use optimization [162–164].

For temperature-based irrigation systems, the LM-35DZ and DS18B20 sensors are among the most widely deployed. The LM-35DZ, an integrated-circuit temperature sensor, outputs voltage linearly proportional to the Celsius temperature [117,165,166]. Operating between –55 °C and +150 °C with a 4–30 V supply, it functions analogously through a diode where voltage increases with temperature [167]. The sensor requires no external calibration and achieves accuracies of ±0.25 °C in ambient and ±0.75 °C in outdoor environments [165]. The DS18B20 is a digital resistor-type (4.7 kΩ) sensor operating across –55 °C to +125 °C with ±5% accuracy [168]. It provides 12-bit resolution, features programmable alarm thresholds, and includes a unique 64-bit factory identifier enabling reliable multi-sensor deployments. Its waterproof construction further enhances suitability for field applications [126,169]. These sensors have been successfully integrated into smart irrigation systems. Nandurkar and Thool [170] utilized LM-35DZ for automatic irrigation control via a P89v51 RD2 microcontroller and PCB-based circuitry, while Ndunagu et al. [171] employed DS18B20 alongside other environmental sensors in an IoT-enabled system based on the ESP8266 NodeMCU platform.

Despite their wide adoption, long-term performance stability remains a critical consideration. For instance, the SP-110 pyranometer exhibits long-term instability below 2% per year under both accelerated aging and field conditions. However, comprehensive data on drift, calibration stability, and measurement degradation under real-world field deployments remain limited. Therefore, systematic long-term performance assessments ($\geq$6 months) across diverse agro-environments are strongly recommended to guide sensor selection and ensure reliable, cost-effective, and sustainable implementation in precision irrigation systems.

5.2.2. Integrated Sensors for Multiple Weather Parameter Measurements

Weather sensors play a critical role in irrigation management by providing continuous measurements of air temperature, relative humidity, wind speed, and solar radiation, which are essential for estimating reference and actual evapotranspiration (ET). Among commercially available sensors, the SHT11 and SHT71 (Sensirion AG, Stäfa, Switzerland) are widely used for air temperature and relative humidity monitoring. The SHT11 measures temperature in the range of −40 to 123 °C (±0.4 °C) and relative humidity (RH) between 0–100% (accuracy 3–3.5%) at an operating voltage of 2.4–5.5 V [123,139,172–174]. It employs a capacitive element for RH and a band-gap sensor for temperature measurement. The SHT71, although more expensive, offers higher precision and faster response. Similarly, the DHT11 and DHT22 sensors are based on thermistor and capacitive principles for temperature and RH measurement [63,67,68,70,175,176]. The DHT11 operates at 3.5–5.5 V and measures temperature from 0–50 °C (±2 °C) and RH from 20–90% (±5%), while the DHT22 extends these ranges to −40–80 °C (±0.5 °C) and 0–100% RH (±2–5%) [126]. Despite their affordability, the SHT and DHT sensors exhibit limited endurance under continuous operation due to degradation of capacitive elements by volatile organic compounds.

For long-term reliability, the HMP50 (Campbell Scientific, Logan, UT, USA) offers enhanced stability by using a 1000 Ω platinum resistance thermometer for temperature measurement and an Intercap 50Y capacitive chip for RH [157]. It measures RH from 0–98% (accuracy 3–5%) and temperature from −40–60 °C (accuracy 0.2–1.6 °C). The VP-3 (METER Group, Pullman, WA, USA) integrates a single sensor chip calibrated for both air temperature and RH and computes vapor pressure from these parameters. It measures RH between 0 and 100% (precision 0.1%, accuracy 2–5%), temperature between −40 and 80 °C (precision 0.1 °C, accuracy 0.5–1 °C), and vapor pressure between 0 and 47 kPa (precision

0.01 kPa, accuracy 0.03–0.5 kPa) [177]. The ATMOS 14 (METER Group) measures RH (0–100%), temperature (−40–80 °C, ±0.2 °C), vapor pressure (0–47 kPa), and barometric pressure (49–109 kPa, ±0.4 kPa) at a supply voltage of 3.6–15 VDC [178]. The ATMOS 41 is a more advanced all-in-one sensor capable of measuring multiple weather parameters, including solar radiation (0–1750 W m^{-2}, ±5%), rainfall (0–1500 mm h^{-1}, ±5%), RH (0–100%), vapor pressure (0–47 kPa), air temperature (−50–60 °C, ±0.2 °C), wind speed, and lightning intensity and direction. These measurements are essential for computing ET and optimizing irrigation schedules.

For wind characterization, the DS-2 Sonic Anemometer measures wind speed (0–30 m s^{-1}, ±0.30 m s^{-1}) and direction (0–359°, ±3°) and operates at 3.6–15 VDC [179]. The HS-50 (Gill Instruments, Hampshire, UK) provides three-axis wind speed measurements (0–45 m s^{-1}) at a 50 Hz update rate with <1% RMS accuracy and wind direction (0–359°, <1% RMS) [180]. The HS-100 offers similar performance with a 100 Hz sampling rate [181]. The R3-50 and R3-100 3-axis anemometers (Gill Instruments, Hampshire, UK) measure wind speeds up to 45 m s^{-1} (<1% RMS) and direction (0–359°, <±1% RMS) at sampling frequencies of 50 Hz and 100 Hz, respectively, and operate between −40 and +60 °C at 9–30 VDC [182,183].

Comparative performance analysis (Figure 8) indicates that ATMOS 14 and ATMOS 41 exhibit superior range and robustness suitable for agricultural applications, while SHT11/SHT71 provide accurate measurements under extreme conditions. DHT11/DHT22 remain cost-effective options with moderate precision, and the HMP50 offers higher accuracy at the expense of greater power demand, posing limitations for low-power field deployments. Figure 8 further illustrates the range and variability in measured air temperature (−40–123.8 °C), RH (0–100%), and voltage (2.4–28 V). Median maximum temperature was 80 °C (IQR = 55–103 °C), and maximum RH was 100% (IQR = 99–100%). Minimum recorded temperature and RH were 0 °C and 0%, respectively, though certain sensors only function above 0 °C and 20% RH. Median supply voltage was 5.5 V (IQR = 5.5–15 V).

Applications of these sensors for irrigation automation have been widely documented. Goumopoulos et al. [123] employed SHT11 for automated irrigation control, while Sangeetha et al. [68] and Kumar et al. [70] used DHT11, and Veerachamy et al. [176] utilized DHT22. King and Shellie [157] deployed HMP50 for air temperature and RH monitoring in smart irrigation, and Müller et al. [184] used VP-3 for real-time humidity and temperature monitoring to estimate ET. Siddiqi and Al-Mulla [185] integrated ATMOS 41 with DS-2 anemometers in soil–plant–atmosphere-based irrigation systems. Long-term field evaluation remains critical for validating sensor reliability (Figure 9). For example, ATMOS 41 demonstrated acceptable performance when compared with a reference weather station over a three-month evaluation, with uncertainties of 0.06 kPa in atmospheric pressure, 3% in solar radiation, and 7.5% in precipitation [186]. Such deviations can be corrected using linear regressions with local reference data.

For direct measurement of actual ET, eddy covariance flux systems comprising gas analyzers (open/closed path), 3D anemometers, and soil heat flux plates offer comprehensive energy and vapor exchange quantification, though cost and power demand limit adoption [187]. The LI-710 miniature ET sensor (LiCOR, Bourne, MA, USA) provides a cost-effective alternative, operating at roughly one-twelfth the price of full systems, with reduced power requirements and simplified installation. Peddinti and Kisekka [188] evaluated LI-710 performance in California across tomato, almond, pistachio, and citrus crops over one- to eight-month periods. Despite an initial energy imbalance causing ET_a underestimation by 20–44%, correction using residual energy balance methods reduced errors to 1–10%.

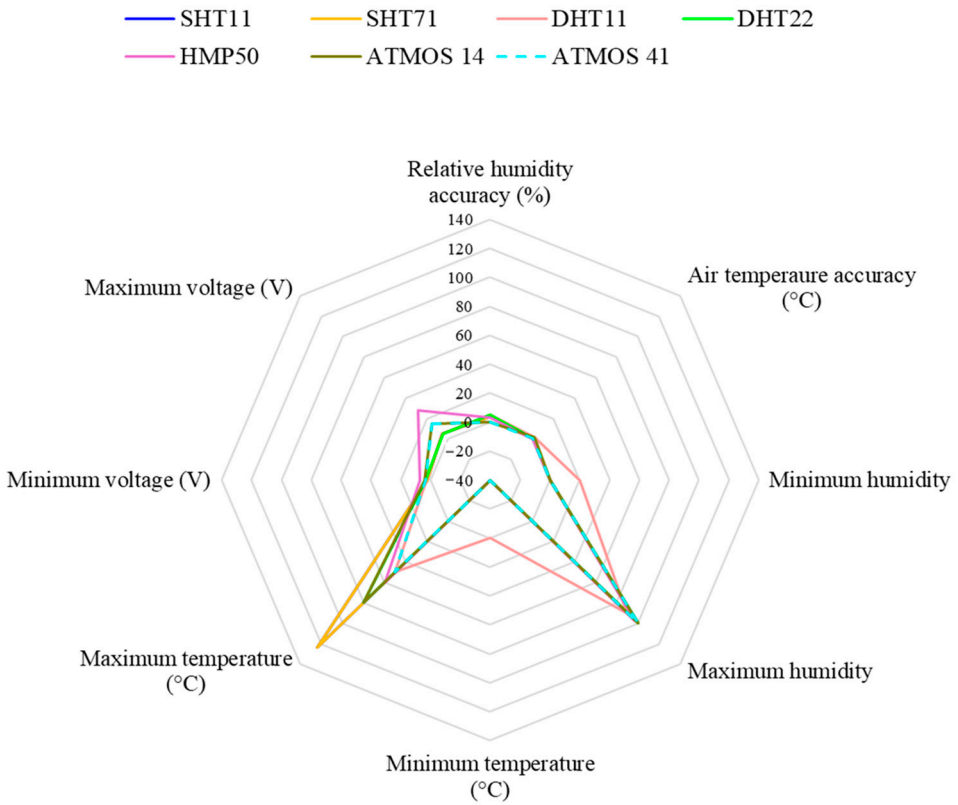


Figure 8. Performance of meteorological sensors widely used in research studies for irrigation management.

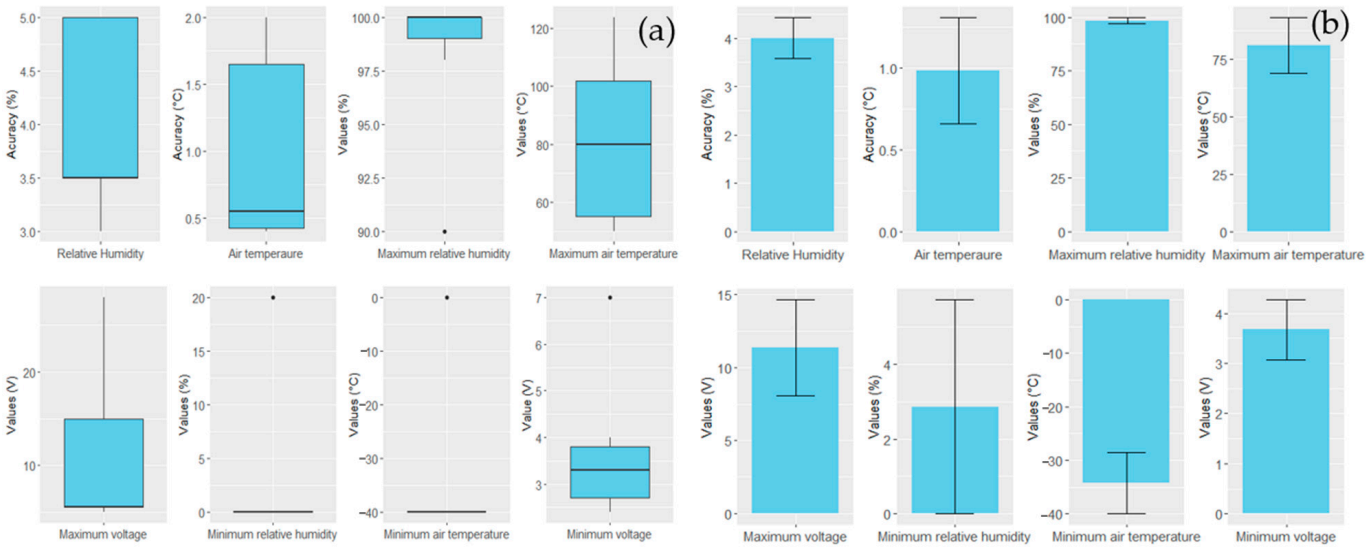


Figure 9. (**a**) Variation in measured weather parameters and power requirements and (**b**) pertaining errors in measurements from different types of weather sensors.

From 2015–2023, the key parameters for determining irrigation water requirements included temperature, RH, wind speed, solar radiation, rainfall, and soil moisture. However, since 2024, primary variables have narrowed to temperature, RH, rainfall, and soil moisture, while the Crop Water Stress Index (CWSI) has gained recognition as an alternative irrigation decision metric. Notably, most existing sensor-based irrigation systems still neglect soil leaching requirements, limiting their applicability in saline environments. In summary, the ATMOS 41 all-in-one weather station and LI-710 ET sensor demonstrate high potential for automated irrigation systems, balancing measurement precision, parameter

coverage, and operational efficiency. Both are compatible with SDI-12 communication protocols, facilitating integration with microcontroller-based platforms such as Arduino for field-deployable smart irrigation solutions.

6. Remote Sensing Approaches

Remote sensing has been extensively utilized for estimating actual crop water requirements in the context of precision irrigation [189–192]. It enables temporal and geospatial (low- to high-resolution) assessment of land surface parameters, including soil characteristics, soil moisture, canopy volume, biomass, plant architecture, water content, and actual evapotranspiration (ET_a). A diverse range of remote sensing platforms such as satellites, small unmanned aerial systems (sUAS), ground-based fixed pole systems, and mobile vehicle-mounted platforms have been deployed for these purposes. These platforms typically integrate various electronic sensors, including spectroradiometers, multispectral and hyperspectral imagers, thermal cameras, meteorological modules, and olfaction-based systems, to characterize crop status and estimate water demand.

Satellite-based systems offer low- to moderate-spatial-resolution data (~10–500 m pixel^{-1}) with extensive spatial coverage and regular temporal frequency, making them valuable for regional-scale monitoring. However, their effectiveness can be constrained by cloud cover, which limits data availability and consistency. In contrast, sUAS platforms provide on-demand, high-resolution data at field or farm scale, with the flexibility to circumvent cloud interference and acquire data at critical crop growth stages [193]. Ground-based fixed pole and mobile systems provide ultra-high-resolution observations, allowing detailed characterization of canopy and soil processes. Nonetheless, these systems are restricted by limited spatial coverage, lower throughput capacity, and increased operational complexity due to the need for human supervision in system deployment, maintenance, and data acquisition. Eventually, the choice of platform depends on the spatial and temporal resolution requirements, the operational scale, and the specific objectives of irrigation management. Studies employing these remote sensing approaches for agricultural water management are summarized in this section.

6.1. Satellite-Based

Satellite-based remote sensing platforms provide data at high spatial coverage and at regular intervals. Such data are available through open sources at moderate to low resolution (~10 m/pixel to 500 km/pixel) as well as at high resolution (0.3–5 m/pixel) for a cost. Satellite-based remote sensing platforms have been used for over two decades now to estimate actual crop water requirements towards precision irrigation. Studies along these lines are described below.

6.1.1. Energy Balance Methods

Karatas et al. [194] assessed the irrigation performance of water user associations in Turkey by applying the SEBAL model to NOAA-16 satellite imagery (1.2 km pixel^{-1} resolution). The model outputs, including potential and actual evapotranspiration, were used to derive five key irrigation performance indicators: overall consumption ratio, relative water supply, depleted water fraction, crop water deficit, and relative ET. The computed values ranged as follows: overall consumption ratio (0.59–2.26), relative water supply (0.47–1.66), depleted fraction (0.43–1.31), crop water deficit (180.5–269.5 mm month^{-1}), and relative ET (0.61–0.74). These results demonstrate the applicability of SEBAL-derived ET for evaluating irrigation performance across large spatial scales.

Veysi et al. [195] estimated the CWSI for irrigation scheduling in sugarcane fields using Landsat thermal infrared (TIR) imagery. Eight imaging campaigns were conducted throughout the growing season, concurrent with in situ canopy temperature and vegetation

water content measurements collected during satellite overpasses. The CWSI was derived using three approaches: (i) the Idso method with infrared thermometer canopy temperature data, (ii) the Idso method with satellite-based TIR data, and (iii) temperature calibration using hot and cold reference pixels within the satellite scene. Field- and satellite-based CWSI estimates exhibited moderate to strong correlation (R^2 = 0.49–0.85) and root mean square error (RMSE) of 0.10–0.29, depending on vegetation cover. These findings confirm the utility of satellite thermal data in field-scale irrigation scheduling when appropriately calibrated.

Bhatti et al. [196] implemented two complementary models for determining crop water requirements and enabling variable-rate irrigation (VRI) management in corn and soybean fields in eastern Nebraska. The first model, the Spatial ET Modeling Interface (SETMI) [197,198], integrates ET estimated via a soil–water balance approach with ET from a two-source energy balance (TSEB) framework. High-resolution PlanetScope multispectral imagery (~3 m pixel^{-1}) was used to compute the Soil Adjusted Vegetation Index (SAVI), which was then correlated with crop coefficients (K_c) derived from soil water depletion measured continuously using a neutron probe. The resulting ET from the soil–water balance model was coupled with ET derived from canopy and surface temperature data obtained via infrared thermometers mounted on center-pivot irrigation systems. Latent heat flux derived from these temperature observations was converted to actual ET. Both ET estimates were merged using a Kalman filter, allowing dynamic water balance correction and reducing model drift [199]. This hybridization enabled ET estimation even on non-imaging days, facilitating irrigation forecasting using historical meteorological inputs.

The second approach utilized the Irrigation Scheduling Supervisory Control and Data Acquisition (ISSCADA) system [200], which integrates mobile and stationary ground-based proximal thermal sensors (infrared thermometers; 8–14 μm spectral range). Mobile IRTs mounted on center pivots acquired canopy temperatures during rotation, while stationary IRTs continuously measured diurnal canopy temperature dynamics across the field. Mobile data were upscaled to minute-level field temperature estimates via reference temperature curves derived from stationary sensors. These were used to calculate instantaneous CWSI every minute, which was integrated over daylight hours (09:00–19:00 h) to trigger irrigation events based on a single CWSI threshold. Results indicated that SETMI- and ISSCADA-based irrigation management reduced water use by over 50% compared to conventional soil-based scheduling, without yield penalties.

Corbari et al. [201] developed a dynamic variable-rate irrigation system in Italy by coupling a crop–energy–water balance framework with satellite-based reflectance and temperature data. The model combined Sentinel-2A multispectral imagery (~10 m pixel^{-1}) with Sentinel-3 land surface temperature (~1 km pixel^{-1}) resampled to Landsat-8 thermal band resolution (~30 m pixel^{-1}). The modeling framework integrated the Simple Algorithm for Yield estimates (SAFY) crop growth model with the Flash-flood Event-based Spatially-distributed rainfall-runoff Transformation–Energy Water Balance (FEST-EWB) model [202]. This coupled system exchanged leaf area index (LAI) and soil moisture (SM) variables in real time—SAFY supplied LAI progression to FEST-EWB for ET computation, while FEST-EWB provided SM feedback to SAFY to model continuous crop water stress. Calibration and validation of the hydrological model enabled generation of dynamic irrigation prescription maps used in VRI systems. Field experiments on soybean demonstrated >10% water savings and >13% improvement in water productivity, without yield reduction, relative to uniform-rate irrigation.

Merlin et al. [203] advanced surface energy balance modeling by introducing a remote sensing-based multi-compartment model representing four surface conditions: non-transpiring green vegetation, bare soil, unstressed green vegetation, and senescent vegetation. The model demonstrated robustness in irrigated agroecosystems using high-resolution

solar and thermal imagery and provided the capability to incorporate microwave-derived soil moisture as an additional constraint on surface energy and water flux partitioning. Singh and Senay [204] compared the METRIC, SEBAL, SEBS, and SSEBop models for ET estimation in corn fields using Landsat imagery. All models effectively captured spatial and temporal ET variation (R^2 = 0.81), with RMSE < 0.93 mm day^{-1} and Nash–Sutcliffe efficiency > 0.80 for METRIC and SSEBop. However, SEBAL and SEBS showed systematic underestimation of daily ET due to reliance on an empirical net radiation equation, particularly when instantaneous net radiation exceeded 100 W m^{-2}. Wagle et al. [205] evaluated SEBAL, Simplified Surface Energy Balance Index (S-SEBI), METRIC, SEBS, and SSEBop for ET estimation in high-biomass sorghum, comparing model outputs to eddy covariance flux measurements. The S-SEBI model showed the best overall agreement, followed by SEBAL and SEBS, though it tended to underestimate ET under humid conditions. Conversely, METRIC tended to overestimate seasonal ET by up to 30%. These findings highlight the trade-offs among model formulations depending on vegetation structure, humidity conditions, and data availability.

6.1.2. Empirical Crop–Coefficient–Vegetation Index Approaches

Pôças et al. [206] developed a remote sensing-based method for estimating real basal crop coefficients (K_{cb}) and composite crop coefficients (K_c) from vegetation indices (VIs), termed K_{cb}–VI and K_c–VI, respectively. The K_c–VI was derived from the vegetation cover fraction coefficient and the crop coefficient for bare soil, both estimated using remotely sensed data. The approach was tested on maize, barley, and olive orchards. Additionally, a hybrid method combining K_{cb}–VI estimation with a soil evaporation coefficient derived from a soil–water balance model was introduced. Strong relationships were observed between K_{cb}–VI and K_{cb} (r = 0.73) and between K_c–VI and K_c (r = 0.71), confirming the potential of VI-based coefficients for representing crop water dynamics in diverse cropping systems. Tadesse et al. [207] evaluated satellite-derived evapotranspiration (ET) using a geospatial statistical exploration framework integrating Normalized Difference Vegetation Index (NDVI) and satellite-based precipitation estimates. Results indicated a robust correlation between satellite-derived precipitation and ET (R^2 > 0.99), while the relationship between NDVI and ET was in the range of R^2 = 0.30–0.84 across 44% of cultivated areas, demonstrating the utility of VIs for ET estimation in water-limited agroecosystems.

Park et al. [208] examined the performance of K_c-based satellite modeling for mixed cropland and forest environments using a dual K_c approach that incorporated NDVI, leaf area index (LAI), and soil moisture in two experimental cases: (1) K_c estimated using NDVI, LAI, and soil moisture and (2) K_c estimated using NDVI and LAI only. Case 1 yielded superior performance, with bias ranging from −0.012 to 0.053, RMSE = 0.144–0.172, and r = 0.463–0.800, compared to Case 2 (bias = −0.058 to 0.088, RMSE = 0.146–0.221, r = 0.434–0.788). When the K_c estimated from Case 1 was multiplied by potential evapotranspiration (ET_p) derived from MODIS data and compared to eddy covariance latent heat fluxes, actual ET biases ranged from −0.224 to 1.364 mm day^{-1} for cropland and 0.711 to 1.055 mm day^{-1} for mixed forest, with RMSE values of 1.952–2.126 mm day^{-1} (cropland) and 1.085–1.878 mm day^{-1} (forest). These findings demonstrate that including soil moisture data improves K_c-based ET modeling accuracy across heterogeneous landscapes.

Zare and Koch [209] estimated crop evapotranspiration and irrigation requirements using empirical K_c–NDVI and K_c–SAVI relationships derived from Landsat 8 reflectance imagery acquired over six satellite passes. NDVI and SAVI were computed to generate spatially distributed K_c values, which were then used to calculate ET and irrigation demand following the FAO-56 Penman–Monteith approach. Comparisons showed strong agreement

between long-term FAO-56 estimates and those derived from remote sensing, confirming the reliability of vegetation-index-based coefficients for irrigation management. Reyes-González et al. [210] applied satellite-derived vegetation indices to estimate ET_a for corn at multiple spatial scales. The study observed lower ET_a values during early growth stages and higher values during mid-season and maturity phases, consistent with crop phenology. The resulting ET_a maps demonstrated the potential of multispectral VI data for quantifying crop water use at both regional and field levels, supporting stage-specific precision irrigation strategies. Wang et al. [211] developed a coupled water–carbon–remote sensing model integrated with crop growth process simulation to estimate ET_a for maize and wheat. The model achieved RMSE values of 0.57 mm day^{-1} for winter wheat and 0.80 mm day^{-1} for maize, indicating high accuracy in capturing crop-specific ET dynamics when linking carbon assimilation and water flux processes.

Mebrie et al. [212] estimated crop coefficients (K_c) based on NDVI and analyzed the spatiotemporal variability of ET_c for wheat using combined MODIS and Sentinel-2B data. MODIS-derived ET was calibrated using the Penman–Monteith equation, while Sentinel-2B NDVI was employed for K_c estimation. The integration of these data sources yielded robust K_c and ET_a estimates, with $R^2 > 0.6$ between MODIS ETp and Penman–Monteith reference ET and $R^2 = 0.95$ between Sentinel-2B-derived NDVI and FAO K_c values. The study highlighted the advantages of combining medium- and high-resolution satellite data for accurate ET monitoring in heterogeneous agricultural fields.

Ihuoma et al. [80] compared the performance of multispectral imagery from unmanned aerial systems (UAS, 12 cm $pixel^{-1}$), PlanetScope (~3 m $pixel^{-1}$), and Sentinel-2A/B (10 m $pixel^{-1}$) for estimating actual ET. The NDVI from each platform was used to derive K_c, followed by ET estimation using the FAO-56 AquaCrop Penman–Monteith module. Sentinel-2-based ET maps were further integrated with soil moisture data to determine field-scale irrigation requirements. Mean NDVI values varied across platforms—UAS (0.87), PlanetScope (0.71), and Sentinel-2 (0.82). Strong correlations were observed between NDVI-derived K_c and satellite data ($R^2 = 0.98$ for Sentinel-2, 0.78 for PlanetScope). Sentinel-2 ET estimates closely matched AquaCrop outputs ($R^2 = 0.94$), confirming the sensor's suitability for high-resolution irrigation assessment and vegetation monitoring.

6.1.3. Google Earth Engine Cloud Computation-Based Methods

Google Earth Engine (GEE) has emerged as an advanced cloud-computation platform that integrates extensive satellite imagery catalogs with geospatial agroclimatic datasets, enabling large-scale data processing for agricultural applications [213]. GEE supports both open-source and subscription-based computations and has been widely used for estimating evapotranspiration (ET) through energy balance and empirical models. For instance, the OpenET API, deployable within GEE, computes daily, monthly, and annual ET using satellite imagery and ensemble energy balance models, including ALEXI/DisALEXI, eeMETRIC, geeSEBAL, PT-JPL, SIMS, and SSEBop [213]. OpenET relies on publicly available datasets from Landsat, Sentinel-2, GOES, and other satellites, combined with meteorological networks and crop boundary datasets. Applications include development of water budgets, sustainable water management, and groundwater resource monitoring. Using GEE and satellite imagery, Gaznayee et al. [214] evaluated center pivot irrigation performance for winter wheat, employing Sentinel-2A/2B multispectral imagery (10 m/pixel) and meteorological data. Leaf relative water content was quantified using the normalized difference moisture index (NDMI), which correlated strongly with irrigation duration, frequency, crop biomass, and water productivity. Further studies have utilized satellite-derived ET coupled with meteorological inputs to determine crop water requirements for diverse cropping systems, providing critical insights for irrigation decision-making even

when precision irrigation is not directly implemented. The GEE-based ET Flux (EEFlux) platform has also been employed for estimating ET near Mediterranean lakes, deriving crop coefficients for vineyard water footprints in central Chile, and calibrating groundwater models [215–217]. EEFlux applies the METRIC model to Landsat multispectral and thermal imagery (~30 m/pixel) to estimate ET, enabling accessible, high-resolution agro-climatic analyses. GEE, along with OpenET and EEFlux, offers scalable, high-performance tools for assessing crop water requirements and optimizing irrigation scheduling. Integration of GEE-derived ET estimates with field-level sensor networks and automated irrigation systems can enable adaptive, real-time irrigation management. Validation across diverse crops, soils, and climatic conditions is recommended to quantify uncertainties and enhance operational reliability for precision irrigation.

6.2. Small Unmanned Aerial System-Based Methods

Satellite-based multispectral and thermal imaging platforms, such as Sentinel, Landsat, and MODIS, provide spatial resolutions ranging from 10 m to 500 m pixel^{-1}, with revisit intervals of 10–16 days. Although high-orbit satellites can achieve sub-meter spatial resolutions ($\leq$0.5 m pixel^{-1}), they typically lack thermal infrared wavebands and exhibit lower temporal frequency. Moreover, cloud cover frequently limits image quality and continuity, constraining the reliability of satellite-derived irrigation estimates. The adoption of small unmanned aerial systems (UASs) has advanced substantially in precision agriculture over the past two decades, though applications in precision irrigation remain in early stages. UAS platforms offer key advantages over satellite imagery, including on-demand and high-spatial-resolution data acquisition (up to millimeter-level detail), minimal cloud interference, and enhanced flexibility for localized monitoring [218]. UAS-based multispectral and thermal imagery has been widely utilized to support irrigation scheduling through derivation of canopy temperature, CWSI, vegetation water content (VWC), and ET_a using surface energy balance, K_c/K_{cb}–VI, and water balance models (Table A3, [80,195,196,208,214,219–228]).

A high-resolution remote-sensing-based soil–water balance model was developed by Thorp et al. [219] to quantify seasonal crop water use across eight cotton cultivars under four irrigation treatments. UAS-derived multispectral imagery was used to estimate canopy fraction for calculating ET, achieving a root mean square error (RMSE) < 5% when compared with measured ET. The derived seasonal crop coefficients were found suitable for precision irrigation scheduling. Similarly, Park et al. [229] estimated instantaneous ET in peach orchards using UAS-based multispectral and thermal imagery with a two-source energy balance (TSEB) model. Tree-level analytical ET maps were generated through canopy segmentation and temperature–leaf area index (LAI) analyses, achieving strong correlation with measured transpiration (R^2 = 0.89). In a related application, García-Vásquez et al. [221] employed UAS-based thermal imagery with a modified SSEBop model to estimate real-time ET and irrigation efficiency in a flood-irrigated pecan orchard. The monthly RMSE between estimated ET and applied water was 8.78 mm, and irrigation efficiency was 74%, closely matching reference estimates (76%). Zhang et al. [222] utilized UAS multispectral and thermal data to estimate maize ET using a refined dual crop coefficient (FAO-56 [82]). The water stress coefficient was derived from CWSI and canopy temperature, while NDVI, SAVI, and EVI were used to compute basal crop coefficients. Combined estimates of basal and stress coefficients yielded ET with R^2 = 0.84 and RMSE = 0.50 mm day^{-1}, with the NDVI–CWSI combination providing optimal results. Mndela et al. [223] demonstrated empirical relationships between UAS-based vegetation indices and relative water content (RWC) across multiple crops. GNDVI showed strong correlations for sweet potato, corn,

sugar beans, and Florida mustard (R^2 = 0.95–1.00), NDVI for Solanum retroflexum, bell pepper, and cabbage (R^2 = 0.95–1.00), and NDRE for peas and green beans (R^2 = 0.96–0.97).

Peng et al. [224] applied a Priestley–Taylor-based TSEB (TSEB-P) model using UAS-derived thermal and multispectral imagery to estimate transpiration, ET, and irrigation demand in potato under differential irrigation treatments. The estimated transpiration exhibited strong agreement with sap-flux-based measurements (R^2 = 0.80). A related development, the Precision Irrigation Soil Moisture Mapper [225], utilized UAS thermal and multispectral data to estimate soil moisture through spatial thermal inertia modeling. VWC predictions achieved R^2 = 0.79, RMSE = 0.04, and MAE = 0.031 against time-domain reflectometry (TDR) measurements, with a ground resolution of 8.6 cm pixel^{-1}. Chandel et al. [230–232] applied UAS thermal and multispectral imagery, integrated with meteorological data, to map geospatial ET for both uniform crops (e.g., spearmint, alfalfa, potato) and heterogeneous crops (e.g., grapevine, apple) using a modified METRIC energy balance model. Model estimates showed close agreement with conventional ET methods (r = 0.64–0.91). Other notable applications include UAS thermal imagery for CWSI mapping in olive orchards [233] and canopy temperature-based water stress detection in almonds [234]. UAS-based thermal and RGB imagery have also been used to evaluate irrigation uniformity across surface, linear-move, and drip systems [235]. Thermal imagery-derived CWSI and RGB-derived Green–Red Vegetation Index (GRVI) indicated uniformities of 82.8% (pre-irrigation), 71.7% (during irrigation), and 81.6% (post-irrigation) for surface systems, compared to 34.3–51% for linear displacement irrigation and 75.5–80.6% for drip systems. These highlight aerial remote sensing to refine irrigation under varying agroclimatic conditions.

Beyond aerial platforms, ground-based remote sensing systems have also been explored for precision irrigation. Mateo-Aroca et al. [236] developed a fixed-pole imaging network that captured high-resolution RGB imagery and environmental parameters (temperature, humidity, pressure) to estimate crop coefficients and ET. The system employed Zigbee wireless communication for node-to-base data transfer, with on-site processing for irrigation scheduling. Although limited in spatial scale and high in deployment cost, such systems enable customized, automated irrigation management. Future developments may focus on low-cost mobile ground platforms capable of autonomous data collection, real-time processing, and geospatially resolved irrigation recommendations.

7. Emergence of Internet of Things (IoT)

An Internet of Things (IoT) network in precision agriculture typically comprises interconnected devices such as sensors, actuators, transceivers, and controllers that enable real-time data exchange for system automation [237]. The integration of advanced wireless communication technologies—including Bluetooth (range ≈ 10 m), Zigbee (range: 10–100 m), Wi-Fi (range: 30–100 m), and Long Range (LoRa) radio communication (range ≈ 3 km)—has substantially expanded the potential of smart irrigation systems [238]. An IoT-based irrigation architecture generally consists of four functional layers: (i) device, (ii) communication, (iii) service, and (iv) application [239,240]. The device layer comprises agroclimatic sensors, controllers, and irrigation actuators. The communication layer handles data transmission to edge or cloud servers. The service layer manages data storage, synchronization, and fusion, while the application layer provides user interfaces for data visualization, alerts, and remote irrigation control [32,238]. These systems typically incorporate soil-buried moisture sensors, microclimate sensors, or imaging sensors integrated with microcontrollers that execute irrigation scheduling commands [241]. Wired or wireless soil-buried sensors are commonly used to estimate irrigation water requirements. However, they are often limited by complex installation, susceptibility to soil-water chemistry

interference, and high maintenance costs [240,241]. Consequently, non-contact sensing approaches—such as fixed or mobile visible, multispectral, and thermal infrared cameras deployed on poles, vehicles, or small UAS platforms—have gained traction as effective alternatives to traditional invasive sensors.

IoT-based smart irrigation systems frequently integrate weather sensors with or without soil moisture probes to estimate evapotranspiration (ET) using the Penman–Monteith equation and crop coefficients [240,242]. Weather-based systems generate irrigation schedules from local meteorological or historical datasets, while soil moisture–based systems enable localized and real-time adjustments [240]. Integrated IoT frameworks combining both weather and soil data can further account for crop type, phenological stage, soil properties, infiltration rates, and environmental variability, enabling estimation of irrigation demand via conventional soil-water and energy balance models as well as modern machine learning (ML) algorithms [32,243–246].

Despite their demonstrated potential, IoT-based irrigation systems face several practical constraints. High initial investment costs are often required to deploy multiple sensor nodes across fields to capture spatial variability [239,247,248]. In addition, field maintenance and sensor calibration demand considerable effort to ensure data reliability [249]. While most systems are wireless, certain configurations still require wired connections that may impede field operations. The development of compact, energy-efficient, all-in-one micro- or nano sensors with integrated wireless communication capabilities could address these limitations and improve scalability.

IoT-enabled irrigation systems primarily base irrigation decisions on real-time soil moisture and weather data. Many systems now employ AI and ML algorithms to model crop water requirements using environmental inputs, triggering actuator-based irrigation scheduling accordingly. More advanced systems integrate multi-source datasets—including satellite imagery, weather forecasts, and historical records—to achieve spatially and temporally comprehensive irrigation control. However, IoT frameworks that rely solely on sensor data and AI models without incorporating crop–soil–water interaction models tend to exhibit reduced robustness and explainability. In contrast, hybrid systems combining agroclimatic data, physically based soil–water balance models, and AI analytics provide a more holistic and interpretable approach, often resulting in improved accuracy and operational resilience.

The increasing availability of cloud computing platforms has further enhanced the functionality of IoT-based irrigation systems. These platforms enable remote data storage, processing, visualization, and control through computers or mobile devices. Real-time alerts and notifications allow users to respond rapidly to changing field conditions, improving irrigation efficiency and decision-making. A detailed summary of recent contributions on IoT-based precision irrigation systems is presented in Table A4 [30–32,59,61,64,67,68,70,84,85,116,126,155,157,168,176,250–285].

Table A5 shows the most widely used communication technologies for smart irrigation applications that include Zigbee, Wi-Fi, LoRa, and LoRaWAN. There are several communication systems available for automated irrigation installations. The choice depends on the user's needs, the price, the area that can be covered by the sensor, the energy consumed, and the speed of data recording, among others. Table A5 also provides an overview of the strengths and weaknesses of each communication technology [24,58,275,286–291].

Multiple wireless communication protocols underpin IoT-based agricultural monitoring and automation systems, each characterized by distinct frequency bands, ranges, and operational features. Wi-Fi (IEEE 802.11) standards operate across several frequency bands. Specifically, 802.11b and 802.11g function in the 2.4 GHz band, 802.11a, 802.11n, and 802.11ac operate in the 5 GHz band, and 802.11ad extends operation to the 60 GHz

millimeter-wave band. More recent standards, including IEEE 802.11ax (Wi-Fi 6), support dual-band operation (2.4/5 GHz), and IEEE 802.11ax-6E (Wi-Fi 6E) and IEEE 802.11be (Wi-Fi 7) extend Wi-Fi operation into the 6 GHz band, enabling higher throughput, lower latency, and reduced interference in field-based data communication networks. However, these Wi-Fi networks tend to be highly expensive. Bluetooth technology operates within the 2.4 GHz Industrial, Scientific, and Medical (ISM) band and is commonly used for short-range ($\leq$10 m), low-power data transmission between proximal sensing or control nodes. LoRa (Long Range) communication functions primarily in the sub-GHz ISM bands (868 MHz in Europe, 915 MHz in North America, and 900 MHz in other regions) [292]. Its extended transmission range (up to several kilometers) and low power consumption make it suitable for distributed agricultural sensor networks where long-distance communication is required. Sigfox technology also utilizes sub-GHz frequencies, specifically 868 MHz in Europe and 902 MHz in the United States, and supports ultra-narrowband communication optimized for low-data-rate IoT applications [292]. Zigbee, another ISM-band protocol, most commonly operates at 2.4 GHz, though regional variants function at 784 MHz (China), 868 MHz (Europe), and 915 MHz (United States and Australia) [293]. Zigbee's mesh networking capability enables reliable communication among dense sensor node deployments in agricultural fields. Radio Frequency Identification (RFID) systems are categorized into four primary frequency classes [294]: (1) Low Frequency (LF): 125–134.2 kHz, with a typical passive communication range of $\leq$20 cm; (2) High Frequency (HF): 13.56 MHz, supporting passive read ranges of approximately 10 cm; (3) Ultra-High Frequency (UHF): Active operation near 433 MHz and passive operation at 860 MHz (Europe) or 915 MHz (USA), with read ranges typically $\leq$3 m; and (4) Microwave (MW): 2.4 GHz, with effective communication ranges around 3 m. Collectively, these communication technologies form the backbone of IoT infrastructure in precision agriculture. Selection depends on the intended application, desired communication range, power constraints, data throughput requirements, and environmental conditions affecting signal propagation.

8. Emergence of Artificial Intelligence for Precision Irrigation

Over the past five decades, artificial intelligence (AI) has demonstrated sustained growth through its robust applications across diverse sectors, including agriculture. In field-based crop production, AI enables data-driven decision-making in complex, multi-directional environments. The past five years (2020–2025) have seen particularly rapid progress in AI integration with automated irrigation systems, aiming to optimize water use efficiency, reduce human intervention, and enhance sustainability.

8.1. Fuzzy Logic Systems

Among the earliest AI applications in irrigation management were fuzzy logic algorithms, which emulate human reasoning for decision-making under uncertainty. Using humidity, temperature, and soil moisture measurements integrated within IoT platforms, fuzzy logic has been employed to control smart irrigation gates equipped with water-level and flow sensors in open-channel irrigation, achieving water savings of up to 70% [295]. Similarly, fuzzy logic controllers have optimized energy and water use by regulating temperature, humidity, and irrigation timing in greenhouse environments, activating control mechanisms in response to deviations from target thresholds [296].

In field applications, fuzzy systems coupled with soil moisture, solar radiation, air temperature, and humidity data have been used to regulate pump operation via microcontrollers, effectively maintaining soil moisture within the optimal range [297]. Further improvements integrated fuzzy algorithms with deep-learning-based crop health classification and weather forecasts, allowing adaptive irrigation scheduling based on rainfall

probability and vegetation condition [298]. More recent implementations combined remote sensing data with soil, weather, and environmental variables (e.g., air temperature, wind speed, soil permeability, vegetation indices, and pollution data) to estimate evapotranspiration (ET), pump runtime, irrigation efficiency, and water loss, yielding up to 70% water savings [261].

However, fuzzy logic models face challenges in constructing robust and generalizable membership functions. Their reliance on expert-defined rules introduces subjectivity and restricts scalability, especially in data-limited conditions. The absence of standardized methodologies for mapping complex input–output relationships also constrain their adaptability across variable agroecosystems.

8.2. Machine Learning and Artificial Neural Networks

Classical machine learning (ML) and artificial neural network (ANN) models have been widely adopted to enhance irrigation system performance and optimize scheduling. For example, Seyedzadeh et al. [299] evaluated emitter flow variability under varying temperature and pressure using four AI models—ANN, neuro-fuzzy sub-cluster (NF-SC), neuro-fuzzy c-means cluster (NF-FCM), and least-squares Support Vector Machine (LS-SVM)—showing improved flow control and system responsiveness. Klyushin and Tymoshenko [300] used AI to simulate water transport based on the Richards–Klute equation, enabling optimized emitter flow rates, precise irrigation timing, and reduced yield losses from system downtime.

ANN-based systems, inspired by biological neural architectures, have been extensively used due to their capacity to model nonlinear, high-dimensional data. For instance, a non-contact RGB camera-based ANN predicted loamy soil irrigation needs using soil color as an indicator of moisture status [241]. To enhance crop-specific precision, Kamyshova et al. [301] integrated crop and environmental data into a phytoindication ANN to generate real-time irrigation prescription maps for center-pivot systems, reducing spatial variability and increasing maize yields by 8.9%.

IoT-integrated ML models using environmental data such as humidity, temperature, soil moisture, and rainfall have achieved up to 98% accuracy in controlling irrigation pumps through K-nearest neighbor (KNN) and long short-term memory (LSTM) models [264]. Incorporating crop physiology and phenology data further enhances model robustness. For instance, Esmail et al. [302] coupled crop development parameters with soil and weather data to forecast irrigation needs, while Katimbo et al. [303] evaluated multiple ML algorithms—including ANN, LSTM, Random Forest (RF), CatBoost, Support Vector Machines (SVM), KNN, Multiple Linear Regression (MLR), and ensemble models—for estimating crop ET and the Crop Water Stress Index (CWSI). CatBoost achieved the highest CWSI accuracy, while stacked regression performed best for ET estimation.

Other ensemble-based algorithms have also been explored. Benhmad et al. [304] applied Gradient Boosted Trees (GBT), emphasizing the method's strong predictive capacity but also its sensitivity to hyperparameters such as tree number, learning rate, and depth, which require careful calibration to avoid overfitting. RF and Naïve Bayes (NB) methods were found most effective in a study by Kaur et al. [305], though both were sensitive to hyperparameter tuning and computationally intensive for large datasets. Oudah [306] developed an IoT-based irrigation decision system that requires further validation in diverse field environments (e.g., bare soil, orchards, vegetable beds) and would benefit from additional soil moisture and air sensors to expand data coverage.

Similarly, Tyagi et al. [307] demonstrated high performance of RF-based irrigation control using soil moisture, temperature, and relative humidity data, while Kaur et al. [305] additionally included wind and rainfall variables, highlighting their influence on irrigation

accuracy. Integrating these factors into a framework could enhance prediction reliability. Field-scale validation across crop types (vegetable, cereal, and tree crops) remains critical for assessing the system's generalizability. Gaitán et al. [279] also noted the need for real condition testing to validate proposed systems. Liu et al. [282] developed a scalable IoT architecture but identified challenges in maintaining performance and energy efficiency in large deployments with thousands of sensor nodes. Addressing these issues will require advanced energy-harvesting mechanisms and efficient routing algorithms tailored for dense networks. Additionally, while GSM-based communication offers cost benefits, it may limit applicability in regions with weak coverage; alternative technologies such as LoRa or satellite networks should be explored to improve system versatility. Comprehensive field validation remains essential for assessing practical applicability and identifying optimization opportunities.

8.3. Deep Learning Approaches

Deep learning (DL) architectures, such as convolutional neural networks (CNNs) and recurrent neural networks (RNNs), have emerged as advanced alternatives to classical ML, offering automatic feature extraction and superior generalization across diverse datasets. A CNN-based DL system was developed to estimate soil moisture classes and irrigation timing using soil imagery, crop coefficients, and irrigation system parameters, achieving a 32.75% improvement in water productivity [308]. Similarly, an LSTM-based DL model using time-series data of soil moisture, temperature, relative humidity, pH, and light intensity accurately predicted irrigation schedules, resulting in 88% water savings and improved germination compared with manual irrigation [309].

Nonetheless, DL approaches are constrained by high computational costs, extensive data requirements, and limited interpretability due to their "black box" nature. Environmental variability and resource scarcity may further limit their robustness. Additionally, cloud-based DL deployments can experience latency in actuation due to delayed communication with irrigation controllers, an issue mitigable by edge computing nodes that enable real-time processing and on-site decision-making [310].

AI-based irrigation systems ranging from rule-based fuzzy controllers to advanced deep learning frameworks have shown substantial potential to improve water-use efficiency, system autonomy, and crop productivity. However, challenges persist regarding data heterogeneity, interpretability, computational demand, and real-world validation. Hybrid approaches that integrate sensor fusion, physics-based crop–soil–water models, and interpretable AI architectures are recommended to enhance reliability and scalability. The incorporation of edge–cloud collaborative architectures, standardized data protocols, and adaptive communication networks will further facilitate real-time, site-specific precision irrigation management. Recent studies that deployed AI and ML for smart irrigation management are summarized in Table A6.

9. Energy Efficiency in Irrigation Management

The transition toward water-efficient agriculture has been accompanied by a substantial increase in energy consumption, particularly over the past decade. All irrigation systems, whether surface, sprinkler, or drip, require energy distributed along the network to extract, convey, and deliver water [311]. Global projections indicate that energy production must increase by approximately 55% by 2030 to meet anticipated demand [312,313]. This escalation stems not only from the intensification of irrigation in arid or drought-prone areas but also from the growing adoption of precision irrigation practices in humid and high-rainfall regions. Consequently, the integration of energy-efficient water management systems and components has become imperative [313,314]. Electric motors remain the

dominant power source for irrigation pumping systems. However, in developing and underdeveloped regions, access to electricity is constrained by (a) limited supply, (b) reliance on non-renewable energy sources, and (c) high per-unit energy costs [315]. These constraints impede the operation of energy-intensive irrigation systems, hindering modernization and scalability [316]. Thus, the deployment of renewable and decentralized energy solutions is critical to support sustainable irrigation expansion.

Among renewable options, solar photovoltaic (PV) technology has emerged as the most widely adopted power source for smart irrigation systems. Over the past decade, rapid technological advancement and price reduction have made solar energy increasingly viable for household, agricultural, and livestock applications [317–319]. PV generators are attractive due to their portability, autonomous operation, low environmental footprint, noiseless performance, and declining cost trajectory—PV module prices halved within five years after 2010 and continue to fall [320]. Solar PV-powered irrigation has been shown to be both economically and environmentally sustainable. Beyond operational efficiency, the sustainability of energy-powered irrigation systems depends on life-cycle impacts, including manufacturing, installation, operation, maintenance, and end-of-life disposal. In addition to operational performance, several studies have explicitly evaluated the environmental and life-cycle trade-offs of different irrigation energy schemes. Comparative analyses indicate that solar photovoltaic–powered irrigation systems exhibit substantially lower life-cycle costs, greenhouse gas emissions, and human toxicity impacts than grid-supplied and diesel-powered alternatives, despite higher initial capital investment and manufacturing-phase energy burdens. For instance, solar systems can save approximately 6.6 million liters of diesel annually, reduce CO_2 emissions by 17,622 tons per year, save 41% of irrigation water, and double farmers' income compared with conventional pumping [321]. The per-unit energy cost of PV systems is estimated to be 4% lower than subsidized grid electricity and 66% lower than diesel-powered alternatives [321]. Similarly, Nikzad et al. [322] reported that PV systems exhibit operation and maintenance (O&M) costs 8.7 times lower and life-cycle costs 29.9% lower than diesel systems. Although the initial investment for off-grid PV systems may be about 2.14 times higher than conventional diesel pumps [322], their significantly lower long-term O&M costs yield favorable life-cycle economics [323]. Mérida García et al. [324] demonstrated that PV installations accounted for only 37% of the total life-cycle cost (LCC) of equivalent diesel systems and 64% of the LCC of grid-powered options when evaluated over 30 years. Despite some environmental burden during panel manufacturing, where materials contribute 29% of CO_2 emissions and 60% of total energy needs, solar PV remains markedly cleaner than fossil-based systems. For diesel-powered irrigation, fuel combustion accounts for 77% of human toxicity potential and 92–97% of other impact categories, underscoring PV's long-term sustainability advantage.

Overall, solar PV adoption not only reduces the carbon footprint but also enhances farm profitability and operational independence [321]. Owing to these benefits, numerous studies have successfully deployed PV-powered irrigation systems, including applications in both stationery and self-propelled platforms by Uddin et al. [36], Al-Ali et al. [48,61], Osroosh et al. [59], Shufian et al. [65], Ramli and Jabbar [67], Sangeetha et al. [68], Kumar et al. [70], Goumopoulos et al. [123], Krishnan et al. [124], and Abayomi-Alli et al. [166].

In addition to solar PV systems, wind energy represents another promising yet underutilized renewable source for powering intelligent irrigation systems. Global onshore wind capacity has expanded from 178 GW to 699 GW between 2010 and 2020 [325]. In the Adrar region, Bouzidi [326] found that wind-powered irrigation demonstrated superior performance and cost efficiency compared with solar PV, yielding a lower cost per cubic meter of pumped water. Wind systems also require less land area than PV arrays, cause

minimal landscape transformation relative to hydroelectric or thermal plants [327], and can significantly reduce energy production costs [328]. However, the intermittent and location-dependent nature of wind resources limits their standalone reliability for irrigation [329–331]. Integrating wind turbines into hybrid renewable systems, combining solar PV, wind, and battery storage, can mitigate these fluctuations by storing surplus energy for later use [330]. Such hybrid configurations are particularly suitable for regions experiencing seasonal variability in solar irradiance and wind availability, enhancing system reliability under diverse agroclimatic conditions. Campana et al. [332] compared solar and wind-powered irrigation systems and found that wind-based solutions are cost-competitive primarily under conditions of high wind speeds and low solar irradiance, whereas PV-based systems ensure more consistent irrigation supply. With the increasing deployment of IoT-enabled irrigation systems, the demand for energy to power sensors, controllers, communication modules, and data processing units has grown substantially. In such scenarios, solar PV has emerged as the preferred renewable energy source due to its scalability, ease of integration, and consistent daytime availability [333].

Overall, the shift toward renewable energy-based irrigation is vital for achieving long-term water–energy–food nexus sustainability. Among the available technologies, solar PV systems currently offer the most mature, cost-effective, and scalable solution, with substantial evidence supporting their environmental and economic advantages. Wind energy and hybrid systems provide complementary benefits and should be evaluated based on site-specific resource availability. Future work should focus on (a) developing hybrid solar–wind–battery configurations optimized for agricultural load profiles; (b) improving energy storage and power management algorithms for IoT-integrated systems; (c) and performing life-cycle assessments that capture both environmental and socioeconomic impacts. Such approaches will enhance the resilience and affordability of renewable-powered irrigation systems across diverse agroecological settings.

10. Limitations and Futuristic Opportunities for Precision Irrigation Also in the Context of Industry/Society 5.0

Smart irrigation systems primarily rely on real-time monitoring or forecasting of soil and climatic parameters to determine irrigation timing and quantities. Existing research has utilized diverse approaches including soil moisture and field capacity measurements, soil water and energy balance models, empirically derived crop coefficients, and reference evapotranspiration (ET) to estimate crop water requirements. However, most studies have overlooked the influence of soil salinity and the additional water required for leaching salts from the root zone. Salinity can reduce crop yields by up to 58% [334], which can significantly constrain the performance of current precision irrigation frameworks, particularly in arid and semi-arid regions. Incorporating leaching water components into existing irrigation algorithms could therefore improve both efficiency and robustness. Determining leaching water requirements necessitates accurate information on soil salinity (typically calibrated using electrical conductivity) and irrigation water salinity. Spatial patterns of soil salinity can be modeled using hyperspectral, advanced multispectral, and radar-based remote sensing data, while in-line salinity sensors can monitor irrigation water quality in real time. Equations used for computing leaching water requirements are detailed in Section 3. In addition, soil organic matter (SOM) often neglected in irrigation models plays a critical role in soil water retention. A 1% increase in SOM can enhance the soil's water-holding capacity by approximately 1.5% of its water weight [335], improving irrigation efficiency and promoting optimal crop growth. Quantification of SOM can be achieved via in situ sensors, remote sensing indices, or periodic soil datasets from repositories such as the Web Soil Survey and SoilGrids.org.

While recent advances increasingly combine remote sensing, IoT, and machine learning to support automated irrigation decision-making, their practical integration into robust decision support systems remains limited. Many reviewed studies rely predominantly on either in situ sensor data or remote sensing products, with limited operational fusion across spatial and temporal scales. Satellite-based observations often suffer from coarse spatial resolution, revisit constraints, cloud contamination, and data latency, which can restrict their direct use for real-time irrigation control. However, UAV- and airborne-based sensing mitigates spatial resolution limitations while introducing constraints related to flight frequency, operational cost, and scalability. Machine learning models developed for irrigation scheduling frequently exhibit strong performance under site-specific conditions but face challenges in generalization across crops, soil types, climatic regimes, and management practices. Limited availability of long-term, high-quality labeled datasets further constrains model transferability and robustness. In addition, most AI-driven approaches remain offline or semi-automated, with decision outputs not fully integrated into closed-loop irrigation control or farmer-oriented decision support interfaces. Real-time implementation poses additional challenges related to data transmission reliability, computational requirements, and synchronization between sensing, analytics, and actuation layers. These limitations highlight the need for tighter coupling between remote sensing products, edge or cloud-based analytics, and decision support systems capable of operating under data uncertainty and infrastructural constraints.

Building on these limitations, although numerous studies have developed algorithms for irrigation requirement estimation, field-level implementation of such precision irrigation systems remains limited. In practice, long-term field testing is frequently omitted due to high deployment and maintenance costs, logistical challenges in managing large sensor networks over multiple seasons, lack of dedicated experimental farms, and the difficulty of controlling environmental variability under real-world agricultural conditions. With advances in remote sensing, IoT, edge and cloud computing, and AI-driven decision tools, seamless integration among sensing, computation, and actuation modules into operational irrigation systems is now achievable. An optimized system architecture could involve high-resolution thermal and multispectral remote sensing platforms equipped with onboard edge-computing and API-enabled wireless communication for near real-time ET, salinity, and SOM estimation. Complementarily, a distributed grid of IoT-enabled in situ sensing nodes integrating soil moisture, salinity, SOM, ET, and microclimatic sensors could refine remote sensing-derived products. Continuous irrigation water salinity monitoring via inline sensors would enhance feedback control. For effective automation, latency-free data exchange and interoperability among all system components are essential. Each node should support SDI-12 communication protocols to ensure compatibility with microcontrollers capable of wireless data acquisition and local storage. Data from field sensors can be transmitted through LoRaWAN, Wi-Fi, or TV White Space technologies to a central base station or cloud-based server. Depending on the system's scale and computational demand, data processing may occur at the edge using single-board computers such as NVIDIA Jetson, Raspberry Pi, or Arduino or in the cloud, using platforms like Google Cloud, MATLAB ThingSpeak, AWS, or Microsoft Azure. The choice between microcontrollers, edge devices, and cloud platforms reflects trade-offs among cost, computational capacity, latency, and scalability. Microcontrollers such as Arduino are well suited for distributed field sensing and control due to their low cost, minimal power requirements, and reliable real-time response, but they lack the computational resources needed for advanced analytics. Edge devices such as NVIDIA Jetson provide substantially higher processing capability, enabling on-site image processing and machine learning inference with low latency while reducing data transmission demands, though at higher cost and power consumption. Cloud plat-

forms offer virtually unlimited storage and computing resources, making them ideal for large-scale data aggregation, multi-year analysis, and training computationally intensive models; however, they introduce recurring operational costs, higher latency, and reliance on network connectivity. Consequently, a hybrid architecture that integrates microcontrollers for data acquisition, edge devices for real-time analytics, and cloud platforms for centralized storage and model development offers a balanced and scalable solution for precision agriculture and IoT systems (Figure 10).

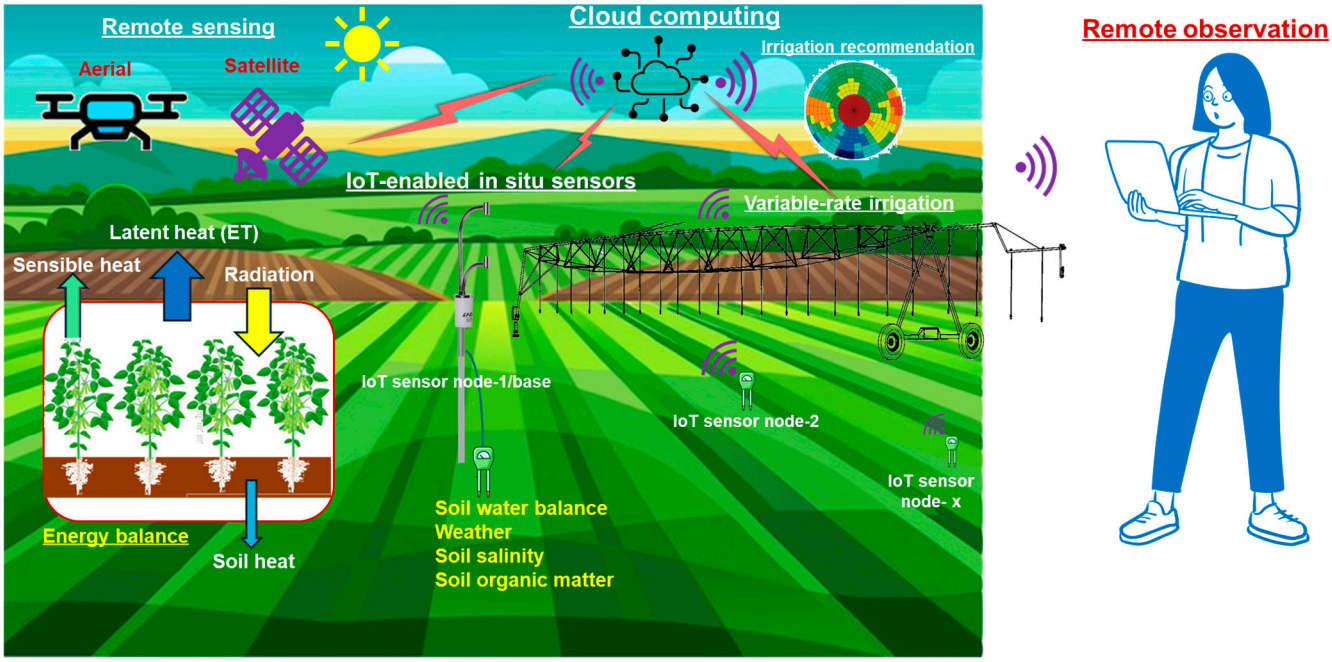


Figure 10. Futuristic approach for designing an integrated automated irrigation system for efficiency, sustainability, and human quality of life.

The analytical workflow would combine energy balance models with remote sensing and local weather data to compute actual ET, while empirical or machine learning (ML) models estimate soil salinity and SOM. Outputs can be cross-validated and refined using in situ measurements. Subsequently, a water balance model integrated with AI-based forecasting can generate irrigation schedules that adapt to both current and predicted climatic conditions. These schedules would be dynamically adjusted for spatial salinity and SOM variability to achieve site-specific precision. The final irrigation prescription maps can be transmitted to controllers equipped with single-board computers and variable-rate irrigation (VRI) mechanisms, enabling automated control of drip lines, sectional nozzles, or mobile irrigation systems. A conceptual schematic of this envisioned architecture is presented in Figure 10. An important operational challenge remains the interpolation of irrigation water requirements during remote sensing data gaps, which can be mitigated through AI-based temporal modeling and sensor-driven predictive calibration.

Despite substantial technological advancement in smart and automated irrigation systems, widespread adoption in real agricultural settings remains limited. This misalignment is not solely attributable to technical constraints but rather to a combination of economic, social, operational, institutional, and user-centric barriers. These challenges are particularly pronounced in developing regions, where limited access to reliable electricity, digital infrastructure, technical training, and financial resources constrain the adoption of advanced smart irrigation technologies, despite their demonstrated potential benefits. Many advanced systems require high initial capital investment, skilled operation, and regular maintenance, which can limit uptake among smallholder and resource-constrained farmers.

In addition, complex system architectures, limited user-friendly interfaces, and insufficient localization of calibration parameters (e.g., crop type, soil condition, and agroclimatic context) reduce practical usability.

Institutional and policy-related challenges further constrain deployment, including limited access to financing mechanisms, lack of standardized guidelines for system evaluation, and insufficient extension support to translate research prototypes into operational tools. To bridge this gap, future smart irrigation systems should prioritize simplified and modular system designs, localized calibration frameworks, and intuitive decision support interfaces tailored to end-user capacity. Policy support in the form of targeted subsidies, incentive schemes for renewable-powered irrigation, and integration with farmer cooperatives and agricultural extension services can further enhance adoption by enabling localized training, participatory system calibration, and sustained technical support beyond pilot deployments. Aligning technological innovation with socioeconomic realities and operational constraints is therefore critical for transitioning smart irrigation systems from experimental deployments to scalable, field-ready solutions. Within these contexts, precision irrigation is undergoing a paradigm shift from static, rule-based automation toward intelligent, adaptive decision support systems aligned with the principles of Industry 5.0 and Society 5.0. Future irrigation systems will move beyond maximizing water use efficiency alone to support farm resilience, environmental sustainability, and farmer agency through the seamless integration of sensing, analytics, and connectivity. This transformation is essential for addressing increasing climate variability, water scarcity, and the need for socially responsible agricultural intensification.

Within the Industry 5.0 framework, next-generation precision irrigation systems will be explicitly designed around a farmer-in-the-loop model, where AI augments human expertise rather than replacing it. Advanced ML models will synthesize multi-modal data streams including soil moisture, crop physiological indicators, microclimate conditions, and management history to generate irrigation recommendations that are both timely and context aware. Critically, these recommendations are supported by explainable AI mechanisms that communicate the key drivers behind each decision, such as soil water deficits, predicted crop stress, or short-term weather forecasts. By making model behavior transparent and interpretable, these systems foster farmer trust, enable informed decision-making, and reduce barriers to adoption.

In the broader Society 5.0 context, human-centered precision irrigation contributes to societal goals that extend beyond individual farm productivity. Data-driven water management supports water conservation, reduces environmental externalities, and strengthens climate resilience of food systems. At the same time, the use of scalable, modular, and cost-effective technologies promotes equitable access to advanced irrigation tools for diverse farming systems, including smallholder and resource-limited operations. By prioritizing transparency, trust, and human agency, future precision irrigation systems can serve as a model for responsible AI deployment in agriculture balancing technological innovation with social and environmental stewardship.

The economic feasibility of an integrated, futuristic precision irrigation framework hinges on its ability to deliver measurable value while remaining accessible, scalable, and resilient across diverse farming systems. Economic viability is not defined solely by technological sophistication but also by how effectively digital systems augment farmer decision-making, reduce input costs, and mitigate production risk under increasing climate and market uncertainty. At the field level, the use of low-cost sensing platforms and modular hardware architecture significantly lowers initial capital investment. Distributed soil and microclimate sensors, combined with simple control units, enable incremental deployment rather than large upfront system installation. This staged adoption model

allows producers to align investment with farm size, crop value, and water scarcity pressures, improving return on investment (ROI) and reducing financial risk, particularly for small and medium-scale operations. Edge computing further enhances economic feasibility by reducing dependence on continuous high-bandwidth data transmission and cloud compute resources. Local processing of high-frequency sensor data and imagery minimizes recurring data transfer and storage costs while enabling timely irrigation decisions that directly translate into water, energy, and labor savings. By avoiding overirrigation and reducing pumping requirements, such systems can generate immediate operational cost reductions, especially in energy-intensive irrigation systems. Cloud platforms do play a complementary economic role by supporting shared infrastructure for data storage, model training, and system-wide optimization. When leveraged strategically such as for periodic model updates rather than continuous real-time processing, cloud-based analytics benefit from economies of scale, distributing computational costs across users and regions. This hybrid edge–cloud approach aligns with Industry 5.0 principles by balancing efficiency with resilience, ensuring that system functionality is maintained even under connectivity constraints. Economic feasibility also encompasses broader value creation beyond individual farm profitability. Improved water-use efficiency reduces long-term resource depletion and regulatory risk, while enhanced climate resilience lowers yield variability and income volatility. Transparent, explainable AI-driven recommendations build farmer trust and reduce the learning curve associated with advanced technologies, increasing adoption rates and shortening payback periods. Moreover, interoperable and open system architectures prevent vendor lock-in, preserving farmer autonomy and fostering competitive technology ecosystems that drive down costs over time.

Collectively, these factors position integrated precision irrigation frameworks as economically viable pathways toward sustainable intensification. By combining incremental investment, reduced operational costs, shared computational infrastructure, and risk-aware decision support, futuristic precision irrigation systems can transition from experimental prototypes to scalable, cost-effective solutions that deliver both private economic returns and public societal benefits.

11. Conclusions

Automated irrigation systems have evolved remarkably since their initial introduction in 1967, when they were first used to simply switch surface irrigation systems ON and OFF. Over time, their objectives have remained consistent to deliver the right amount of water, at the right frequency and location, minimizing waste while supporting crop productivity. The broader goals of these systems are equally critical: reducing human intervention and labor, conserving water amid increasing scarcity, addressing land-use limitations, mitigating climatic uncertainties, and advancing agricultural sustainability. Despite substantial progress in developed countries, the pace of adoption in developing and underdeveloped regions remains limited due to infrastructure, cost, and technical barriers.

While in situ sensors offer reliable, high-frequency data on soil moisture, temperature, or microclimate, their spatial representativeness is inherently restricted. Conversely, remote sensing technologies from satellites and small UASs to ground-based mobile platforms enable field- to plant-scale insights into crop water requirements through energy and water balance modeling or crop-coefficient-based approaches. However, most studies have investigated these technologies in isolation, without establishing the full feedback loop between data acquisition, processing, and irrigation actuation. Bridging these gaps through the integration of multimodal sensing, AI-driven analytics, and automated control remains a key frontier in achieving true precision irrigation.

A next-generation precision irrigation system would seamlessly combine real-time remote sensing, IoT-based in situ monitoring, cloud and edge computing, and intelligent actuation. Such a system can dynamically compute and deliver irrigation schedules using energy balance, soil–water balance, or machine learning models, refined through ground-based data. The inclusion of soil salinity and organic matter content often neglected in current studies can substantially enhance system robustness and water-use efficiency. Accounting for salinity is vital, as it can reduce crop yields by up to 58%, and incorporating leaching requirements based on soil and irrigation water conductivity would ensure sustainable soil health. Likewise, a 1% increase in soil organic matter can enhance soil-water storage capacity by up to 1.5 times, directly influencing irrigation needs. Quantifying these parameters through hyperspectral and radar-based remote sensing, in situ sensors, or soil databases could enable data-driven correction of irrigation prescriptions.

Communication and computation form the core of next-generation precision irrigation systems. Low-power, long-range networks such as LoRaWAN, Wi-Fi, and TV White Space enable connectivity across distributed sensor grids, while edge computing platforms (e.g., NVIDIA Jetson, Raspberry Pi, Arduino) support low-latency, on-site data processing. Cloud-based infrastructures (e.g., AWS, Google Cloud, Azure) further facilitate large-scale data storage, model training, and automated decision execution. However, several computational challenges remain unresolved, including real-time fusion of heterogeneous data streams (remote sensing, in situ sensors, and weather forecasts), scalable processing across thousands of sensor nodes, and synchronization between sensing, analytics, and irrigation actuation.

Energy efficiency and scalability remain persistent challenges. Large-scale agricultural deployments involving thousands of nodes must balance data accuracy, transmission efficiency, and energy recovery. Solutions may involve integrating energy-harvesting technologies, adaptive routing algorithms, and hybrid communication infrastructures. Furthermore, validation under real-world conditions across diverse cropping systems including vegetables, cereals, and trees will be crucial to refine model generalization and system resilience.

In conclusion, precision irrigation is transitioning from data collection and standalone estimation toward computationally driven, closed-loop automation. The fusion of remote and proximal sensing, AI-driven modeling, and intelligent actuation enhanced by salinity and organic matter considerations marks a decisive step toward sustainable, energy-efficient, and self-adaptive irrigation ecosystems. Future research in precision irrigation must prioritize computational approaches that are not only technically advanced but also human-centered, resilient, and sustainable. Key research directions include the following: (i) the development of robust multimodal data fusion frameworks that integrate satellite, UAV, and in situ observations across spatial and temporal scales to provide context-aware insights rather than isolated measurements; (ii) machine learning models designed for transferability and fairness, capable of generalizing across diverse crops, soils, climates, and management practices while minimizing site-specific bias; (iii) uncertainty-aware and adaptive decision algorithms that explicitly quantify human confidence, remain reliable under sensor noise and data gaps, and transparently communicate risk to support informed farmer decision-making; (iv) intelligent edge–cloud orchestration strategies that balance latency, energy consumption, and computational load to ensure timely, efficient, and resilient operation under variable connectivity; and (v) interoperable, open decision-support architectures that enable closed-loop irrigation control while preserving farmer oversight and system transparency. Addressing these together with agronomic and environmental considerations such as soil salinity dynamics, organic matter preservation, energy efficiency, and real-world deployment constraints is essential for transitioning precision irrigation

from experimental and site-specific implementations toward scalable, trustworthy, and economically viable solutions that support sustainable food systems and societal well-being as water scarcity intensifies and climatic unpredictability grows.

Author Contributions: Conceptualization, A.S., A.K.C., L.D., Y.M.S., and A.K.T.; methodology, A.S., A.K.C., L.D., and A.M.; investigation, A.S.; writing—original draft preparation, A.S.; writing—review and editing A.S., A.K.C., L.D., Y.M.S., A.K.T., S.H., and A.M.; supervision, A.K.C. and Y.M.S. All authors have read and agreed to the published version of the manuscript and have contributed substantially to the work reported.

Funding: This work is partially supported by the USDA-NIFA NAPDC, project award no. USDA-NIFA 2023-77039-41033; USDA-NIFA hatch projects VA-643 160181, VA-136412, VA-136438, and VA-136452; and faculty startup funds from Virginia Tech College of Agriculture and Life Sciences. Aminata Sarr would like to thank the Regional Scholarship and Innovation Fund/Partnership in Applied Sciences, Engineering and Technology (Rsif/PASET) for support towards completing a part of her PhD at Virginia Tech, USA.

Data Availability Statement: The original contributions presented in this study are included in the article. Further inquiries can be directed to the corresponding author.

Acknowledgments: We would like to thank Ajay Maurya for his initial feedback on this study. Any opinions, findings, conclusions, or recommendations expressed in this publication are those of the authors and should not be construed to represent any official USDA or U.S. Government determination or policy.

Conflicts of Interest: The authors declare that they have no conflicts of interest.

Appendix A Evidence Tables Supporting Precision Irrigation Technologies Synthesis

Table A1. Summary of different automatic irrigation systems developed and deployed.

Sensor Network (Sensor, Operating Range, Accuracy, Power)	Data Handling and Processing Components	Data Communication Unit	Irrigation Type and Automation Components	Energy Source And Type of Test	Irrigation Requirements/Scheduling Determination	Test Crop/Impact on Water Use or/and Crop Yield	Reference
• Air temperature (LM-35, −55–150 °C, ±¼ – ±¾ °C, 4 to 30 V) • Relative humidity (SY-HS-220, 20 to 95%, ±5%, 5 V) • Soil moisture	• Microcontroller PIC 18F458 (CAN bus, In-built ADC): manages data and controls irriga-tion automation • Display (LCD)	• 3 nodes (2 sensing and 1 receiver) with each having sensors, Zigbee device, and microcontroller • Zigbee facilitates data transmission between nodes	• Motor Pump • Relay • Drip irrigation	• Type of energy used not given • Field test	• Monitoring and controlling soil moisture, relative humidity, and air temperature to detect the threshold value of the crop • Buzzer signals to switch ON/OFF motor	• Wheat, rice, sorghum, pearl millet • Short-term test to validate proper system operation	[58]
• Air temperature (109, CampbellScientific, −50 – 70 °C, ±0.6 °C) • Infrared Thermometers (IRT/c.2: Type J, Exergen, −45 – 650 °C, ±0.01 °C), • Relative humidity, temperature, solar radiation, wind speed (local weather station)	• CR10(X) datalogger with 900 MHz spread-spectrum radio, connected to a laptop computer • Control computer with graphical user interface (GUI) developed in VB.Net to collect sensor and weather data for processing and scheduling irrigation	• 900 MHz spread-spectrum radio transmits data and receives control signal to/from the control computer	• Drip irrigation • Lateral lines controlled using Solenoid valves based on the signals	• Batteries and photovoltaic solar energy (10 W solar panel) • Field test	• The graphical interface collected data from sensor nodes and real time weather data from the Web, ran the adaptive irrigation algorithm and automatically scheduled irrigation • Adaptive crop water stress index (CWSI) algorithm: (i) no irrigation if the index has a declining trend, (ii) stop irrigation after several successive irrigation events exceeding the soil's water retention capacity if the index does not decline, and (iii) no irrigation if evaporation is too low	• Apple trees • Long-term test: 2013 growing season • CWSI treatment had lower mean soil water deficit than neutron probe (NP) treatment with $p < 0.05$	[59]
• Soil moisture (YL-69, 3.3 to 5 V)	• Node with Arduino Uno (clock rate of 16 MHz) directly connected for computing irrigation requirements and irrigation actuation • ThingSpeak cloud displays current water sprinkler status	• GSM-GPRS SIM900A Modem facilitates data transmission from Arduino to ThingSpeak cloud server	• Motor • Sprinklers	• Energy used not given • Field test	• Set a threshold value from which irrigation starts, depending on soil type • Sprinklers are activated when the sensors detect a moisture level below the threshold • Avoid overirrigation by stopping the sprinklers as soon as the sensor reading is 100%	• Crop not given • Short-term test to validate proper system operation	[60]

Table A1. *Cont.*

Sensor Network (Sensor, Operating Range, Accuracy, Power)	Data Handling and Processing Components	Data Communication Unit	Irrigation Type and Automation Components	Energy Source And Type of Test	Irrigation Requirements/Scheduling Determination	Test Crop/Impact on Water Use or/and Crop Yield	Reference
• Air temperature sensor • Relative humidity • Soil moisture sensors	• MyRIO (clock rate of 40 MHz clock) composed of dual core ARM® Cortex™-A9 real-time processor and Artix-7 field programmable gate array • MyRIO: connect float switches, sensors, and charge controller	• Digital and analog inputs on the controller interface with the float switches and sensors	• Bilge pump: Bilge pump is submerged and extracts water into the underground to stores it in the tank • Diaphragm pump: pumps water from the reservoir to irrigate crops • Drip pipe	• Photovoltaic solar energy (100 W PV solar panel) • Buck converter of 12 V to 5 V: steps down the 12 V supply voltage from the charge controller to 5 V • Relay board of 5 V: connect the diaphragm pump and a bilge pump • Laboratory test	• Smart irrigation system uses a control algorithm based on fuzzy logic • Raw sensor values converted into linguistic terms and membership functions created accordingly • Relative humidity, temperature, and soil moisture values taken as inputs and membership functions created using linguistics terms • Four linguistic terms for temperature (very hot, hot, cold, and very cold), three for relative humidity (high, medium, and low), and three for soil moisture (high, medium, and low) • Fuzzy output values created and defuzzified into real outputs for controlling the diaphragm pump by switching it on or off	• Crop not given • Short-term test to validate proper system operation	[61]
• Irradiance • Pressure meter • Soil moisture	• Database (commercial database accessible by TCP/IP connection and Structured Query Language (SQL) server and open database consisted of relational tables and implemented in MATLAB™, using SQL server): collect data • Irrigation controller: controls all process of all irrigation system elements through its database • Middleware and GUI RESSIM: collects climatic data from open websites and manages the entire PV irrigation systems • Weather stations platform: allows to collect agroclimatic data	• Real-time Smart Solar Irrigation Manager (RESSIM): connect smart PV irrigation management, database, field sensing, agroclimatic information, irrigation control, and GUI	• Pump • Electro valves • Emitter • Hydrant	• Photovoltaic solar energy • Field test	• Daily crop irrigation requirement, calculated from evapotranspiration and precipitation data and crop data • Daily soil–water balance calculated by considering the soil as a water storage reservoir • If the water in the soil is sufficient to make up the irrigation deficit after verification, there is no irrigation, and if not, the next day's irrigation time is increased to compensate for the irrigation deficit	• Olive trees • Long-term test to validate proper system operation	[31]

Table A1. *Cont.*

Sensor Network (Sensor, Operating Range, Accuracy, Power)	Data Handling and Processing Components	Data Communication Unit	Irrigation Type and Automation Components	Energy Source And Type of Test	Irrigation Requirements/Scheduling Determination	Test Crop/Impact on Water Use or/and Crop Yield	Reference
• Air temperature and relative humidity (DHT) • Soil moisture	• Arduino board: type not specified • Cloud (Adafruit IO): upload the data, display real-time data online, and connect the system to internet	• Node MCU	• Pump • Solenoid valve • Irrigation system not given during this test: emitter	• Photovoltaic solar energy • Charge controller: deliver power to the Arduino for charge the battery • Buck converter of 12 V to 5 V: connected to Arduino • Laboratory test	• Fuzzy logic code is written and uploaded to the Arduino, which is connected to the solenoid value • Input values are collected from sensors (soil moisture, air temperature, and humidity sensors), and output is assigned to the solenoid valve. • Valve opens only when current is applied to solenoid. Four functions are used for air temperature (very hot, hot, cold, and very cold) and three for relative humidity and soil moisture (high, medium, and low) • Output value "True" means that the solenoid valve is supplied with power and the crops are irrigated, and "False" means that the solenoid valve is not powered and the valve is kept closed.	• Summer crop • Short-term test to validate proper system operation	[62]
• Air temperature and relative humidity (DHT11, 0–50 °C, ±2 °C for temperature and 20–90%, ±5 %RH for relative humidity, 3.5–5.5 V) • Soil moisture (0–45%, ±4%, 3–5 V) • Precipitation (rain detector, 0–300 mm/h, ±2%, 3.5–5 V)	• ARM 7 Microcontroller (clock rate of 1 MHz to 25 MHz)	• GSM module to transmit data to farmers in mobile	• Pump motor • Drip irrigated	• Energy used not specified • Field test	• Pump starts and stops depending on soil moisture and the occurrence or absence of rain • Irrigation stops when the threshold is reached	• Paddy field • Tomato • Water savings of 42% compared with manual flood irrigation and 14% compared with manual drip irrigation	[63]

Table A1. *Cont.*

Sensor Network (Sensor, Operating Range, Accuracy, Power)	Data Handling and Processing Components	Data Communication Unit	Irrigation Type and Automation Components	Energy Source And Type of Test	Irrigation Requirements/Scheduling Determination	Test Crop/Impact on Water Use or/and Crop Yield	Reference
• Air temperature (VP3, METER Group, −40 – 80 °C, ±1.0 °C, 3.5–15 V) • Soil moisture (10HS, METER Group, 0–57%, ±3%, 3–15 V)	• Datalogger (CR800 model): records sensors and command irrigation valves • CR Basic: implements the functionalities of the irrigation automation	• 3 G modem MTX-3 G-JAVA: allows Remote communication • Multiplexer AM16/32: Connected to the datalogger to increase the number of sensor channels • Relay LR4: allows the datalogger open and close the irrigation valves • IRRIX: sends the irrigation doses of each sector to the datalogger • API PackBus SDK: ensures communication between the IRRIX server and the datalogger	• Pump • Solenoid valve • Drip irrigation	• Not given • Field test	• Web application queries the datalogger for new sensor data and once a day (at 02:30 GMT), IRRIX sends the irrigation requirements for each sector to the datalogger, for the new day • During the day, at the scheduled time (8:00 AM), the datalogger starts irrigation and ends when it has measured the programmed irrigation requirement • Crop water requirements calculated using water balance method, and sensor data used to empirically adjust irrigation doses for each sector	• Apple trees • In the large-tree zone, the amount of water applied was similar to that applied during manual irrigation • In the small-tree zone, the proposed system applied an average of 25.4% and 24% less water compared to the large-tree zone and manual irrigation, respectively	[64]
• Dynamic water above and below ground surface (HCSR04 Ultrasonic sensor)	• Arduino Uno (clock rate of 16 MHz) • LCD display monitoring and online monitoring (ThingSpeak) • ThingSpeak cloud	• ESP8266 Wi-Fi Module: control automated online monitoring to collect sensor feedback	• Motor and pump • Relay • Surface irrigation	• Photovoltaic solar energy (60 W solar panel) • Voltage controller • Buck converter • Battery (12 V lead acid battery) • Field test	• The ultrasonic sensor detects and measures the water level in the rice plot • If the water level reaches the water depletion threshold, • Arduino sends a signal to automatically turn on the pump to irrigate the plot • If the water level reaches the maximum, Arduino sends a signal to stop the pump	• Rice • Can save up to 30% of irrigation water	[65]
• Soil moisture (V1.2, ±2%, 3.3–5.5 V) • Ultrasonic sensor (JSN-SR04T JSN-SR04T-2.0)	• Arduino Nano V3.0 microcontroller (clock rate of 16 MHz) • Ultrasonic sensor to protect the gate from being struck by the ground when closing and the top when opening	• LoRa HPD Tek HPD13A1.1V to transmit soil moisture readings to the gate • GSM Module Simcom for cloud server connection	• Aluminum automatic check gate • DC motor/actuator • Surface irrigation	• Photovoltaic solar energy (10 W solar panel) • Battery (12 V battery) • Field test	• Gate is opened and closed according to the minimum and maximum soil moisture thresholds set in the system	• Bare soil conditions • Application efficiency improved by 86.6%	[66]

Table A1. *Cont.*

Sensor Network (Sensor, Operating Range, Accuracy, Power)	Data Handling and Processing Components	Data Communication Unit	Irrigation Type and Automation Components	Energy Source And Type of Test	Irrigation Requirements/Scheduling Determination	Test Crop/Impact on Water Use or/and Crop Yield	Reference
• Moisture (FC-28, 3.3 5 V) • Air temperature and humidity (DHT11, 0–50 °C, ±2 °C for temperature and 20–90%, ±5%RH for relative humidity, 3.5–5.5 V)	• NodeMCU ESP8266 Microcontroller (clock rate of 80 MHz) • Blynk mobile application: save collected data and controls pump operation	• Node MCU: also ensures communication between sensors and Blynk IoT cloud server • Graphical User Interface: Remotely monitor the conditions in the farm	• Pump • Relay • Micro-irrigation (pipe with multinozzles)	• Photovoltaic solar energy (two 50 W PV panel) • Charge controller • Field test	• Irrigation is based on data from soil moisture, relative humidity, and air temperature sensors • If data reaches predefined thresholds, the pump is automatically activated, and irrigation is triggered	• Crop not specified • Test to validate proper system operation	[67]
• Humidity and temperature (DHT11, 0–50 °C, ±2 °C for temperature and 20–90%, ±5%RH for relative humidity, 3.5–5.5 V) • Pressure (BMP280, 300–1100, ±1 hPa, 3–3.3 V) • Soil moisture (YL-69, 3.3–5 V)	• Node MCU (ESP 8266, clock rate of 80 MHz) Microcontroller • Resistor: decrease flow of current, modify signal power, separate amperage, bias active ingredients, and break transmission lines	• Node MCU	• Pump • Relay • Transistor (BC548) • Sprinkler irrigation	• Photovoltaic solar energy • Laboratory test	• A server manages data such as air temperature, relative humidity, and soil moisture • When 30% of the total accessible soil moisture is consumed, the moisture sensors start to irrigate	• Crop not specified • Test to validate proper system operation	[68]
• Soil moisture (Watermark 200SS-5, 0–239 kPa, ±3%, 2.5–5 V) • Water pressure	• Vinduino board (clock rate of 16 MHz) • IoT server: The Things Network or Things Stack • All Things Talk: to store and display data and control the valves	• LoRaWAN gateway	• Solenoid valve • Drip irrigation	• Photovoltaic solar energy • Battery (5000 mAh LiPo battery) • Field test	• Irrigation is triggered based on soil moisture threshold	• Tomato • Use of watermark 200SS-5 thresholds of −40 kPa resulted in water savings of 30.6% and a yield close to the FAO56 ET method • Use of watermark 200SS-5 thresholds of −60 kPa resulted in water savings of 3.4 compared to the FAO56-ET method with a yield increase of 15.2%	[69]

Table A1. *Cont.*

Sensor Network (Sensor, Operating Range, Accuracy, Power)	Data Handling and Processing Components	Data Communication Unit	Irrigation Type and Automation Components	Energy Source And Type of Test	Irrigation Requirements/Scheduling Determination	Test Crop/Impact on Water Use or/and Crop Yield	Reference
• Moisture sensors (V2.0, 3.3–5 V) • Soil temperature (DS18B20, −55 to 125 °C, ±5%, 3–5.5 V) • Air temperature and humidity (DHT11, 0–50 °C, ±2 °C for temperature and 20–90%, ±5% RH for relative humidity, 3.5–5.5 V)	• ESP-32 (clock rate of 80 MHz to 240 MHz) • Microcontroller: process different algorithm	• ESP8266 Wi-Fi Module sends data recorded by the sensors to an IoT platform (ThingSpeak) wirelessly	• Pump • Solenoid valve • Drip irrigation	• Photovoltaic solar energy (10 W PV panel) • Field test	• Solenoid valves and pump are activated by real-time soil moisture data • Solenoid valves are activated, and irrigation starts based on a soil moisture sensor's threshold value	• Sweet corn • Proposed system applying capacity saves 11% water compared with the ETc method, with a 12.05% increase in yield	[70]
• Soil moisture • Air temperature and humidity (DHT11, 0–50 °C, ±2 °C for temperature and 20–90%, ±5%RH for relative humidity, 3.5–5.5 V)	• Arduino Nano Microcontroller (clock rate of 16 MHz)	• GPRS based, and Zigbee-based WSNs • NI CompactRIO Controller • Cloud-based IoT Platform	• Pump • Smart Relay • Drip irrigation	• Photovoltaic solar energy lithium-ion • Battery (batteries with capacity of 3.3 kWh) • Field test	• The system starts and stops depending on the maximum and minimum threshold values of soil moisture and the weather forecast • If there is an 80% probability of rain within the next 3 h, then the maximum threshold is adjusted anticipating rainfall and minimizing water use • If there is less than an 80% probability of rain, then the system checks if the soil moisture is below the minimum threshold to start irrigation	• Crop not specified	[71]
• Soil moisture (resistive soil moisture) • Air temperature and humidity (DHT11, 0–50 °C, ±2 °C for temperature and 20–90%, ±5%RH for relative humidity, 3.5–5.5 V)	• Arduino Uno R3 (clock rate of 16 MHz) • ESP8266	• Arduino IoT Cloud and Blynk, • AdaFruit IO	• Motor pump • Relay • Drip irrigation	• Photovoltaic solar energy (85 W PV panel) • Battery (12 V battery) • Laboratory test	• Irrigation is triggered based on soil moisture threshold	• Test on bare soil to validate proper system operation	[72]
• Water level	• AVR ATmega 16 Microcontroller (clock rate of 16 MHz)	• 433 MHz RF transmitter-receiver • HT12E IC to convert parallel data into a serial signal for transmission • HT12D IC to convert the serial signal back into parallel data	• Motor • Electrical switches	• Photovoltaic solar energy (5 W PV panel) • Field test	• Comparison between threshold value and water level measured by sensor	• Rice • Irrigation water productivity increased by 3.09 kg/ha/mm • Water savings of 36%	[73]

Table A1. *Cont.*

Sensor Network (Sensor, Operating Range, Accuracy, Power)	Data Handling and Processing Components	Data Communication Unit	Irrigation Type and Automation Components	Energy Source And Type of Test	Irrigation Requirements/Scheduling Determination	Test Crop/Impact on Water Use or/and Crop Yield	Reference
• Soil moisture	• NodeMCU ESP8266 (clock rate of 80 MHz)	• NodeMCU ESP8266 • Cloud servers: think blynk application	• DC 3–6 V Mini Submersible Pump • Motor	• Lawnmower's electrical power • Battery (12 V battery) • Laboratory test	• The motor is controlled by the microcontroller depending on soil moisture • Through a mobile application, farmers are able to send feedback to the controller	• Test on bare soil to validate proper system operation	[74]
• Air pressure, air temperature, humidity, precipitation, wind speed, solar radiation (mini-weather station in remote area) • Soil water potential (EQ15)	• JN5139 wireless microprocessor module	• Zigbee wireless sensor network	• Drip irrigation • Control valve	• Mains power • Photovoltaic solar energy • Field test	• Irrigation time calculated based on evapotranspiration and soil water potential using fuzzy logic • Five linguistic variables are used and are named very small, small, medium, large, and very large	• Crop not specified • Water savings of 36%	[75]
• Soil moisture (V1.2, 3.3–5 V) • Air temperature and humidity (DHT22, −40–80 °C, ±0.5 °C for temperature and 0–100%, ±2–5%RH for relative humidity, 3.5–5.5 V)	• NodeMCU ESP8266 (clock rate of 80 MHz)	• NodeMCU ESP8266 • Raspberry Pi 4 for pump control • Message Queuing Telemetry Transport (MQTT) protocol	• Relay • Motor pump	• Photovoltaic solar energy (20 W PV panel) • Battery (12 V DC lead-acid battery) • Laboratory test	• The pump is activated based on a soil moisture threshold set at 45% for the purposes of this study	• Crop not specified • Test to validate proper system operation	[76]
• Soil moisture (V2.0, 3.3.-5) • Air temperature (DS18B20, −55 to 125 °C, ±5%, 3–5.5 V and bias of −0.9 °C) • Humidity (DHT22, −40–80 °C, ±0.5 °C for temperature and 0–100%, ±2–5% RH for relative humidity, 3.5–5.5 V and bias of –0.2%)	• NodeMCU ESP8266 (clock rate of 80 MHz)	• NodeMCU ESP8266 • Cloud servers: think blynk application and ThingSpeak platform	• Relay module • Pump	• Type of energy not specified • Daily energy Consumption of the system 24 Wh • Field test	• Relay module activates when the pump soil moisture is below 60%, which is the moisture threshold	• Crop not specified	[77]

Table A2. Case studies of crop evapotranspiration estimation using satellite-based remote sensing and energy balance models.

Authors	Methods	Climatic Conditions or Location	Crop	Results
[94]	• METRIC algorithm	Saudi Arabia	Alfalfa	• A 6.6% overestimation of hourly ET and a 4.2% underestimation of daily ET compared to eddy covariance method
[95]	• METRIC algorithm	Western region of the state of Bahia, Brazil	Soybeans	• Good agreement between ETa EEFlux and ETa FAO method based on the d-index (0.83–0.89) • Slightly underestimate ETa
[106]	• METRIC algorithm	St. John, WA, and Genesee, ID, USA	Spring wheat, winter pea, and winter wheat rainfed conditions	• EEFlux ET overestimation during crop senescence
[107]	• Operational Simplified Surface Energy Balance (SSEBop)	New Delhi, India	Maize and wheat	• Compared with the Bowen Ratio Energy Balance (BREB) method, the SSEBop gave an R^2 of 0.76, a d-index of 0.92, and a root mean square error of 0.48 mm/day
[89]	• METRIC algorithm • QWaterModel • Surface Energy Balance System (SEBS) model	Southern Italy near the Tyrrhenian Sea	Rotational irrigated field: maize, fennel, ryegrass-clover	Compared to the eddy covariance measurement method: • METRIC-EEFlux achieved an R^2 of 0.65, RMSE of 1.13 mm/day, mean percentage error (MPE) of 10.7%, and mean bias error (MBE) of 0.34 • SEBS obtained an R^2 of 0.58, RMSE of 0.71 mm/day, MBE of −0.05, and MPE of 10.3% • QWaterModel yielded an R^2 of 0.09, RMSE of 2.65 mm/day, and MPE of 14%
[108]	• METRIC algorithm	Southern California's Imperial Valley/ hot and dry climate	Alfalfa and sugar beet	• For alfalfa, the mean square error was 1.22 mm/day and the mean absolute error was 1.19 mm/day when comparing the EEFlux method with the FAO-56 method • For sugar beet, the mean square error was 1.5 to 3.3 mm/day, and the mean absolute error was 1.3 to 2.7 mm/day

Table A2. *Cont.*

Authors	Methods	Climatic Conditions or Location	Crop	Results
[109]	• METRIC algorithm • Surface Energy Balance Algorithm for Land (SEBAL)	Markazi province, Central part of Iran	Maize	• METRIC-EEFLux evapotranspiration was 7.71% higher than SEBAL Performance was evaluated by comparison with a lysimeter • For the EEFLux method, the RMSE was 0.711, Nash–Sutcliffe coefficient of efficiency (NSE) was 0.807, percent bias error (PBIAS) was 7.398 and R^2 was 0.885 • For the SEBAL method, RMSE was 1.046, NSE was 0.582, PBIAS was 15.080 and R^2 was 0.793
[110]	• METRIC algorithm • Atmosphere–Land Exchange Inverse/Disaggregation of the Atmosphere–Land Exchange Inverse (ALEXI/DisALEXI) • Surface Energy Balance Algorithm for Land using Google Earth Engine (geeSEBAL) • Priestley–Taylor Jet Propulsion Laboratory (PT-JPL) • Satellite Irrigation Management Support (SIMS) • Operational Simplified Surface Energy Balance (SSEBop)	Northern New Mexico	Maize	• The average percentage error between 2017 and 2022 is −2.58% for eeMETRIC, −13.01% for SSEBop, −7.74% for SIMS, −24.87% for PT-JPL, −13.92% for DisALEXI, and −10.86% for geeSEBAL • Average MBE between 2017 and 2022 is −0.11 mm/day for eeMETRIC, −0.55 mm/day for SSEBop, −0.33 mm/day for SIMS, −1.06 mm/day for PT-JPL, −0.59 mm/day for DisALEXI, and −0.46 mm/day for geeSEBAL • Average RMSE between 2017 and 2022 is 1.25 mm/day for eeMETRIC, 1.41 mm/day for SSEBop, 1.24 mm/day for SIMS, 1.70 mm/day for PT-JPL, 1.60 mm/day for DisALEXI, and 1.52 mm/day for geeSEBAL
[111]	• Modified Priestley–Taylor (MPT) model	Udham Singh Nagar district of Uttarakhand, India	Chickpea	• Estimation of evapotranspiration using the MPT model compared with the lysimeter yielded an R^2 of 0.71, a mean biased error of 0.04 mm/day, a root mean square error of 0.62 mm/day, and an agreement index of 0.914

Table A2. *Cont.*

Authors	Methods	Climatic Conditions or Location	Crop	Results
[112]	• CropSyst-W model • METRIC algorithm • OpenET	Texas, USA	Maize	• Compared with the lysimeter method, the CropSyst-W, METRIC algorithm, and OpenET models for estimating evapotranspiration yielded average normalized root mean square deviations of 0.31, 0.47, and 0.32, respectively

Table A3. Data processing methods deployed with small UAS and satellite-based imagery for estimating crop water use.

Methods	Data Processing Techniques	Crops Considered	Study Area	Sources
UAS	• Thermal camera (Optris PI 450 LightWeight infrared camera, Irvine, CA, USA) • Fixed-wing UAV (Q300, QuestUAV, Northumberland, UK) • Flight altitude of 90 m • Use of SkyCircuits Ground Control Station software SC2 • Use of TSEB (two-source energy balance) model (TSEB-PT: PT for Priestley–Taylor) and a dual-temperature difference (DTD)	Barley	Denmark	[233]
	• ImperX Bobcat B8430 digital cameras (Boca Raton, FL, USA) and thermal imagery (ThermaCAM SC640, Wilsonville, OR, USA) • Variation of flight height between 240 m and 480 m • Resolution for thermal camera varied between 0.38 and 0.66 • Resolution for multispectral camera varied between 0.05 and 0.1 • Use of two-source energy balance (TSEB) model and Deriving Atmosphere Turbulent Transport Useful To Dummies Using Temperature (DATTUTDUT) model	Vineyard	California, USA	[234]
	• Octocopter (MikroKopter OktoXL, Moormerland, Germany) • Compact digital camera (Samsung ES80, Seoul, South Korea) and thermal imager (Optris Pi 400, Irvine, CA, USA) • Flight altitude of 25 m • Use of one-source energy balance model (OSEB) and two-source energy balance model (TSEB)	Grassland	Luxembourg	[235]

Table A3. *Cont.*

Methods	Data Processing Techniques	Crops Considered	Study Area	Sources
UAS	• Five-band multispectral camera aboard a custom-built hexacopter or a four-band multispectral camera • Fixed-wing drone (eBee, SenseFly, Cheseaux-sur-Lausanne, Switzerland) • 80% image overlap along flight paths • Flight altitude of 75 m • Use of commercial photogrammetry software: Pix4DMapperPro, Pix4D S.A., Lausanne, Switzerland • Estimation of fractional vegetation (fc) cover from drone measurements and use of fc for basal crop coefficient calculation, which is used in ETc calculation	Cotton	Arizona, USA	[219]
	• Multispectral and thermal cameras • Flight altitude of 450 m • 0.15 m pixel resolution in the visible and near-infrared bands and 0.60 m resolution in the thermal infrared • TSEB-PT use of and DTD	Vineyard	California, USA	[236]
	• A thermal infrared camera and multispectral camera integrated with five bands with a GPS in an onboard CPU for geo-tagging • Flight altitude of 90 m • 80% forward overlap and 40% side overlap • Radiometric calibration target for TIR and MS images and ground control point (GCP) and ground artificial feature (GAF) for image processing • Use of high-resolution mapping of evapotranspiration (HRMET) model	Peach and nectarine	Tatura, Victoria, Australia	[208]
	• Thermal sensor • Flight altitude of 70–80 m • Modified Simplified Surface Energy Balance (SSEBop) model	Orchard	New Mexico, USA	[221]
	• Micasense RedEdge multispectral camera (Seattle, WA, USA) • Resolution of the camera of 1280 mm × 960 mm • Drone2Map extension of the ArcGIS 8.1 software package • Use of spectral values of NDVI, GNDVI, NDRE, and OSAVI were set as predictor variables (x), and the crop water content was set as the dependent variable (y)	Crop diversification and crop rotation with a variety of crops	South Africa	[223]

Table A3. *Cont.*

Methods	Data Processing Techniques	Crops Considered	Study Area	Sources
UAS	• Thermal camera Tau 2 encompassing a single 7.5–13.5 µm broadband channel with 19 mm focal length • RGB camera Zenmuse X3 (Nanshan, Shenzhen, China) • Flight altitude of 60 m • Thermal data obtained and saved as video, and images extracted from the video frame by ThermoViewer ver. 2.1.7 (Wilnsdorf, Germany) and mosaicked by Agisoft Metashape ver. 1.6.4 (St. Petersburg, Russia) • RGB camera Zenmuse X3 images processed by Pix4Dmapper with the "Ag RGB" template • Use of Priestley–Taylor Equation (TSEB-PT)	Potato	Denmark	[224]
	• Multispectral with 5 bands and thermal cameras • 85% front and side image overlaps • Flight altitude of 60 m for thermal and 70 m multispectral images • Pix4Dmapper software was used to mosaic and orthorectify the UAS RGB, multispectral, and thermal images • Use of stress coefficient applied with NDVI, SAVI, and EVI to evaluate based crop coefficient values	Maize	Zhaojun Town, China	[222]
	• Micasense RedEdgeTM camera (Seattle, WA, USA) • FLIR Vue Pro R • Flight altitude of 70 m • 80% vertical and horizontal photo overlap • Use of Pix4DMapperPr	Trees	North central Texas, USA	[224]
Satellite	• Landsat 8 satellite images • Use of split-window (SW) algorithm to retrieve LST from Landsat 8 TIR bands	Sugarcane	Southwest of Iran	[195]
	• Satellite imagery from Sentinel-2A and 2B • Multispectral imagery from PlanetScope • NDVI calculated for all multispectral images with ArcMap • Crop evapotranspiration is estimated from satellite images using the empirical relationship between NDVI and Kc	Tomato	Ontario, Canada	[80]
	• IRTs mounted on stationary posts for canopy temperature • PlanetScope satellite multispectral imager • Use of red and near-infrared bands of the multispectral imagery to compute the Soil Adjusted Vegetation Index (SAVI) • Spatial Evapotranspiration Modeling Interface (SETMI) model	Maize and soybean	Nebraska, USA	[196]

Table A3. *Cont.*

Methods	Data Processing Techniques	Crops Considered	Study Area	Sources
Satellite	• Sentinel-2 A/B • Sentinelsat Python API ver. 0.4.1 used to get data for the study area and time period of interest, subsequently preprocessed in Google Earth Engine (GEE) to acquire surface reflectance values • Resampling of data to a standardized spatial resolution of 10 m, masking of clouds and cloud shadows using the SCL band, and application of a correction to the bidirectional reflectance distribution function • Extraction of individual tiles based on their geographic coordinates and zoom level using the GEE platform function ee.data.getTileUrl • Import GeoTIFF format into QGIS	Wheat	North Erbil, Iraq	[214]

Table A4. Systems that have deployed agroclimatic sensors, Internet of Things, and real-time data processing for irrigation management.

Input Parameters	Communication Protocol	Irrigation Scheduling Method (RS, S, IWRM)	Contribution	Authors
T, RH, U2, G, P, M	Wireless sensor network, ECHERP	S and IWRM	• Proposal of a system that takes into account historical data and changing weather values to calculate the amount of water required for irrigation in automated irrigation systems	[250]
T, RH, U2, G, M	900 MHz spread spectrum radio	S and IWRM	• Development and evaluation of an adaptive CWSI-based irrigation algorithm with a dynamic threshold (CWSI-DT) to maintain the trees in a well-watered condition and to avoid over irrigation mainly due to erroneous irrigation signals on cool and humid days, caused by temporary weather conditions, and canopy growth	[59]

Table A4. *Cont.*

Input Parameters	Communication Protocol	Irrigation Scheduling Method (RS, S, IWRM)	Contribution	Authors
T, RH, U2, G, P, M	N/A	S and IWRM	• Implementation of long-term memory network models (LSTM) for soil moisture prediction • The models generate a one-day prediction of volumetric water content, based on previous measurements of soil moisture, precipitation, and climate data	[251]
T, RH, G, M	• Zigbee for real-time sensor data collection • Wi-Fi to control the relay switch connected to the pump and to collect weather information available online	S	• Implementation of a new soil moisture forecasting algorithm, based on machine learning techniques applied to weather prediction and sensor node data	[30]
T, RH, M	Wi-Fi	S	• Development of a system in which sensing and controlling drip irrigation are handled by a single microcontroller-based system that utilizes a fuzzy-logic algorithm for decision-making and control • Use solar cells to handle the temporary loss of power supplied by the utility company • Development of a wireless monitoring system interface, which can allow a remote user to remotely monitor the status of a farm from the convenience of a mobile phone or a computer.	[61]
T, RH, U2, G, P, M	Wired internet	RS and IWRM	• Development of a system for operative irrigation water management based on the coupling of remote sensing data, distributed water-energy hydrological model, and meteorological forecasts	[252]

Table A4. *Cont.*

Input Parameters	Communication Protocol	Irrigation Scheduling Method (RS, S, IWRM)	Contribution	Authors
M	N/A	S	• Calibration of the YL-69 sensor and comparing its accuracy with two commercial ECH2O probes	[253]
T, RH, U2, G, P, M	Internet	S and IWRM	• Development of a new middleware called Real-time Smart Solar Irrigation Manager (RESSIM), which processes data collected from the irrigation controller and weather web platforms to control the operation of a smart photovoltaic irrigation system in real time	[31]
T, RH, U2, G, P, M	nRF24L01 (single-chip radio transceiver for 2.4 to 2.5 GHz) Internet	S and IWRM	• Implementation of the Smart & Green framework to offer smart irrigation services, such as data monitoring, fusion, storage, pre-processing, synchronization, and irrigation management improved by predicted soil humidity • Development of a forecasting model for estimating matrix potential using meteorological data in fields without soil moisture sensors • Application of the predicted matric potential approach to estimate the moisture used in an irrigation management scheme using the an Genutchen model	[32]
T, M	Internet	S and IWRM	• Demonstrate the feasibility of automated scheduling irrigation in orchards, where, in practice, size and structure of the canopy can be a common source of variation. The trial looked at how the automated system behaved on sectors with different tree vigor and whether, with identical configuration, it was able to provide differential irrigation according to the differences in tree vigor.	[64]

Table A4. *Cont.*

Input Parameters	Communication Protocol	Irrigation Scheduling Method (RS, S, IWRM)	Contribution	Authors
T, RH, G	Internet	RS	• Estimating potential evapotranspiration using the ECOsystem Spaceborne Thermal Radiometer Experiment on Space Station (ECOSTRESS)	[254]
T, RH, U2, P, M	Internet	S and IWRM	• Implementation of an integrated modeling approach based on the linking of an automated irrigation system with IrrigWeb. The approach offers scope for including closed-loop feedback to apply the right amount of water at the right time • Design of an Uplink program to connect WiSA to IrrigWeb to allow effortless irrigation record keeping and data importing • Development of downlink program to perform efficient irrigation scheduling to WiSA through IrrigWeb	[255]
T, RH, M, water level	Ethernet /Wi-Fi	S and IWRM	• Implementation of an automated real-time irrigation controller based on fuzzy inference and implemented in LabVIEW. The system uses data from soil moisture, air temperature, and water level sensors to schedule irrigation according to soil–water balance, weather conditions, crop growth stage, and water and energy availability, with communication provided by the GSM/GPRS module	[256]
T, RH, M	nRF24L01 Wi-Fi	S	• Implementing a mesh network of wireless sensors and actuators as an alternative method to collect and measure environmental parameters in smart irrigation systems • Mesh network manages the addition and subtraction of sensor nodes, enabling self-rearrangements of the latter to adapt the system to changes in the network	[257]

Table A4. *Cont.*

Input Parameters	Communication Protocol	Irrigation Scheduling Method (RS, S, IWRM)	Contribution	Authors
S	N/A	RS	• Implementation of a new non-contact vision system based on an RGB camera to predict the irrigation requirements of loam soil based on deep learning using a feed-forward back propagation neural network	[241]
T, RH, U2, G, P, M	Zigbee	S and IWRM	• Identification and validation of the specific process dynamics for the pecan crop irrigation system • Implementation of a model-based self-triggered monitoring algorithm to minimize the communication messages number while meeting the monitoring objectives • Estimation of the energy consumption improvement in the wireless sensor nodes due to the use of this control approach in comparison with the duty-cycle periodical scheduling technique	[258]
T, RH, U2, G, P, M	Radio-transmission units	S and IWRM	• Implementation of a scalable weighing lysimeter prototype for determining the ET, using real-time soil–water balance monitoring managed by an irrigation automation protocol, which includes a soil-based irrigation scheduling protocol that calculates the correct irrigation dose based on a feedback strategy involving replenishing the water used by the plants based on changes in volumetric soil water content as a control system variable	[259]
T, RH, U2, G, M	Internet	S and IWRM	• Implementation of a fully automated subsurface irrigation system with sensor-based/time-based irrigation scheduling methods	[85]

Table A4. *Cont.*

Input Parameters	Communication Protocol	Irrigation Scheduling Method (RS, S, IWRM)	Contribution	Authors
T, RH, U2, P, M	N/A	IWRM	• Development of a Deep Q-Network for irrigation scheduling and irrigation water estimation using a long-term agent memory model that predicts the total amount of water in the soil profile the next day and another long-term agent memory model that estimates the yield as a function of environmental conditions over a season and measures the net yield	[260]
T, RH, U2, P, M, air pollution	GSM	IWRM	• Development of an automated irrigation system based on the calculation of irrigation water requirements considering soil data, climatic data, vegetation, and air pollution using fuzzy logic	[261]
Climate data (exact parameters not specified)	N/A	RS and IWRM	• Evaluation of the performance of remote sensing-based soil–water balance (RS-SWB) using FAO56 dual crop coefficient methodology to derive remote sensing-based irrigation water accounting (RS-IWA) for complete surveillance of diverse and extended irrigated surfaces	[262]
T, RH, U2, P, G, M, daytime, visibility, pressure, heat index, water flow	LoRa network	S and IWRM	• Implementation of a smart, knowledge-based irrigation system based on big data, combining historical local weather data, weather forecasts, irrigation logs, and real-time sensor data • The model examines the internal relationships between the data to form a big data fusion system for optimizing irrigation	[263]

Table A4. *Cont.*

Input Parameters	Communication Protocol	Irrigation Scheduling Method (RS, S, IWRM)	Contribution	Authors
T, RH, P, S	Wi-Fi and Bluetooth	S	• Use of an irrigation prediction approach to efficiently manage intelligent automatic irrigation. • Using the Node-RED platform, whose objective is to facilitate supervision, storage, and notification • Processing the collected data using algorithms namely: KNN, neural networks, Support Vector Machine, Naive Bayes, and Logistic	[264]
T, RH, U2, G, P, M	Edge-computing and communication	S and IWRM	• Development of a framework based on deep neural network architectures to build prediction models for soil moisture • Tackle the problem of missing data for the dataset features using data imputation, which requires filling in the values of features that are unknown (or missing) with values that ensure a desired degree of reliability	[265]
T, M	Edge-computing and wired communication	S	• Integration of soil moisture, temperature, and flow sensors with the input pins of the Arduino and the relay module connected to the water pump to collect hourly measures in the CSV file via serial communication • Implementation of a system that provides optimum irrigation by switching the pumping motor automatically through the relay module, depending on the threshold value of soil moisture and temperature	[168]
T, RH, M	Wi-Fi	S	• Proposition of a new combination of optimized intelligent smart irrigation systems to improve the energy management performance of the system	[266]

Table A4. *Cont.*

Input Parameters	Communication Protocol	Irrigation Scheduling Method (RS, S, IWRM)	Contribution	Authors
RGB images of soil	N/A	RS	• Implementation of a proximal sensing system by means of using a color camera towards smart irrigation based on computer vision and deep learning to identify water requirements of three soil texture classes under different illumination conditions	[240]
T, RH, M	Wi-Fi	S	• Design and fabrication of a cost-effective solar-powered water pump with IoT integration for the smart irrigation system	[67]
T, RH, M	Wi-Fi	S	• Development of a method that ensures an agricultural model for measuring the use of water to minimize pollutants and to create a software framework that would help farmers control soil quality and regulate the irrigation system through a digital application of some kind	[68]
S, T, RH, U2, G, P, M	N/A	S	• Proposition of machine learning (ML) good practices for data-driven soil moisture (SM) forecast and organize modeling planning steps in a reference guide for solution designers • Proposition of an alternative to solely using domain-knowledge features about evapotranspiration, crop phenology, and soil properties models as input data with an entirely data-driven approach • Evaluation of the impact of IoT data quality issues on ML-based SM forecasting and explore alternatives to deal with these issues	[267]

Table A4. *Cont.*

Input Parameters	Communication Protocol	Irrigation Scheduling Method (RS, S, IWRM)	Contribution	Authors
T, RH, P, M, water flow level	Wi-Fi	S	• Proposition of a system that can be switched into automatic and manual modes. In manual mode, the farmer gets an alert through the mobile application and can manually initiate or shut the irrigation. In automatic mode, the system controls the irrigation based on the preset soil moisture values. It estimates the threshold soil moisture value and irrigates the fields when the soil moisture is low.	[176]
T, RH, U2, G, P, M	OPC Unified Architecture	S and IWRM	• Validating a system capable of monitoring the farm's environment and monitoring and controlling an irrigation system. The solution presented in this paper presents a closed-loop monitoring and control system for irrigation based on data from the weather, soil, and crops. The soil probe is simulated with data from field tests, the weather data is collected from external services, and the irrigation system behavior is simulated in the Plat Simulation software.	[268]
T, RH, U2, G, P, M	GSM	S and IWRM	• Development of a soil moisture dynamics model in an open field agricultural system to aid model-based irrigation management for enhancement of water use efficiency in arid and semi-arid regions	[84]
M and water height	LoRaWAN	S	• Assessment of the performance of automated surface irrigation in aerobic rice cultivation in temperate Australia and control dynamic of water in rice ponds, allowing the application of strategic deep water during cold-sensitive conditions	[269]

Table A4. *Cont.*

Input Parameters	Communication Protocol	Irrigation Scheduling Method (RS, S, IWRM)	Contribution	Authors
T, RH, U2, G, P, M	LoRaWAN	S and IWRM	• Analysis and dissemination of soil moisture variability against weather data using statistical techniques • Prediction of soil moisture at multiple depths against seasonal segmentation and depths against the weather using a machine learning model	[246]
T, RH, G, M	Zigbee	S	• Design and implementation of an intelligent irrigation system that uses fuzzy logic and IoT for real-time acquisition of weather and soil data to schedule irrigation • Automatic motor deactivation based on rainfall to save electrical resources	[270]
T, RH, M	Wi-Fi	S	• Development of novel IoT-enabled smart drip irrigation system using a sensor fusion method that helps in the reduction of excess water and electricity and minimization of labor by controlling using android mobile	[116]
T, RH, U2, G, M	RavenXTA CDMA or RV50 Sierra wireless AirLink, Campbell Scientific Inc	S and IWRM	• Development of a CWSI-based IoT DSS for precision irrigation of wine grapes under semiarid conditions • Field test of the CWSI-based IoT DSS in two small acreage commercial estate vineyards over four growing seasons • Performing validation of the IoT derived CWSI values by statistical correlation with LWP and fASW at each vineyard site and evaluate vineyard	[157]

Table A4. *Cont.*

Input Parameters	Communication Protocol	Irrigation Scheduling Method (RS, S, IWRM)	Contribution	Authors
T, RH, M	Wi-Fi	S, RS	• Implementation and evaluation of an IoT-based wireless smart drip irrigation system to enhance field application efficiency. For the developed data acquisition systems, an attempt is made to determine the best location, depth, and the number of soil moisture sensors	[70]
T, RH, U2, G, P, M	GSM	S, RS and IWRM	• Evaluation of the accuracy of the yield prediction of the biophysical model and comparison of field performance of irrigation strategies: uniform irrigation and variable-rate irrigation using a fixed underlying map, soil water sensors, and Model Predictive Control	[271]
T, RH, M	Wi-Fi	S	• Use of a low-cost ESP32 microcontroller that also monitors the humidity and notifies the user when the humidity is too low or too high • Use of temperature readings to ensure that the crops are watered at the best temperature for maximum water absorption	[126]
T, RH, U2, G, P, M	Internet	S and IWRM	• Design and implementation of a decision support system through a low-cost IoT-based platform that provides irrigation management and plant protection advice to Mediterranean olive farmers. • Estimation of irrigation dose based on real-time computation, based on soil information, while weather information assists decision-making regarding plant protection	[272]

Table A4. *Cont.*

Input Parameters	Communication Protocol	Irrigation Scheduling Method (RS, S, IWRM)	Contribution	Authors
T, RH, M	Global System for Mobile (GSM)	S and IWRM	• Evaluation of smart irrigation management in maize grain cultivation and comparison with irrigation based on long-term weather statistics	[273]
M	Wi-Fi	S and IWRM	• Implementation of low-cost IoT soil moisture tensiometer prototype to compare weather-based irrigation to soil water moisture-based irrigation in terms of yield and crop water productivity	[155]
T, RH, M	NRF24L01 radio module to transmit data collected from smallholder farmers Wi-Fi	S	• Development of a new, low-cost Fog-IoT-Cloud system to store, analyze, and use vast volumes of acquired data to help smallholder farming communities (SFCs) manage the irrigation mechanism efficiently • Comparison between autoencoders (AE) and generative adversarial networks (GAN) to detect anomalies in data on environmental factors • Prediction of soil moisture, air temperature, and air humidity-based data from field sensory and weather forecast with CNN/BiLSTM architecture	[274]
T, RH, P, M	LoRa	S and IWRM	• Combining long-range technology (LoRa) wireless communication and fuzzy logic with cloud-based weather forecasting services to control irrigation and reduce water consumption in agriculture	[275]
M	LoRa to transmit sensor data to the main station Wi-Fi to transmit real-time data to the cloud and switch on the pump	S	• Design and implement a solar-powered intelligent irrigation system based on IoT for rice field that uses solar tracking to generate energy to run the pump, detecting soil moisture levels and periodically controlling the pump's operation when soil moisture is below a certain level	[276]

Table A4. *Cont.*

Input Parameters	Communication Protocol	Irrigation Scheduling Method (RS, S, IWRM)	Contribution	Authors
T, P, G, M	N/A	IWRM	• Assessing the potential of deep reinforcement learning to schedule irrigation based on variations of climate data and on water use restrictions	[277]
T, M	N/A	RS and IWRM	• Optimization of the Random Forest (RF) model using the Sparrow Search Algorithm (SSA) and the Ant Colony Optimization (ACO) algorithm, forming two new hybrid models called ACO-RF and SSA-RF that are used to predict soil moisture at different depths of the citrus orchard based on Landsat-8 and Sentinel-1 multi-temporal data, used for making large-scale intelligent irrigation decisions	[278]
T, RH, M	WebSocket	S	• Integration of artificial intelligence with highly scalable nationwide IoT networks and interactive geospatial visualization • Use of OpenAI models to schedule irrigation based on historical trends and real-time sensor data	[279]
M, T, RH	Wi-Fi	S	• Irrigation programming with a closed loop using real-time data of relative humidity, temperature, and soil moisture and historical data with predictive autoregressive model	[280]
T, RH, G, U2	N/A	S and IWRM	• Development of an automatic irrigation system based on hourly cumulative evapotranspiration • Comparison of different irrigation levels using field sensors, Korea Meteorological Administration, and virtual sensors based on a machine learning model	[281]

Table A4. *Cont.*

Input Parameters	Communication Protocol	Irrigation Scheduling Method (RS, S, IWRM)	Contribution	Authors
T, RH, M, P, evaporation rate	GSM Internet	S and IWRM	• Integration of fuzzy logic-based irrigation control to ensure adaptive and precise irrigation control, deep neural networks (DNN) to refine predictions based on environmental conditions, and energy-efficient Open Shortest Path First (OSPF) to improve network energy efficiency	[282]
M, T, RH, water level	Wi-Fi	S	• Design of an intelligent irrigation system based on the use of real-time data, using IoT, Hypertext Transfer Protocol (http), Server-Sent Event (SSE), Hypertext Markup Language (HTML), and Cascading Style Sheets (CSS) • Use of SSE protocol for automatic and continuous data updating on a user-friendly interface	[283]
M, T, RH	Wi-Fi	S	• Implementation of automated irrigation system based on IoT, embedded systems, fuzzy logic, which is used for decision-making in irrigation to adjust it dynamically according to changing environmental conditions and a cloud layer using ThingSpeak to collect and analyze data in real time via HTTP protocol	[284]
M, T, RH, P, light intensity	Wi-Fi	S	• Implementation of an IoT-based automated shed and irrigation system for opening and closing depending on moisture, precipitation, temperature, and light intensity	[285]

Table A5. Most widely used wireless communication technologies for smart irrigation systems.

Technologies	Advantages	Limitations
Bluetooth low energy (BLE)	• Low power and low cost, support an unlimited number of nodes in a star topology and has a lower connection time [24] • Communication range: 100 m [286]	• Operates in the 2.4 GHz [287] • Max data rate of 3 Mbps [286] • Low security and can lose connection during communication [288]
Bluetooth	• Low power [287,288]	• Operates in the 2.4 GHz, communication range of 10 to 20 m and data rate of 1 Mbps to 3 Mbps [287]
Zigbee	• Ultralow power consumption [24] • Low cost [58,286] • Has a flexible network structure, long battery life [288] • Communication range: 10–100 m [58,286])	• Operates in the 2.4 GHz [287] • Max data rate of 250 kbps [58,286]
Wi-Fi	• Communication range: up to 35 m for indoor applications and up to 100 m for outdoor applications [24] • Typical data rate of 54 Mbps [286] • Advanced versions offer up to 46 Gbps but are very expensive	• Operates at 2.4 GHz [287] • Latest versions (Wi-Fi 5, 6, 6E, and 7) operate at 5 GHz and 6 GHz • High cost [286]
LoRa	• Low power and can operate at 868 MHz [275]	• Communication range: Over short compared to BLE, Zigbee, and Wi-Fi: 5 in in urban areas and 15 km or more in rural areas [275] • Max data rate of 0.3 kbps to 50 kbps [287]
LoRaWAN	• Low power [24,288] • Communication range: 5 to 10 km [24,288]	• Max data rate of 0.3 kbps to 50 kbps [24]
Sigfox	• Communication range: 40 km in rural area and low power consumption [289]	• Low data rates: 100 bps [289]
6LoPWAN	• Low cost because of the low bandwidth and low power consumption [288]	• Communication range: 2–5 km in urban and 15 km in suburban and data rate of 0.3 to 50 kbps [288]
Cellular network (LTE)	• Max data rate of 100 Mbps [286,290] • Communication range: 2.5 km [286]	• Operates in 1800 MHz [286] • Very high cost and high powee [286]
Radio frequency identification (RFID)	• Max data rate of 10 Mbps [286] • Low cost and low power [286,291]	• Operates in 125 kHz [286] • Communication range: 10–20 cm [288]
Global System for Mobile (GSM)/General Packet Radio Service (GPRS)	• Communication range: 1–10 km [289]	• Licensed bands from 900 to 1800 MHz, data rate up to 170 kbps and power consumption [289]

Table A6. Recent use-cases of machine learning and artificial intelligence in smart irrigation.

Authors	Methods	Data input	Outputs	Results
[304]	• Automated irrigation method based on IoT and artificial intelligence using the Gradient Boosted Trees (GBT) algorithm	Soil moisture, air temperature, relative humidity, solar radiation, wind speed, wind direction, atmospheric pressure and rainfall	Date palm water requirements	• Reduction of water resources by 35% and increased yields by 25%
[305]	• Automated irrigation system based on IoT and ML • ML algorithms including: • K-nearest neighbor (KNN) • Naïve Bayes (NB) • Random Forest (RF) • Support Vector Machine (SVM) • Logistic regression (LR)	soil moisture, temperature, humidity, wind, rain and water level (in the dam)	Determine time to turn on or off the motor	• NB and RF models gave an estimated better accuracy of 98.8% and a root mean square error of 0.16 • LR gave accuracy of 98.3% and MSE of 1.66 • KNN has accuracy of 99.3% and MSE of 0.66 • SVM gaves accuracy of 99.5% and MSE of 0.5
[306]	• Automated irrigation system based on computer vision technology • Autonomous Raspberry Pi imaging system and color observation of the soil • Classification of soil images using the Random Forest algorithm	Soil type changes in soil color by using images	Determine when to irrigate	• Prediction accuracy of 0.921
[307]	• Integration of IoT and ML (ML) and Deep Learning (DL) models for irrigation automation • Data was processed using ML models (Random Forest Classifier, Logistic Regression, Support Vector Model, Gaussian Naïve Byes, Decision Tree Classifier, and KNeighbors) and DL models (AdaBoost Classifier, XGBoost Classifier, and MLPClassifier)	Soil moisture, air temperature, and humidity	Collecting and storing data using IoT and a cloud connection, thereby providing a model that allows calculation of optimal irrigation parameters	• Random Forest classifier performed best, with an accuracy of 94.77%
[279]	• Smart irrigation system based on the use of IoT and AI • OpenAI models to generate predictive recommendations for irrigation based on these real-time and historical data	Soil moisture, air temperature, and humidity	Adjustment of irrigation scheduling and irrigation water requirements	• 25% increase in the irrigation water use efficiency index
[281]	• Comparison between field sensors (FS), Korea Meteorological Administration (KMA), and virtual sensors based on a ML model (ML) model to calculate hourly ET and automate irrigation • Irrigation using 40%, 60%, 80%, and 100% of ETc for each case	Air temperature, humidity, wind speed, and solar radiation, relative	Irrigation automation based on cumulative hourly evapotranspiration	• Crop growth and irrigation water productivity higher in the FS and KMA treatments at 60% of ETc, with water use of 8.90 and 9.07 L/plant, respectively • Crop growth and water productivity for ML treatment were higher at 80% of ETc, with water use of 8.93 L/plant

Table A6. *Cont.*

Authors	Methods	Data input	Outputs	Results
[282]	• Deep neural networks (DNN) that refine predictions based on environmental conditions • Fuzzy inference systems (FIS) for irrigation scheduling • Energy-efficient Open Shortest Path First (OSPF) routing mechanism to optimize water use and improve network lifespan	Crop growth stage, evaporation rate, air temperature, rainfall, soil moisture, crop water requirements, and irrigation type, planting schedule, geographic location	Proposal for a sensor-based method enabling optimal irrigation and efficient information transmission through a fast fuzzy logic-based routing mechanism	• Evaluate the system's performance by comparing it with reference methods: Discrete Linear Quadratic Regulator (DLQR), Smart Precision Irrigation System (SPIS), Fuzzy Water Irrigation System (FWIS) • Proposed system has a higher number of active nodes over time • Improvement of the packet delivery rate (PDR), by 1.29% compared to the best-performing reference method

References

1. United Nations. *World Population to Reach 8 Billion on 15 November 2022*; United Nations: New York, NY, USA, 2022.
2. Dorin, B. *Agricultural Dynamics in Sub-Saharan Africa: A Perspective to 2050 on Structural Transformation Challenges*; Research Report; Centre de Sciences Humaines (CSH): New Delhi, India, 2014.
3. FAO. *The State of Food Insecurity in the World: Economic Crises—Impacts and Lessons Learned*; FAO: Rome, Italy, 2009.
4. FAO. *Save and Grow: A Policymaker's Guide to the Sustainable Intensification of Smallholder Crop Production*; FAO: Rome, Italy, 2011.
5. GIZ. *What Is Sustainable Agriculture?* GIZ: Bonn, Germany, 2016.
6. Wise, T.A. *Can We Feed the World in 2050? A Scoping Paper to Assess the Evidence*; Global Development and Environment Institute Working Paper No. 13-04; GDAE, Tufts University: Medford, MA, USA, 2013.
7. FAO. *Coping with Water Scarcity: An Action Framework for Agriculture and Food Security*; FAO: Rome, Italy, 2012.
8. Denier-Pasquier, F. *Water Management and Use in Agriculture*; Economic, Social and Environmental Council: Paris, France, 2013.
9. FAO. *The State of Food and Agriculture 2020: Overcoming Water Challenges in Agriculture*; FAO: Rome, Italy, 2020. [CrossRef]
10. Hulotet, J.F.; Pagnon, J. *Water Management in Agriculture: What Do European Recovery Plans Provide?* Institute for European Environmental Policy: Brussels, Belgium; London, UK, 2022.
11. FAO. *The State of the World's Land and Water Resources for Food and Agriculture: Managing Systems at Risk*; FAO: Rome, Italy, 2011.
12. UNESCO. *United Nations World Water Development Report 2020: Water and Climate Change*; UNESCO: Paris, France, 2020.
13. DGCID. *Prospects for Irrigated Agriculture in Sub-Saharan Africa: Cooperation Strategy for the Sustainability of Large Irrigation Schemes*; DGCID: Paris, France, 2020.
14. Jamahiriya, L.A. Water for Agriculture and Energy in Africa: Resources and Challenges in the Context of Climate Change. 2008. Available online: https://www.fao.org/4/i2345e/i2345e.pdf (accessed on 5 January 2026).
15. Mafuta, C. The Value of Green Water Management in Sub-Saharan Africa: A Review. *J. Contemp. Water Res. Educ.* **2018**, *165*, 67–75. [CrossRef]
16. FAO. *Water for Sustainable Food and Agriculture: A Report Produced for the G20 Presidency of Germany*; FAO: Rome, Italy, 2017.
17. Plusquellec, H. Is the daunting challenge of irrigation achievable? *Irrig. Drain.* **2002**, *51*, 185–198. [CrossRef]
18. Bwambale, E.; Abagale, F.K.; Anornu, G.K. Smart irrigation monitoring and control strategies for improving water use efficiency in precision agriculture: A review. *Agric. Water Manag.* **2022**, *260*, 107324. [CrossRef]
19. Gobarah, M.E.; Tawfik, M.M.; Thalooth, A.M.; El-Housini, E.A. Water conservation practices in agriculture to cope with water scarcity. *Int. J. Water Resour. Arid Environ.* **2015**, *4*, 20–29.
20. Qureshi, A.S. Water Management for Sustainable Agriculture. 2018. Available online: https://oar.icrisat.org/10959/1/Chapter-Water-Productivity-Published.pdf (accessed on 5 January 2026).
21. Pereira, L.; Paredes, P.; Jovanovic, N. Soil water balance models for determining crop water and irrigation requirements and irrigation scheduling focusing on the FAO56 method and the dual Kc approach. *Agric. Water Manag.* **2020**, *241*, 106357. [CrossRef]
22. Touil, S.; Richa, A.; Fizir, M.; Argente-García, J.; Skarmeta-Gómez, A. A review on smart irrigation management strategies and their effect on water savings and crop yield. *Irrig. Drain.* **2022**, *71*, 1396–1416. [CrossRef]
23. Ighrakpata, U.; Chouikha, M.; Ejofodomi, O.A.; Ofualagba, G. Automation of irrigation systems and design of automated irrigation systems. *Int. J. Water Resour. Manag. Irrig. Eng. Res.* **2019**, *2*, 11–27.
24. Khriji, S.; El Houssaini, D.; Kammoun, I.; Kanoun, O. Precision Irrigation: An IoT-Enabled Wireless Sensor Network for Smart Irrigation Systems. In *Women in Precision Agriculture*; Hamrita, T., Ed.; Springer: Cham, Switzerland, 2021. [CrossRef]

25. Singh, A.K.; Singh, A.K.; Bhardwaj, A.K.; Verma, C.L.; Mishra, V.K.; Arora, S.; Sharma, N.; Ojha, R.P. Automation in scheduling irrigation: A review of concepts and latest recommendations in technology. *J. Nat. Resour. Conserv. Manag.* **2021**, *2*, 47–56. [CrossRef]
26. Koech, R.; Langat, P. Improving irrigation water use efficiency: A review of advances, challenges and opportunities in the Australian context. *Water* **2018**, *10*, 1771. [CrossRef]
27. Rathika, S.; Ramesh, T.; Priyadharshini, V.; Prasanth, A.S.; Shanmugapriya, P. Automation in irrigation—A review. *Int. J. Curr. Microbiol. Appl. Sci.* **2020**, *9*, 2974–2990. [CrossRef]
28. Obaideen, K. An overview of smart irrigation systems using IoT. *Energy Nexus* **2022**, *7*, 100124. [CrossRef]
29. Zhang, S.; Wang, M.; Shi, W.; Zheng, W. Construction of intelligent water saving irrigation control system based on water balance. *IFAC Proc.* **2010**, *51*, 466–471. [CrossRef]
30. Goap, A.; Sharma, D.; Shukla, A.K.; Krishna, C.R. An IoT-based smart irrigation management system using machine learning and open-source technologies. *Comput. Electron. Agric.* **2018**, *155*, 41–49. [CrossRef]
31. Perea, R.G.; Mérida-García, A.; Fernández-García, I.; Poyato, E.C.; Montesinos, P.; Rodríguez Díaz, J.A. Middleware to operate smart photovoltaic irrigation systems in real time. *Water* **2019**, *11*, 1508. [CrossRef]
32. Campos, N.G.S.; Rocha, A.R.; Gondim, R.; Coelho da Silva, T.L.; Gomes, D.G. Smart & Green: An Internet-of-Things framework for smart irrigation. *Sensors* **2020**, *20*, 190. [CrossRef]
33. Gomathy, C.K.; Vamsikumar, A.; Karthik, B.; Purushothamreddy, A. The smart irrigation system using IoT. *Int. Res. J. Eng. Technol. (IRJET)* **2021**, *8*, 462–468.
34. Abdulaziz, W.B.; Croock, M.S. Design of smart irrigation system for vegetable farms based on efficient wireless sensor networks. *Iraqi J. Comput. Commun. Control Syst. Eng.* **2022**, *22*, 72–85. [CrossRef]
35. Mahmud, B.; Hong, G.; Bernard, F. A study of human–AI symbiosis for creative work: Recent developments and future directions in deep learning. *ACM Trans. Multimed. Comput. Commun. Appl.* **2023**, *20*, 1–21. [CrossRef]
36. Uddin, J.; Taslim Reza, S.M.; Newaz, Q.; Uddin, J.; Islam, T.; Kim, J. Automated irrigation system using solar power. In Proceedings of the 7th International Conference on Electrical and Computer Engineering, Dhaka, Bangladesh, 20–22 December 2012.
37. Gutiérrez, J.; Villa-Medina, J.F.; Nieto-Garibay, A.; Porta-Gándara, M.A. Automated irrigation system using a wireless sensor network and GPRS module. *IEEE Trans. Instrum. Meas.* **2013**, *63*, 166–176. [CrossRef]
38. Rani, M.U.; Kamalesh, S. Web-based service to monitor automatic irrigation system for the agriculture field using sensors. In Proceedings of the 2014 International Conference on Advances in Electrical Engineering (ICAEE), Vellore, India, 9–11 January 2014. [CrossRef]
39. Humpherys, A.S. Control structures for automatic surface irrigation systems. *Trans. ASAE* **1967**, *10*, 21–23. [CrossRef]
40. Humpherys, A.S. Automatic furrow irrigation systems. *Trans. ASAE* **1971**, *14*, 466–470. [CrossRef]
41. Humpherys, A.S. *Improving Farm Irrigation Systems by Automation*; International Commission on Irrigation and Drainage (ICID): New Delhi, India, 1978.
42. Phene, C.J.; Howell, T.A. Soil sensor control of high-frequency irrigation systems. *Trans. ASAE* **1984**, *27*, 392–396. [CrossRef]
43. Evett, S.R.; Howell, T.A.; Schneider, A.D.; Upchurch, D.R.; Wanjura, D.F. Canopy temperature-based automatic irrigation control. In Proceedings of the International Conference on Evapotranspiration and Irrigation Scheduling, San Antonio, TX, USA, 3–6 November 1996; pp. 207–213.
44. Bravdo, B.; Sharon, Y. A fully automated orchard irrigation system based on continuous monitoring of turgor potential with a leaf sensor. In Proceedings of the 3rd International Symposium on Sensors in Horticulture, 2001, Haifa, Israël, 17–21 August 1997; Volume 562, pp. 55–61.
45. Kuyper, M.C.; Balendonck, J. Application of dielectric soil moisture sensors for real-time automated irrigation control. In Proceedings of the 3rd International Symposium on Sensors in Horticulture, 2001, Haifa, Israël, 17–21 August 1997; Volume 562, pp. 71–79.
46. Ravina, I.; Paz, E.; Sofer, Z.; Marm, A.; Schischa, A.; Sagi, G.; Yechialy, Z.; Lev, Y. Control of clogging in drip irrigation with stored treated municipal sewage effluent. *Agric. Water Manag.* **1997**, *33*, 127–137. [CrossRef]
47. Abraham, N.; Hema, P.S.; Saritha, E.K.; Subramannian, S. Irrigation automation based on soil electrical conductivity and leaf temperature. *Agric. Water Manag.* **2000**, *45*, 145–157. [CrossRef]
48. Al-Ali, A.R.; Rehman, S.; Al-Agili, S.; Al-Omari, M.H.; Al-Fayezi, M. Usage of photovoltaics in an automated irrigation system. *Renew. Energy* **2001**, *23*, 17–26. [CrossRef]
49. Stringam, B.L.; Sauer, B.W.; Pugh, C.A. Accurate water delivery using a simplified automated farm turnout. *Irrig. Drain.* **2003**, *52*, 355–361. [CrossRef]
50. Morari, F.; Giardini, L. Irrigation automation with heterogeneous vegetation: The case of the Padova botanical garden. *Agric. Water Manag.* **2002**, *55*, 183–201. [CrossRef]
51. Nogueira, L.C.; Dukes, M.D.; Haman, D.Z.; Scholberg, J.M.; Cornejo, C. Data acquisition system and irrigation controller based on CR10X datalogger and TDR sensor. *Proc. ASAE* **2003**, *62*, 38–46.

52. Rafea, A.; Hassen, H.; Hazman, M. Automatic knowledge acquisition tool for irrigation and fertilization expert systems. *Expert Syst. Appl.* **2003**, *24*, 49–57. [CrossRef]
53. Font, L.; Kōrtösi, F.; Farkas, I. Machine vision system for water shortage indication of tomato plants using local orientation. *IFAC Proc.* **2004**, *37*, 34–39. [CrossRef]
54. Benzekri, A.; Meghriche, K.; Refoufi, L. PC-based automation of a multi-mode control for an irrigation system. In Proceedings of the International Symposium on Industrial Embedded Systems (SIES), Costa da Caparica, Portugal, 4–6 July 2007; pp. 310–315. [CrossRef]
55. Zhou, Y.; Yang, X.; Wang, L.; Ying, Y. A wireless design of low-cost irrigation system using ZigBee technology. In Proceedings of the International Conference on Network Security, Wireless Communications and Trusted Computing, Wuhan, China, 25–26 April 2009; pp. 572–575. [CrossRef]
56. Yang, G.; Liu, Y.; Zhao, L.; Cui, S.; Meng, Q.; Chen, H. Automatic irrigation system based on wireless network. In Proceedings of the IEEE International Conference on Control and Automation (ICCA), Xiamen, China, 9–11 June 2010; pp. 2120–2125. [CrossRef]
57. Ooi, S.K.; Cooley, N.; Mareels, I.; Dunn, G.; Dassanayake, K.; Saleem, K. Automation of on-farm irrigation: Horticultural case study. *IFAC Proc.* **2010**, *43*, 256–261. [CrossRef]
58. Chikankar, P.B.; Mehetre, D.; Das, S. An automatic irrigation system using ZigBee in wireless sensor network. In Proceedings of the International Conference on Pervasive Computing (ICPC), Pune, India, 8–10 January 2015.
59. Osroosh, Y.; Peters, R.T.; Campbell, C.S.; Zhang, Q. Automatic irrigation scheduling of apple trees using theoretical crop water stress index with an innovative dynamic threshold. *Comput. Electron. Agric.* **2015**, *118*, 193–203. [CrossRef]
60. Rawal, S. IoT-based smart irrigation system. *Int. J. Comput. Appl.* **2017**, *159*, 7–11. [CrossRef]
61. Al-Ali, A.R.; Al Nabulsi, A.; Mukhopadhyay, S.; Awal, M.S.; Fernandes, S.; Ailabouni, A. IoT–solar energy powered smart farm irrigation system. *J. Electron. Sci. Technol.* **2019**, *17*, 100017. [CrossRef]
62. Sudharshan, N.; Kasturi Karthik, A.V.S.; Sandeep Kiran, J.S.; Geetha, S. Renewable energy-based smart irrigation system. *Procedia Comput. Sci.* **2019**, *165*, 615–623. [CrossRef]
63. Barkunan, S.R.; Bhanumathi, V.; Balakrishnan, V. Automatic irrigation system with rainfall detection in agricultural field. *Measurement* **2020**, *156*, 107552. [CrossRef]
64. Domínguez-Niño, J.M.; Oliver-Manera, J.; Girona, J.; Casadesús, J. Differential irrigation scheduling by an automated algorithm of water balance tuned by capacitance-type soil moisture sensors. *Agric. Water Manag.* **2020**, *228*, 105880. [CrossRef]
65. Shufian, A.; Haider, M.R.; Hasibuzzaman, M. Results of a simulation to propose an automated irrigation and monitoring system in crop production using fast charging and solar charge controller. *Clean. Eng. Technol.* **2021**, *4*, 100165. [CrossRef]
66. Pramanik, M.; Khanna, M.; Singh, M.; Singh, D.K.; Sudhishri, S.; Bhatia, A.; Ranjan, R. Automation of soil moisture sensor-based basin irrigation system. *Smart Agric. Technol.* **2022**, *2*, 100032. [CrossRef]
67. Ramli, R.M.; Jabbar, W.A. Design and implementation of solar-powered IoT-enabled portable irrigation system. *Internet Things Cyber-Phys. Syst.* **2022**, *2*, 212–225. [CrossRef]
68. Sangeetha, B.P.; Kumar, N.; Ambalgi, A.P.; Haleem, S.L.A.; Thilagam, K.; Vijayakumar, P. IoT-based smart irrigation management system for environmental sustainability in India. *Sustain. Energy Technol. Assess.* **2022**, *52*, 101973. [CrossRef]
69. Zhang, H.; He, L.; Gioia, F.D.; Choi, D.; Elia, A.; Heinemann, P. LoRaWAN-based Internet of Things system for precision irrigation in plasticulture fresh-market tomato. *Smart Agric. Technol.* **2022**, *2*, 100053. [CrossRef]
70. Kumar S, V.; Singh, C.D.; Rao, K.V.R.; Kumar, M.; Rajwade, Y.A.; Babu, B.; Singh, K. Evaluation of IoT-based smart drip irrigation and ETc-based system for sweet corn. *Smart Agric. Technol.* **2023**, *5*, 100248. [CrossRef]
71. Et-taibi, B.; Abid, M.R.; Boufounas, E.-M.; Morchid, A.; Bourhnane, S.; Abu Hamed, T.; Benhaddou, D. Enhancing water management in smart agriculture: A cloud- and IoT-based smart irrigation system. *Results Eng.* **2024**, *22*, 102283. [CrossRef]
72. Borges, R.C.; Beuter, C.H.; Dourado, V.C.; Bento, M.E.C. Internet of Things application in an automated irrigation prototype powered by photovoltaic energy. *Energies* **2024**, *17*, 2219. [CrossRef]
73. Kumar, M.; Sahni, R.K.; Waghaye, A.M.; Kumar, M.; Randhe, R.D. Electronic sensor-based automated irrigation system for rice cultivated under alternate wetting and drying technique. *AgriEngineering* **2024**, *6*, 4720–4738. [CrossRef]
74. Muthuramalingam, R.; Rathnam Velu, R.; Baskar, H.; Vellan Saminathan, M.H. An IoT-based smart irrigation system. *Eng. Proc.* **2024**, *66*, 13. [CrossRef]
75. Prasad, R.; Srivastava, A.K.; Tiwari, R. Fuzzy logic-based sprinkler controller for a precision irrigation system: A case study of semi-arid regions in India. *Eng. Proc.* **2024**, *82*, 103. [CrossRef]
76. Al Mamun, M.R.; Ahmed, A.K.; Upoma, S.M.; Haque, M.; Ashik-E-Rabbani, M. IoT-enabled solar-powered smart irrigation for precision agriculture. *Smart Agric. Technol.* **2025**, *10*, 100773. [CrossRef]
77. Saputri, F.R.; Linelson, R.; Salehuddin, M.; Nor, D.M.; Ahmad, M.I. Design and development of an irrigation monitoring and control system based on Blynk Internet of Things and ThingSpeak. *PLoS ONE* **2025**, *20*, e0321250. [CrossRef]
78. Döll, P.; Siebert, S. Global modeling of irrigation water requirements. *Water Resour. Res.* **2002**, *38*, 1–10. [CrossRef]

79. Shi, J.; Wu, X.; Wang, X.; Zhang, M.; Han, L.; Zhang, W.; Liu, W.; Zuo, Q.; Wu, X.; Zhang, H.; et al. Determining threshold values for root–soil water weighted plant water deficit index-based smart irrigation. *Agric. Water Manag.* **2020**, *230*, 105979. [CrossRef]
80. Ihuoma, S.O.; Madramootoo, C.A.; Kalacska, M. Integration of satellite imagery and in situ soil moisture data for estimating irrigation water requirements. *Int. J. Appl. Earth Obs. Geoinf.* **2021**, *102*, 102396. [CrossRef]
81. Mérida García, A.; Fernández García, I.; Camacho Poyato, E.; Montesinos Barrios, P.; Rodríguez Díaz, J.A. Coupling irrigation scheduling with solar energy production in a smart irrigation management system. *J. Clean. Prod.* **2018**, *175*, 670–682. [CrossRef]
82. Allen, R.G.; Pereira, L.S.; Raes, D.; Smith, M. *Crop Evapotranspiration—Guidelines for Computing Crop Water Requirements*; FAO Irrigation and Drainage Paper No. 56; FAO: Rome, Italy, 1998.
83. Sheikh, S.S.; Javed, A.; Anas, M.; Ahmed, F. Solar-based smart irrigation system using PID controller. *IOP Conf. Ser. Mater. Sci. Eng.* **2018**, *414*, 012040. [CrossRef]
84. Bwambale, E.; Abagale, F.K.; Anornu, G.K. Data-driven modelling of soil moisture dynamics for smart irrigation scheduling. *Smart Agric. Technol.* **2023**, *5*, 100251. [CrossRef]
85. Mohammed, M.; Riad, K.; Alqahtani, N. Efficient IoT-based control for a smart subsurface irrigation system to enhance irrigation management of date palm. *Sensors* **2021**, *21*, 3942. [CrossRef]
86. McShane, R.R.; Driscoll, K.P.; Sando, R. *A Review of Surface Energy Balance Models for Estimating Actual Evapotranspiration with Remote Sensing at High Spatiotemporal Resolution over Large Extents*; U.S. Geological Survey Scientific Investigations Report 2017–5087; U.S. Geological Survey: Reston, VA, USA, 2017. [CrossRef]
87. Senay, G.B.; Budde, M.; Verdin, J.P.; Melesse, A.M. A coupled remote sensing and simplified surface energy balance approach to estimate actual evapotranspiration from irrigated fields. *Sensors* **2007**, *7*, 979–1000. [CrossRef]
88. Salgado, R.; Mateos, L. Evaluation of different methods of estimating evapotranspiration for the performance assessment of irrigation schemes. *Agric. Water Manag.* **2021**, *243*, 106450. [CrossRef]
89. Nisa, Z.; Khan, M.S.; Govind, A.; Marchetti, M.; Lasserre, B.; Magliulo, E.; Manco, A. Evaluation of SEBS, METRIC-EEFlux, and QWaterModel actual evapotranspiration for a Mediterranean cropping system in southern Italy. *Agronomy* **2021**, *11*, 345. [CrossRef]
90. Cutting, N.G.; Kaur, S.; Singh, M.C.; Sharma, N.; Mishra, A. Estimating crop evapotranspiration in data-scarce regions: A comparative analysis of eddy covariance, empirical and remote-sensing approaches. *Water Conserv. Sci. Eng.* **2024**, *9*, 65. [CrossRef]
91. Li, Y.; Peng, X.; Liu, Z.; Lu, X.; Gu, X.; Yu, L.; Xu, J.; Cai, H. A machine learning-driven semi-mechanistic model for estimating actual evapotranspiration: Integrating photosynthetic indicators with vapor pressure deficit. *Agric. Water Manag.* **2025**, *315*, 109563. [CrossRef]
92. Ragab, R.; Evans, J.G.; Battilani, A.; Solimando, D. Towards accurate estimation of crop water requirement without the crop coefficient Kc: New approach using modern technologies. *Irrig. Drain.* **2017**, *66*, 469–477. [CrossRef]
93. Dingre, S.K.; Gorantiwar, S.D. Determination of the water requirement and crop coefficient values of sugarcane by field water balance method in semiarid region. *Agric. Water Manag.* **2020**, *232*, 106042. [CrossRef]
94. Madugundu, R.; Al-Gaadi, K.A.; Tola, E.; Hassaballa, A.A.; Patil, V.C. Performance of the METRIC model in estimating evapotranspiration fluxes over an irrigated field in Saudi Arabia using Landsat-8 images. *Hydrol. Earth Syst. Sci.* **2017**, *21*, 6135–6151. [CrossRef]
95. Venancio, L.P.; Eugenio, F.C.; Filgueiras, R.; da Cunha, F.F.; dos Santos, R.A.; Ribeiro, W.R.; Mantovani, E.C. Mapping within-field variability of soybean evapotranspiration and crop coefficient using the Earth Engine Evaporation Flux (EEFlux) application. *PLoS ONE* **2020**, *15*, e0235620. [CrossRef]
96. Xiong, Y.; Chen, X.; Tang, L.; Wang, H. Comparison of surface renewal and Bowen ratio derived evapotranspiration measurements in an arid vineyard. *J. Hydrol.* **2022**, *613*, 128474. [CrossRef]
97. Irmak, S. Bowen ratio energy balance system-measured evapotranspiration, surface energy fluxes, single and basal crop coefficients and energy partitioning for subsurface drip-irrigated maize canopy. *J. Nat. Resour. Agric. Ecosyst.* **2025**, *3*, 101–120. [CrossRef]
98. Ding, J.; Li, S.; Wang, H.; Wang, C.; Zhang, Y.; Yang, D. Estimation of evapotranspiration and crop coefficient of Chinese cabbage using eddy covariance in Northwest China. *Water* **2021**, *13*, 2781. [CrossRef]
99. Moorhead, J.E.; Marek, G.W.; Gowda, P.H.; Lin, X.; Colaizzi, P.D.; Evett, S.R.; Kutikoff, S. Evaluation of evapotranspiration from eddy covariance using large weighing lysimeters. *Agronomy* **2019**, *9*, 99. [CrossRef]
100. Denager, T.; Looms, M.C.; Sonnenborg, T.O.; Jensen, K.H. Comparison of evapotranspiration estimates using the water balance and the eddy covariance methods. *Vadose Zone J.* **2020**, *19*, e20032. [CrossRef]
101. Gokool, S.; Clulow, A.; Araya, N.A. Assessing the potential of the cloud-based EEFlux tool to monitor the water use of Moringa oleifera in a semi-arid region of South Africa. *Geomatics* **2025**, *5*, 18. [CrossRef]
102. Dong, Y.; Hansen, H. Development and design of an affordable field scale weighing lysimeter using a microcontroller system. *Smart Agric. Technol.* **2023**, *4*, 100147. [CrossRef]

103. Kebede, N.; Ayana, M.; Mekonnen, B.; Beri, H. Design, construction, and calibration of a weighable lysimeter for measuring water requirements of field crops for data-scarce areas of Ethiopia. *Heliyon* **2024**, *10*, e36968. [CrossRef]
104. Liu, B.; Cui, Y.; Shi, Y.; Cai, X.; Luo, Y.; Zhang, L. Comparison of evapotranspiration measurements between eddy covariance and lysimeters in paddy fields under alternate wetting and drying irrigation. *Paddy Water Environ.* **2019**, *17*, 725–739. [CrossRef]
105. Ghiat, I.; Mackey, H.R.; Al-Ansari, T. A review of evapotranspiration measurement models, techniques and methods for open and closed agricultural field applications. *Water* **2021**, *13*, 2523. [CrossRef]
106. Kadam, S.A.; Stöckle, C.O.; Liu, M.; Gao, Z.; Russell, E.S. Suitability of Earth Engine Evaporation Flux (EEFlux) estimation of evapotranspiration in rainfed crops. *Remote Sens.* **2021**, *13*, 3884. [CrossRef]
107. Mukherjee, J.; Sharma, A.; Dhakar, R.; Sehgal, V.K.; Chakraborty, D.; Das, D.K. Estimation and validation of actual evapotranspiration (ETa) of maize–wheat cropping system using SSEBop model over IARI research farm, New Delhi, India. *J. Indian Soc. Remote Sens.* **2021**, *49*, 1823–1837. [CrossRef]
108. Poudel, U.; Stephen, H.; Ahmad, S. Evaluating irrigation performance and water productivity using EEFlux ET and NDVI. *Sustainability* **2021**, *13*, 7967. [CrossRef]
109. Kamyab, A.D.; Mokhtari, S.; Jafarinia, R. A comparative study in quantification of maize evapotranspiration for Iranian maize farm using SEBAL and METRIC-1 EEFlux algorithms. *Acta Geophys.* **2022**, *70*, 319–332. [CrossRef]
110. Djaman, K.; Mohammed, A.T.; Koudahe, K. Accuracy of estimated crop evapotranspiration using locally developed crop coefficients against satellite-derived crop evapotranspiration in a semiarid climate. *Agronomy* **2023**, *13*, 1937. [CrossRef]
111. Satpathi, A.; Danodia, A.; Abed, S.A.; Nain, A.S.; Al-Ansari, N.; Ranjan, R.; Vishwakarma, D.K.; Gacem, A.; Mansour, L.; Yadav, K.K. Estimation of the crop evapotranspiration for Udham Singh Nagar district using modified Priestley–Taylor model and Landsat imagery. *Sci. Rep.* **2024**, *14*, 21463. [CrossRef]
112. Stöckle, C.O.; Liu, M.; Kadam, S.A.; Evett, S.R.; Marek, G.W.; Colaizzi, P.D. Comparing evapotranspiration estimations using crop model–data fusion and satellite data-based models with lysimetric observations: Implications for irrigation scheduling. *Agric. Water Manag.* **2025**, *311*, 109372. [CrossRef]
113. Letey, J.; Dinar, A.; Knapp, K.C. Crop-water production function model for saline irrigation waters. *Soil Sci. Soc. Am. J.* **1985**, *49*, 1005–1009. [CrossRef]
114. Dudley, L.M.; Ben-Gal, A.; Shani, U. Influence of plant, soil, and water on the leaching fraction. *Vadose Zone J.* **2008**, *7*, 420–425. [CrossRef]
115. Corwin, D.L.; Rhoades, J.D.; Šimůnek, J. Leaching requirement for soil salinity control: Steady-state versus transient models. *Agric. Water Manag.* **2007**, *90*, 165–180. [CrossRef]
116. Jain, R.K. Experimental performance of smart IoT-enabled drip irrigation system using and controlled through web-based applications. *Smart Agric. Technol.* **2023**, *4*, 100215. [CrossRef]
117. Zaher, A.; Hamwi, H.; Almas, A.; Al-Baitamouni, S.; Al-Bathal, M. Automated smart solar irrigation system. In Proceedings of the Smart Cities Symposium, Bahrain, 22–23 April 2018; pp. 1–6. [CrossRef]
118. Tornese, I.; Matera, A.; Rashvand, M.; Genovese, F. Use of probes and sensors in agriculture—Current trends and future prospects on intelligent monitoring of soil moisture and nutrients. *AgriEngineering* **2024**, *6*, 234. [CrossRef]
119. Cobos, D.R.; Chambers, C. *Calibrating ECH$_2$O Soil Moisture Sensors: Application Note*; Decagon Devices: Pullman, WA, USA, 2010.
120. Spelman, D.; Kinzli, K.-D.; Kunberger, T. Calibration of the 10HS soil moisture sensor for southwest Florida agricultural soils. *J. Irrig. Drain. Eng.* **2013**, *139*, 965–971. [CrossRef]
121. Mittelbach, H.; Lehner, I.; Seneviratne, S.I. Comparison of four soil moisture sensor types under field conditions in Switzerland. *J. Hydrol.* **2012**, *430–431*, 39–49. [CrossRef]
122. Dursun, M.; Özden, S. An efficient improved photovoltaic irrigation system with artificial neural network based modeling of soil moisture distribution—A case study in Turkey. *Comput. Electron. Agric.* **2014**, *102*, 120–126. [CrossRef]
123. Goumopoulos, C.; O'Flynn, B.; Kameas, A. Automated zone-specific irrigation with wireless sensor/actuator network and adaptable decision support. *Comput. Electron. Agric.* **2014**, *105*, 20–33. [CrossRef]
124. Santhana Krishnan, R.; Golden Julie, E.; Robinson, Y.H.; Raja, S.; Kumar, R.; Thong, P.H.; Son, L.H. Fuzzy logic based smart irrigation system using Internet of Things. *J. Clean. Prod.* **2020**, *252*, 119902. [CrossRef]
125. Decagon Devices. *EC-20, EC-10, EC-5 Soil Moisture Sensors: User's Manual*; Decagon Devices: Pullman, WA, USA, 2010.
126. Pereira, G.P.; Chaari, M.Z.; Daroge, F. IoT-enabled smart drip irrigation system using ESP32. *IoT* **2023**, *4*, 221–243. [CrossRef]
127. Topp, G.C.; Davis, J.L.; Annan, A.P. Electromagnetic determination of soil water content: Measurements in coaxial transmission lines. *Water Resour. Res.* **1980**, *16*, 574–582. [CrossRef]
128. Datta, S.; Taghvaeian, S.; Ochsner, T.E.; Moriasi, D.; Gowda, P.; Steiner, J.L. Performance assessment of five different soil moisture sensors under irrigated field conditions in Oklahoma. *Sensors* **2018**, *18*, 3786. [CrossRef]
129. Wilson, T.B.; Diamond, H.J.; Kochendorfer, J.; Meyers, T.P.; Hall, M.; Casey, N.W.; Baker, C.B.; Leeper, R.; Palecki, M.A. Evaluating time domain reflectometry and coaxial impedance sensors for soil observations by the U.S. Climate Reference Network. *Vadose Zone J.* **2020**, *19*, e20013. [CrossRef]

130. Marek, G.W.; Evett, S.; Marek, T.H.; Porter, D.O.; Schwartz, R.C. Field evaluation of conventional and downhole TDR soil water sensors for irrigation scheduling in a clay loam soil. *Appl. Eng. Agric.* **2023**, *39*, 495–507. [CrossRef]
131. Ferrarezi, R.S.; Nogueira, T.A.R.; Zepeda, S.G.C. Performance of soil moisture sensors in Florida sandy soils. *Water* **2020**, *12*, 358. [CrossRef]
132. Wilson, T.B.; Kochendorfer, J.; Diamond, H.J.; Meyers, T.P.; Hall, M.; French, B.; Myles, L.; Saylor, R.D. A field evaluation of the SoilVUE10 soil moisture sensor. *Vadose Zone J.* **2023**, *22*, e20241. [CrossRef]
133. Campbell Scientific. *GS1: Ruggedized Soil Water Content Sensor*; Campbell Scientific Inc.: Logan, UT, USA, 2019.
134. Salman, A.K.; Aldulaimy, S.E.; Mohammed, H.J.; Abed, Y.M. Performance of soil moisture sensors in gypsiferous and salt-affected soils. *Biosyst. Eng.* **2021**, *209*, 200–209. [CrossRef]
135. Mendis, S.S.; Udawatta, R.P.; Anderson, S.H.; Nelson, K.A.; Cordsiemon, R.L. Effects of cover crops on soil moisture dynamics of a corn cropping system. *Soil Secur.* **2022**, *8*, 100072. [CrossRef]
136. Liu, Y.; Razman, M.R.; Syed Zakaria, S.Z.; Lee, K.E.; Khan, S.U.; Albanyan, A. Personalized context-aware systems for sustainable agriculture development using ubiquitous devices and adaptive learning. *Comput. Hum. Behav.* **2024**, *160*, 108375. [CrossRef]
137. Singh, J. Performance Assessment of Electromagnetic Soil Water Sensors in Different Soil Textural, Temperature, and Salinity Conditions. Ph.D. Thesis, University of Nebraska–Lincoln, Lincoln, NE, USA, 2017.
138. Burns, T.T.; Adams, J.R.; Berg, A.A. Laboratory calibration procedures of the Hydra Probe soil moisture sensor: Infiltration wet-up vs. dry-down. *Vadose Zone J.* **2014**, *13*, 1–10. [CrossRef]
139. López Riquelme, J.A.; Soto, F.; Suardíaz, J.; Sánchez, P.; Iborra, A.; Vera, J.A. Wireless sensor networks for precision horticulture in southern Spain. *Comput. Electron. Agric.* **2009**, *68*, 25–35. [CrossRef]
140. Kodikara, J.; Rajeev, P.; Chan, D.; Gallage, C. Soil moisture monitoring at the field scale using neutron probe. *Can. Geotech. J.* **2014**, *51*, 332–345. [CrossRef]
141. CPN International. *CPN 503 Elite HYDROPROBE™: Operating Manual*; CPN International Inc.: Martinez, CA, USA, 2015.
142. Sriram, A.; Sharmau, N.; Reddy, K.S.; Anand Babu, G.L. Automated irrigation system for agriculture. *Int. J. Innov. Technol. Explor. Eng.* **2019**, *8*, 53–56. [CrossRef]
143. Kamelia, L.; Ramdhani, M.A.; Faroqi, A.; Rifadiapriyana, V. Implementation of automation system for humidity monitoring and irrigation system. *IOP Conf. Ser. Mater. Sci. Eng.* **2018**, *288*, 012092. [CrossRef]
144. Muñoz-Carpena, R.; Li, Y.C.; Klassen, W.; Dukes, M.D. Field comparison of tensiometer and granular matrix sensor automatic drip irrigation on tomato. *HortTechnology* **2005**, *15*, 584–590. [CrossRef]
145. Millán, S.; Casadesús, J.; Campillo, C.; Moñino, M.J.; Prieto, M.H. Using soil moisture sensors for automated irrigation scheduling in a plum crop. *Water* **2019**, *11*, 2061. [CrossRef]
146. de Moura Campos, H.; de Oliveira, H.F.E.; Mesquita, M.; de Castro, L.E.V.; Ferrarezi, R.S. Low-cost open-source platform for irrigation automation. *Comput. Electron. Agric.* **2021**, *190*, 106481. [CrossRef]
147. Casadesús, J.; Mata, M.; Marsal, J.; Girona, J. A general algorithm for automated scheduling of drip irrigation in tree crops. *Comput. Electron. Agric.* **2012**, *83*, 11–20. [CrossRef]
148. Guevara, S.; Singh, Y.; Shores, A.; Mercado, J.; Postigo, M.; Garcia, J.; Newell, B. Development of a pilot smart irrigation system for Peruvian highlands. *J. Contemp. Water Res. Educ.* **2020**, *171*, 49–62. [CrossRef]
149. Vories, E.; Sudduth, K. Determining sensor-based field capacity for irrigation scheduling. *Agric. Water Manag.* **2021**, *250*, 106860. [CrossRef]
150. Jimenez, A.-F.; Cardenas, P.-F.; Jimenez, F.; Ruiz-Canales, A.; López, A. A cyber-physical intelligent agent for irrigation scheduling in horticultural crops. *Comput. Electron. Agric.* **2020**, *178*, 105777. [CrossRef]
151. Bernier, M.H.; Madramootoo, C.A.; Mehdi, B.B.; Gollamudi, A. Assessing on-farm irrigation water use efficiency in southern Ontario. *Can. Water Resour. J.* **2010**, *35*, 115–130. [CrossRef]
152. Kim, Y.; Evans, R.G.; Iversen, W.M. Evaluation of closed-loop site-specific irrigation with wireless sensor network. *J. Irrig. Drain. Eng.* **2009**, *135*, 25–31. [CrossRef]
153. Nandi, R.; Shrestha, D. Assessment of low-cost and higher-end soil moisture sensors across various moisture ranges and soil textures. *Sensors* **2024**, *24*, 5886. [CrossRef]
154. Dafalla, M. Using 5TE sensors for monitoring moisture conditions in green parks. *Sensors* **2024**, *24*, 3479. [CrossRef]
155. Abdelmoneim, A.A.; Khadra, R.; Elkamouh, A.; Derardja, B.; Dragonetti, G. Towards affordable precision irrigation: An experimental comparison of weather-based and soil water potential-based irrigation using low-cost IoT-tensiometers on drip irrigated lettuce. *Sustainability* **2024**, *16*, 306. [CrossRef]
156. Schwamback, D.; Persson, M.; Berndtsson, R.; Bertotto, L.E.; Kobayashi, A.N.A.; Wendland, E.C. Automated low-cost soil moisture sensors: Trade-off between cost and accuracy. *Sensors* **2023**, *23*, 2451. [CrossRef]
157. King, B.A.; Shellie, K.C. A crop water stress index based Internet of Things decision support system for precision irrigation of wine grape. *Smart Agric. Technol.* **2023**, *4*, 100202. [CrossRef]
158. Met One Instruments. *034B Wind Sensor*; Met One Instruments Inc.: Grants Pass, OR, USA, 2018.

159. Kolapkar, M.M.; Khirade, P.W.; Sayyad, S.B. Design and development of embedded system for measurement of humidity, soil moisture and temperature in polyhouse using 89E516RD microcontroller. *Int. J. Adv. Agric. Sci. Technol.* **2016**, *5*, 96–110. [CrossRef]
160. Adat, D.M.; Mane-Deshmukh, P.V.; Tilekar, S.K.; Ladgaonkar, B. Mixed signal based VLSI technology for wireless sensor network. *Int. J. Eng. Res. Appl.* **2015**, *5*, 307–312.
161. Pawar, A.M.; Deshpande, J.D.; Patil, S.N. Development of smart electronic system for realization smart home. *Manag. J. Digit. Signal Process.* **2020**, *8*, 16–27.
162. Anand, T. AGRARIAN—Automatic plant irrigation system. *Int. J. Comput. Appl.* **2015**, *132*, 22–26. [CrossRef]
163. Shruthi, G.; Selva Kumari, B.; Rani, R.P.; Preyadharan, R. A real-time smart sprinkler irrigation control system. In Proceedings of the 2017 IEEE International Conference on Electrical, Instrumentation and Communication Engineering (ICEICE), Karur, India, 27–28 April 2017; pp. 1–5. [CrossRef]
164. Al-Humairi, S.N.S.; Manimaran, P.; Abdullah, M.I.; Daud, J. A smart automated greenhouse: Soil moisture, temperature monitoring and automatic water supply system. In Proceedings of the 2019 IEEE Conference on Sustainable Utilization and Development in Engineering and Technologies (CSUDET), Penang, Malaysia, 7–9 November 2019; pp. 111–115. [CrossRef]
165. Monica, M.; Yeshika, B.; Abhishek, G.S.; Sanjay, H.A.; Dasiga, S. IoT based control and automation of smart irrigation system. In Proceedings of the 2017 International Conference on Recent Innovations in Signal processing and Embedded Systems (RISE), Bhopal, India, 27–29 October 2017; pp. 601–607. [CrossRef]
166. Abayomi-Alli, O.; Odusami, M.; Ojinaka, D.; Shobayo, O.; Misra, S.; Damasevicius, R. Smart-solar irrigation system (SMIS) for sustainable agriculture. In *Applied Informatics*; Springer: Cham, Switzerland, 2018; pp. 198–212. [CrossRef]
167. Bagaria, R.; Periyasamy, S.; Nandakumar, S. Smart irrigation and farm field monitoring system using Internet of Things. Proceedings of International Conference on Sustainable Computing in Science, Technology and Management (SUSCOM), Jaipur, India, 26–28 February 2019. [CrossRef]
168. El Mezouari, A.; El Fazziki, A.; Sadgal, M. Smart irrigation system. *IFAC-PapersOnLine* **2022**, *55*, 3298–3303. [CrossRef]
169. Yudhana, A.; Kusuma, A.C. Water quality monitoring at paddies farming based on Android. *IOP Conf. Ser. Mater. Sci. Eng.* **2018**, *403*, 012042. [CrossRef]
170. Nandurkar, S.R.; Thool, V.R. Design of a soil moisture sensing unit for smart irrigation application. In *International Conference on Emerging Technology Trends on Advanced Engineering Research (ICETT 2012)*; International Journal of Computer Applications (IJCA): Wilmington, NC, USA, 2012.
171. Ndunagu, J.N.; Ukhurebor, K.E.; Akaaza, M.; Onyancha, R.B. Development of a wireless sensor network and IoT-based smart irrigation system. *Appl. Environ. Soil Sci.* **2022**, *2022*, 7678570. [CrossRef]
172. Wang, K.; Ma, B.; Lui, F.; Luo, H.; Dong, H. A WSN-based system for environment monitoring and energy saving control in hull workshop. *Sens. Transducers* **2013**, *158*, 135–140.
173. Sensirion. *Datasheet SHT1x (SHT10, SHT11, SHT15) Humidity and Temperature Sensor*; Sensirion AG: Staefa, Switzerland, 2011.
174. Suárez Barón, J.C.; Suárez Barón, M.J. Application of SHT71 sensor to measure humidity and temperature with a WSN. In Proceedings of the 2014 IEEE 9th IberoAmerican Congress on Sensors, Bogota, Colombia, 15–18 October 2014; pp. 1–7. [CrossRef]
175. Tan, P.; Gebremariam, E.T.; Rahman, M.S.; Salman, H.; Xu, H. Design and implementation of soil moisture monitoring and irrigation system based on ARM and IoT. *Procedia Comput. Sci.* **2022**, *208*, 486–493. [CrossRef]
176. Veerachamy, R.; Ramar, R.; Balaji, S.; Sharmila, L. Autonomous application controls on smart irrigation. *Comput. Electr. Eng.* **2022**, *100*, 107855. [CrossRef]
177. Decagon Devices. *P-3 Vapor Pressure, Temperature & Relative Humidity Sensor: Operator's Manual*; Decagon Devices: Pullman, WA, USA, 2015.
178. METER Group. *ATMOS-14 Manual*; METER Group Inc.: Pullman, WA, USA, 2018.
179. Decagon Devices. *DS-2 Sonic Anemometer Operator's Manual*; Decagon Devices: Pullman, WA, USA, 2014.
180. Gill Instruments. *HS-50: 3-Axis Horizontal-Head Research Anemometer*; Gill Instruments Ltd.: Lymington, UK, 2019.
181. Gill Instruments. *HS-100: 3-Axis Horizontal-Head Research Anemometer*; Gill Instruments Ltd.: Lymington, UK, 2019.
182. Gill Instruments. *R3-50: 3-Axis Ultrasonic Anemometer*; Gill Instruments Ltd.: Lymington, UK, 2022.
183. Gill Instruments. *R3-100: 3-Axis Ultrasonic Anemometer*; Gill Instruments Ltd.: Lymington, UK, 2023.
184. Müller, T.; Ranquet Bouleau, C.; Perona, P. Optimizing drip irrigation for eggplant crops in semi-arid zones using evolving thresholds. *Agric. Water Manag.* **2016**, *177*, 54–65. [CrossRef]
185. Siddiqi, S.A.; Al-Mulla, Y. Wireless sensor network system for precision irrigation using soil- and plant-based near-real-time monitoring sensors. *Procedia Comput. Sci.* **2022**, *203*, 407–412. [CrossRef]
186. Dombrowski, O.; Hendricks Franssen, H.-J.; Brogi, C.; Bogena, H.R. Performance of the ATMOS41 all-in-one weather station for weather monitoring. *Sensors* **2021**, *21*, 741. [CrossRef]
187. LI-COR Environmental. *LI-710 Evapotranspiration Sensor Instruction Manual*; LI-COR Biosciences: Lincoln, NE, USA, 2025.
188. Peddinti, S.R.; Kisekka, I. Evaluation of the LI-710 evapotranspiration sensor in comparison to full eddy covariance for monitoring energy fluxes in perennial and annual crops. *Agric. Water Manag.* **2025**, *313*, 109501. [CrossRef]

189. Menenti, M.; Nieuwenhuis, G.J.A. Remote sensing in the water management practice. *Neth. J. Agric. Sci.* **1986**, *34*, 317–328. [CrossRef]
190. Bastiaanssen, W.G.M.; Thiruvengadachari, S.; Sakthivadivel, R.; Molden, D.J. Satellite remote sensing for estimating productivities of land and water. *Int. J. Water Resour. Dev.* **1999**, *15*, 181–194. [CrossRef]
191. Plant, R.E.; Monk, D.S. Application of remote sensing to irrigation management in California cotton. In *Proceedings of the Fourth International Conference on Precision Agriculture*; American Society of Agronomy, Inc.; Crop Science Society of America, Inc.; Soil Science Society of America, Inc.: Madison, WI, USA, 1999; pp. 1511–1521. [CrossRef]
192. Alvino, A.; Marino, S. Remote sensing for irrigation of horticultural crops. *Horticulturae* **2017**, *3*, 40. [CrossRef]
193. Dutta, G.; Goswami, P. Application of drone in agriculture: A review. *Int. J. Chem. Stud.* **2020**, *8*, 181–187. [CrossRef]
194. Karatas, B.S.; Akkuzu, E.; Unal, H.B.; Asik, S.; Avci, M. Using satellite remote sensing to assess irrigation performance in water user associations in the Lower Gediz Basin, Turkey. *Agric. Water Manag.* **2009**, *96*, 982–990. [CrossRef]
195. Veysi, S.; Naseri, A.A.; Hamzeh, S.; Bartholomeus, H. A satellite-based crop water stress index for irrigation scheduling in sugarcane fields. *Agric. Water Manag.* **2017**, *189*, 70–86. [CrossRef]
196. Bhatti, S.; Heeren, D.M.; O'Shaughnessy, S.A.; Neale, C.M.U.; LaRue, J.; Melvin, S.; Wilkening, E.; Bai, G. Toward automated irrigation management with integrated crop water stress index and spatial soil water balance. *Precis. Agric.* **2023**, *24*, 2223–2247. [CrossRef]
197. Geli, H.M.E.; Neale, C.M.U. Spatial evapotranspiration modelling interface (SETMI). *Remote Sensing for Hydrology* **2012**, 171–174.
198. Neale, C.M.U.; Geli, H.M.E.; Kustas, W.P.; Alfieri, J.G.; Gowda, P.H.; Evett, S.R.; Prueger, J.H.; Hipps, L.E.; Dulaney, W.P.; Chávez, J.L.; et al. Soil water content estimation using a remote sensing-based hybrid evapotranspiration modeling approach. *Adv. Water Resour.* **2012**, *50*, 152–161. [CrossRef]
199. Barker, J.B.; Heeren, D.M.; Neale, C.M.U.; Rudnick, D.R. Evaluation of variable rate irrigation using a remote-sensing-based model. *Agric. Water Manag.* **2018**, *203*, 63–74. [CrossRef]
200. Evett, S.R.; O'Shaughnessy, S.A.; Peters, R.T. Irrigation Scheduling and Supervisory Control and Data Acquisition System for Moving and Static Irrigation Systems. U.S. Patent 8,924,031, 2014.
201. Corbari, C.; Gabrieli, D.; Furlan, L.; Furlanetto, J.; Skokovic, D.; Sobrino, J.; Morari, F. Optimizing variable rate irrigation using model- and satellite-based dynamic prescription maps. *Agric. Water Manag.* **2024**, *299*, 108896. [CrossRef]
202. Corbari, C.; Ben Charfi, I.; Al Bitar, A.; Skokovic, D.; Sobrino, J.A.; Perelli, C.; Branca, G.; Mancini, M. A fully coupled crop–water–energy balance model based on satellite data for maize and tomato crop yield estimates: The FEST-EWB-SAFY model. *Agric. Water Manag.* **2022**, *272*, 107850. [CrossRef]
203. Merlin, O.; Chirouze, J.; Olioso, A.; Jarlan, L.; Chehbouni, G.; Boulet, G. An image-based four-source surface energy balance model to estimate crop evapotranspiration from solar reflectance/thermal emission data (SEB-4S). *Agric. For. Meteorol.* **2014**, *184*, 188–203. [CrossRef]
204. Singh, R.K.; Senay, G.B. Comparison of four different energy balance models for estimating evapotranspiration in the Midwestern United States. *Water* **2016**, *8*, 9. [CrossRef]
205. Wagle, P.; Bhattarai, N.; Gowda, P.H.; Kakani, V.G. Performance of five surface energy balance models for estimating daily evapotranspiration in high biomass sorghum. *ISPRS J. Photogramm. Remote Sens.* **2017**, *128*, 192–203. [CrossRef]
206. Pôças, I.; Paço, T.A.; Paredes, P.; Cunha, M.; Pereira, L.S. Estimation of actual crop coefficients using remotely sensed vegetation indices and soil water balance modelled data. *Remote Sens.* **2015**, *7*, 2373–2399. [CrossRef]
207. Tadesse, T.; Senay, G.B.; Berhan, G.; Regassa, T.; Beyene, S. Evaluating a satellite-based seasonal evapotranspiration product and its relationship with other satellite-derived products and crop yield: A case study for Ethiopia. *Int. J. Appl. Earth Obs. Geoinf.* **2015**, *40*, 39–54. [CrossRef]
208. Park, J.; Baik, J.; Choi, M. Satellite-based crop coefficient and evapotranspiration using surface soil moisture and vegetation indices in Northeast Asia. *CATENA* **2017**, *156*, 305–314. [CrossRef]
209. Zare, M.; Koch, M. Computation of irrigation water demand using FAO-56 and satellite-estimated crop coefficients. *Interdiscip. Res. Rev.* **2017**, *12*, 16.
210. Reyes-González, A.; Kjaersgaard, J.; Trooien, T.; Hay, C.; Ahiablame, L. Estimation of crop evapotranspiration using satellite remote sensing-based vegetation index. *Adv. Meteorol.* **2018**, *2018*, 4525021. [CrossRef]
211. Wang, X.; Lei, H.; Li, J.; Huo, Z.; Zhang, Y.; Qu, Y. Estimating evapotranspiration and yield of wheat and maize croplands through a remote sensing-based model. *Agric. Water Manag.* **2023**, *282*, 108294. [CrossRef]
212. Mebrie, D.W.; Assefa, T.T.; Yimam, A.Y.; Belay, S.A. Remote sensing-based estimation of variable crop coefficient and evapotranspiration in the Ethiopian highlands. *Appl. Water Sci.* **2023**, *13*, 168. [CrossRef]
213. Melton, F.S.; Huntington, J.; Grimm, R.; Herring, J.; Hall, M.; Rollison, D.; Erickson, T.; Allen, R.; Anderson, M.; Fisher, J.; et al. OpenET: Filling a critical data gap in water management for the Western United States. *JAWRA* **2022**, *58*, 971–994. [CrossRef]

214. Gaznayee, H.A.A.; Zaki, S.H.; Al-Quraishi, A.M.F.; Aliehsan, P.H.; Hakzi, K.K.; Razvanchy, H.A.S.; Riksen, M.; Mahdi, K. Integrating remote sensing techniques and meteorological data to assess ideal irrigation system performance scenarios. *Water* **2023**, *15*, 1605. [CrossRef]
215. Carrasco-Benavides, M.; Ortega-Farías, S.; Gil, P.M.; Knopp, D.; Morales-Salinas, L.; Lagos, L.O.; de la Fuente, D.; López-Olivari, R.; Fuentes, S. Vineyard water footprint assessment using ancillary data and EEFlux satellite images. *Sci. Total Environ.* **2022**, *811*, 152452. [CrossRef]
216. Fadel, A.; Mhawej, M.; Faour, G.; Slim, K. Application of METRIC-GEE to estimate spatial and temporal evaporation rates in a Mediterranean lake. *Remote Sens. Appl. Soc. Environ.* **2020**, *20*, 100431. [CrossRef]
217. Blin, N.; Suárez, F. Evaluating satellite-derived evapotranspiration for groundwater model calibration using EEFlux. *Sci. Total Environ.* **2023**, *858*, 159764. [CrossRef] [PubMed]
218. Chandel, A.K.; Khot, L.R.; Yu, L.-X. Alfalfa crop vigor and yield characterization using high-resolution aerial multispectral and thermal infrared imagery. *Comput. Electron. Agric.* **2021**, *182*, 105999. [CrossRef]
219. Thorp, K.R.; Thompson, A.L.; Harders, S.J.; French, A.N.; Ward, R.W. High-throughput phenotyping of crop water use efficiency via multispectral drone imagery. *Remote Sens.* **2018**, *10*, 1682. [CrossRef]
220. Nieto, H.; Kustas, W.P.; Torres-Rúa, A.; Alfieri, J.G.; Gao, F.; Anderson, M.C.; White, W.A.; Song, L.; Alsina, M.d.M.; Prueger, J.H.; et al. Evaluation of TSEB turbulent fluxes using UAV thermal imagery. *Irrig. Sci.* **2019**, *37*, 389–406. [CrossRef]
221. Garcia-Vasquez, A.C.; Mokari, E.; Samani, Z.; Fernald, A. UAV-thermal imaging to estimate crop water use and irrigation efficiency. *Agric. Water Manag.* **2022**, *272*, 107824. [CrossRef]
222. Zhang, Y.; Han, W.; Zhang, H.; Niu, X.; Shao, G. Evaluating maize evapotranspiration using high-resolution UAV imagery and FAO-56 dual crop coefficient approach. *Agric. Water Manag.* **2023**, *275*, 107551. [CrossRef]
223. Mndela, Y.; Ndou, N.; Nyamugama, A. Irrigation scheduling for small-scale crops using UAV multispectral imagery. *Sustainability* **2023**, *15*, 12034. [CrossRef]
224. Peng, J.; Nieto, H.; Andersen, M.N.; Kørup, K.; Larsen, R.; Morel, J.; Parsons, D.; Zhou, Z.; Manevski, K. Accurate estimates of land surface energy fluxes and irrigation requirements from UAV-based sensors. *ISPRS J. Photogramm. Remote Sens.* **2023**, *198*, 238–254. [CrossRef]
225. Wienhold, K.J.; Li, D.; Fang, Z.N. Precision irrigation soil moisture mapper using UAV multispectral imagery. *Remote Sens.* **2024**, *16*, 1660. [CrossRef]
226. Hoffmann, H.; Nieto, H.; Jensen, R.; Guzinski, R.; Zarco-Tejada, P.; Friborg, T. Estimating evaporation with thermal UAV data and two-source energy balance models. *Hydrol. Earth Syst. Sci.* **2016**, *20*, 697–713. [CrossRef]
227. Xia, T.; Kustas, W.P.; Anderson, M.C.; Alfieri, J.G.; Gao, F.; McKee, L.; Prueger, J.H.; Geli, H.M.E.; Neale, C.M.U.; Sanchez, L.; et al. Mapping evapotranspiration with high-resolution aircraft imagery. *Hydrol. Earth Syst. Sci.* **2016**, *20*, 1523–1545. [CrossRef]
228. Brenner, C.; Thiem, C.E.; Wizemann, H.; Bernhardt, M.; Schulz, K. Estimating turbulent heat fluxes from UAV thermal imagery. *Int. J. Remote Sens.* **2017**, *38*, 3003–3026. [CrossRef]
229. Park, S.; Ryu, D.; Fuentes, S.; Chung, H.; O'Connell, M.; Kim, J. Mapping very-high-resolution evapotranspiration from UAV im-agery. *ISPRS Int. J. Geo-Inf.* **2021**, *10*, 211. [CrossRef]
230. Chandel, A.K.; Molaei, B.; Khot, L.R.; Peters, R.T.; Stöckle, C.O. High-resolution geospatial evapotranspiration mapping using UAV imagery with METRIC model. *Drones* **2020**, *4*, 52. [CrossRef]
231. Chandel, A.K.; Khot, L.R.; Molaei, B.; Peters, R.T.; Stöckle, C.O.; Jacoby, P.W. High-resolution spatiotemporal water use mapping of drip-irrigated grapevines using UAS. *Remote Sens.* **2021**, *13*, 954. [CrossRef]
232. Chandel, A.K.; Khot, L.R.; Stöckle, C.O.; Kalcsits, L.; Mantle, S.; Rathnayake, A.P.; Peters, T.R. Canopy transpiration mapping in an apple orchard using airborne imagery. *AgriEngineering* **2025**, *7*, 154. [CrossRef]
233. Berni, J.A.J.; Zarco-Tejada, P.J.; Sepulcre-Cantó, G.; Fereres, E.; Villalobos, F. Mapping canopy conductance and CWSI using high-resolution thermal imagery. *Remote Sens. Environ.* **2009**, *113*, 2380–2388. [CrossRef]
234. Gonzalez-Dugo, V.; Testi, L.; Villalobos, F.; López-Bernal, Á.; Orgaz, F.; Zarco-Tejada, P.J.; Fereres, E. Empirical validation of the relationship between crop water stress index and transpiration. *Agric. For. Meteorol.* **2020**, *292–293*, 108128. [CrossRef]
235. Meron, M.; Peres, M.; Levin-Orlov, V.; Shoshani, G.; Marchaim, U.; Chen, A. Irrigation uniformity assessment with high-resolution aerial sensors. *Int. J. Appl. Earth Obs. Geoinf.* **2025**, *137*, 104446. [CrossRef]
236. Mateo-Aroca, A.; García-Mateos, G.; Ruiz-Canales, A.; Molina-García-Pardo, J.M.; Molina-Martínez, J.M. Remote image capture system for precision irrigation. *Water* **2019**, *11*, 255. [CrossRef]
237. Thakur, D.; Kumar, Y.; Vijendra, S. Smart irrigation and intrusion detection using IoT. *Procedia Comput. Sci.* **2020**, *167*, 154–162. [CrossRef]
238. Gimpel, H.; Graf-Drasch, V.; Hawlitschek, F.; Neumeier, K. Designing smart and sustainable irrigation: A case study. *J. Clean. Prod.* **2021**, *315*, 128048. [CrossRef]
239. García, L.; Parra, L.; Jimenez, J.M.; Lloret, J.; Lorenz, P. IoT-based smart irrigation systems: An overview of recent trends on sensors and IoT systems for irrigation in precision agriculture. *Sensors* **2020**, *20*, 1042. [CrossRef] [PubMed]

240. Kurtulmus, E.; Arslan, B.; Kurtulmus, F. Deep learning for proximal soil sensor development towards smart irrigation. *Expert Syst. Appl.* **2022**, *198*, 116812. [CrossRef]
241. Al-Naji, A.; Fakhri, A.B.; Gharghan, S.K.; Chahl, J. Soil color analysis based on an RGB camera and an artificial neural network towards smart irrigation: A pilot study. *Heliyon* **2021**, *7*, e06078. [CrossRef] [PubMed]
242. Zhang, X.; Khachatryan, H. Investigating homeowners' preferences for smart irrigation technology features. *Water* **2019**, *11*, 1996. [CrossRef]
243. Putjaika, N.; Phusae, S.; Chen-Im, A.; Phunchongharn, P.; Akkarajitsakul, K. A control system in intelligent farming using Arduino technology. In *2016 Fifth ICT International Student Project Conference (ICT-ISPC)*; IEEE: New York, NY, USA, 2016; pp. 53–56. [CrossRef]
244. Goldstein, I.; Kopelowitz, T.; Lewenstein, M.; Porat, E. Conditional lower bounds for space/time tradeoffs. In *Algorithms and Data Structures*; Springer: Cham, Switzerland, 2017; pp. 421–436. [CrossRef]
245. Chandrappa, V.Y.; Ray, B.; Ashwath, N.; Shrestha, P. Application of IoT to develop a smart watering system for Cairns parklands: A case study. In *2020 IEEE Region 10 Symposium (TENSYMP)*; IEEE: New York, NY, USA, 2020; pp. 1118–1122. [CrossRef]
246. Chandrappa, V.Y.; Ray, B.; Ashwatha, N.; Shrestha, P. Spatiotemporal modeling to predict soil moisture for sustainable smart irrigation. *Internet Things* **2023**, *21*, 100671. [CrossRef]
247. Blonquist, J.M., Jr.; Jones, S.B.; Robinson, D.A. A time domain transmission sensor with TDR performance characteristics. *J. Hydrol.* **2005**, *314*, 235–245. [CrossRef]
248. Ortiz, D.; Litvin, A.G.; Fernandez, M.G.S. A cost-effective and customizable automated irrigation system for precise high-throughput phenotyping in drought stress studies. *PLoS ONE* **2018**, *13*, e0198546. [CrossRef] [PubMed]
249. Pierce, F.J.; Elliott, T.V. Regional and on-farm wireless sensor networks for agricultural systems in eastern Washington. *Comput. Electron. Agric.* **2008**, *61*, 32–43. [CrossRef]
250. Nikolidakis, S.A.; Kandris, D.; Vergados, D.D.; Douligeris, C. Energy-efficient automated control of irrigation in agriculture using wireless sensor networks. *Comput. Electron. Agric.* **2015**, *113*, 154–163. [CrossRef]
251. Adeyemi, O.; Grove, I.; Peets, S.; Domun, Y.; Norton, T. Dynamic neural network modelling of soil moisture content for predictive irrigation scheduling. *Sensors* **2018**, *18*, 3408. [CrossRef]
252. Corbari, C.; Salerno, R.; Ceppi, A.; Telescac, V.; Mancini, M. Smart irrigation forecast using satellite LANDSAT data and meteohydrological modeling. *Agric. Water Manag.* **2019**, *212*, 283–294. [CrossRef]
253. Jiménez, A.d.l.Á.C.; Cabral de Almeida, C.D.G.; Júnior, J.A.S.; de Morais, E.D.F.; de Almeida, B.G.; de Andrade, F.H.N. Accuracy of capacitive sensors for estimating soil moisture in northeastern Brazil. *Soil Tillage Res.* **2019**, *195*, 104413. [CrossRef]
254. Kohli, G.; Lee, C.M.; Fisher, J.B.; Halverson, G.; Variano, E.; Jin, Y.; Carney, D.; Wilder, B.A.; Kinoshita, A.M. ECOSTRESS and CIMIS: A comparison of potential and reference evapotranspiration in Riverside County, California. *Remote Sens.* **2020**, *12*, 4126. [CrossRef]
255. Wang, E.; Attard, S.; Linton, A.; McGlinchey, M.; Xiang, W.; Philippa, B.; Everingham, Y. Development of a closed-loop irrigation system for sugarcane farms using the Internet of Things. *Comput. Electron. Agric.* **2020**, *172*, 105376. [CrossRef]
256. Jaiswal, S.; Ballal, M.S. Fuzzy inference-based irrigation controller for agricultural demand-side management. *Comput. Electron. Agric.* **2020**, *175*, 105537. [CrossRef]
257. Tiglao, N.M.; Alipio, M.; Balanay, J.V.; Saldivar, E.; Tiston, J.L. Agrinex: A low-cost wireless mesh-based smart irrigation system. *Measurement* **2020**, *161*, 107874. [CrossRef]
258. Lozoya, C.; Favela-Contreras, A.; Aguilar-Gonzalez, A.; Félix-Herrán, L.C.; Orona, L. Energy-efficient wireless communication strategy for precision agriculture irrigation control. *Sensors* **2021**, *21*, 5541. [CrossRef]
259. Mira-García, A.B.; Vera, J.; Conejero, W.; Conesa, M.R.; Ruiz-Sánchez, M.C. Evapotranspiration in young lime trees with automated irrigation. *Sci. Hortic.* **2021**, *288*, 110396. [CrossRef]
260. Alibabaei, K.; Gaspar, P.D.; Assunção, E.; Alirezazadeh, S.; Lima, T.M. Irrigation optimization with a deep reinforcement learning model: A case study in Portugal. *Agric. Water Manag.* **2022**, *263*, 107480. [CrossRef]
261. Baradaran, A.A.; Tavazoei, M.S. Fuzzy system design for automatic irrigation of agricultural fields. *Expert Syst. Appl.* **2022**, *210*, 118602. [CrossRef]
262. Garrido-Rubio, J.; González-Piqueras, J.; Campos, I.; Osann, A.; González-Gómez, L.; Calera, A. Remote sensing-based soil water balance for irrigation water accounting at plot and water user association scales. *Agric. Water Manag.* **2020**, *238*, 106236. [CrossRef]
263. Gong, L.; Yan, J.; Chen, Y.; An, J.; He, L.; Zheng, L.-R.; Zou, Z. An IoT-based intelligent irrigation system with data fusion and a self-powered wide-area network. *J. Ind. Inf. Integr.* **2022**, *29*, 100367. [CrossRef]
264. Tace, Y.; Tabaa, M.; Elfilali, S.; Leghris, C.; Bensag, H.; Renault, E. Smart irrigation system based on IoT and machine learning. *Energy Rep.* **2022**, *8*, 1025–1036. [CrossRef]
265. Cordeiro, M.; Markert, C.; Araújo, S.S.; Campos, N.G.S.; Gondim, R.S.; Coelho da Silva, T.L.; da Rocha, A.R. Towards smart farming: Fog-enabled intelligent irrigation system using deep neural networks. *Future Gener. Comput. Syst.* **2022**, *129*, 115–124. [CrossRef]

266. Khan, A.I.; Alsolami, F.; Alqurashi, F.; Abushark, Y.B.; Sarker, I.H. Novel energy management scheme in IoT-enabled smart irrigation systems using optimized intelligence methods. *Eng. Appl. Artif. Intell.* **2022**, *114*, 104996. [CrossRef]
267. Togneri, R.; dos Santos, D.F.; Camponogara, G.; Nagano, H.; Custódio, G.; Prati, R.; Fernandes, S.; Kamienski, C. Soil moisture forecast for smart irrigation: The primetime for machine learning. *Expert Syst. Appl.* **2022**, *207*, 117653. [CrossRef]
268. Alves, R.G.; Maia, R.F.; Lima, F. Development of a digital twin for smart farming: Irrigation management for water saving. *J. Clean. Prod.* **2023**, *388*, 135920. [CrossRef]
269. Champness, M.; Vial, L.; Ballester, C.; Hornbuckle, J. Evaluating the performance and opportunity cost of a smart-sensed automated irrigation system for water-saving rice cultivation. *Agriculture* **2023**, *13*, 903. [CrossRef]
270. Hoque, M.J.; Islam, M.S.; Khaliluzzaman, M. A fuzzy logic- and IoT-based smart irrigation system. *Eng. Proc.* **2023**, *58*, 93. [CrossRef]
271. McCarthy, A.; Foley, J.; Raedts, P.; Hills, J. Field evaluation of automated site-specific irrigation using soil-water sensors and model predictive control. *Agric. Water Manag.* **2023**, *277*, 108098. [CrossRef]
272. Tzerakis, K.; Psarras, G.; Kourgialas, N.N. Developing an open-source IoT platform for optimal irrigation scheduling and decision-making. *Water* **2023**, *15*, 1739. [CrossRef]
273. Sharifnasab, H.; Mahrokh, A.; Dehghanisanij, H.; Łazuka, E.; Łagód, G.; Karami, H. Evaluating intelligent IoT-based irrigation systems for grain corn. *Water* **2023**, *15*, 1394. [CrossRef]
274. Benameur, R.; Dahane, A.; Kechar, B.; Benyamina, A.E.H. Smart and sustainable low-cost irrigation system for anomaly detection using deep learning. *Sensors* **2024**, *24*, 1162. [CrossRef]
275. Artetxe, E.; Barambones, O.; Martín Toral, I.; Uralde, J.; Calvo, I.; del Rio, A. Smart IoT irrigation system based on fuzzy logic, LoRa, and cloud integration. *Electronics* **2024**, *13*, 1949. [CrossRef]
276. Dey, P.K.; Banu, S.; Milufarzana, M.; Robin, S.; Mazumdar, N.C.; Samsuzzaman, S.; Kabir, M.S.N. IoT-based solar-powered smart irrigation system with solar tracker for rice fields. *Precis. Agric. Sci. Technol.* **2024**, *6*, 59–70. [CrossRef]
277. Kelly, T.D.; Foster, T.; Schultz, D.M. Assessing the value of deep reinforcement learning for irrigation scheduling. *Smart Agric. Technol.* **2024**, *7*, 100403. [CrossRef]
278. Wu, Z.; Cui, N.; Zhang, W.; Gong, D.; Liu, C.; Liu, Q.; Zheng, S.; Wang, Z.; Zhao, L.; Yang, Y. Inversion of large-scale citrus soil moisture using multi-temporal Sentinel-1 and Landsat-8 data. *Agric. Water Manag.* **2024**, *294*, 108718. [CrossRef]
279. Gaitan, N.C.; Batinas, B.I.; Ursu, C.; Crainiciuc, F.N. Integrating artificial intelligence into an automated irrigation system. *Sensors* **2025**, *25*, 1199. [CrossRef]
280. Gupta, S.; Chowdhury, S.; Govindaraj, R.; Amesho, K.T.T.; Shangdiar, S.; Kadhila, T.; Iikela, S. Smart agriculture using IoT for automated irrigation, water and energy efficiency. *Smart Agric. Technol.* **2025**, *12*, 101081. [CrossRef]
281. Lee, Y.; Ha, S.; Wang, X.; Hahm, S.; Lee, K.; Park, J. Automatic irrigation based on hourly cumulative evapotranspiration. *Agriculture* **2025**, *15*, 308. [CrossRef]
282. Liu, X.; Zhao, Z.; Rezaeipanah, A. Intelligent and automatic irrigation system based on IoT using fuzzy control technology. *Sci. Rep.* **2025**, *15*, 14577. [CrossRef] [PubMed]
283. Morchid, A.; Et-Taibi, B.; Oughannou, Z.; El Alami, R.; Qjidaa, H.; Jamil, M.O.; Boufounas, E.M.; Abid, M.R. IoT-enabled smart agriculture for improving water management. *Sci. Afr.* **2025**, *27*, e02527. [CrossRef]
284. Morchid, A.; Said, Z.; Abdelaziz, A.Y.; Siano, P.; Qjidaa, H. Fuzzy logic-based IoT system for optimizing irrigation with cloud computing. *Smart Agric. Technol.* **2025**, *11*, 100979. [CrossRef]
285. Sarker, K.K.; Kabir, M.S.; Biswas, S.K.; Niloy, K.M.; Mofazzol, M.I.H.; Hossain, A.; Mahboob, M.G. Sensor-driven automated shed and irrigation for summer tomato production in Bangladesh. *Results Eng.* **2025**, *26*, 104993. [CrossRef]
286. Pathmudi, V.R.; Khatri, N.; Kumar, S.; Abdul-Qawy, A.S.H.; Vyas, A.K. A systematic review of IoT technologies and their constituents for smart and sustainable agriculture applications. *Sci. Afr.* **2023**, *19*, e01577. [CrossRef]
287. Abderrahmane, T.; Nourredine, A.; Mohammed, T. Experimental analysis for comparison of wireless transmission technologies: Wi-Fi, Bluetooth, ZigBee and LoRa for mobile multi-robot in hostile sites. *Int. J. Electr. Comput. Eng.* **2024**, *14*, 2753–2761. [CrossRef]
288. Shafi, U.; Mumtaz, R.; García-Nieto, J.; Hassan, S.A.; Zaidi, S.A.R.; Iqbal, N. Precision agriculture techniques and practices: From considerations to applications. *Sensors* **2019**, *19*, 3796. [CrossRef]
289. Borrero, J.D.; Zabalo, A. An autonomous wireless device for real-time monitoring of water needs. *Sensors* **2020**, *20*, 2078. [CrossRef]
290. Zhang, X.; Andreyev, A.; Zumpf, C.; Negri, M.C.; Guha, S.; Ghosh, M. Thoreau: A subterranean wireless sensing network for agriculture and the environment. In Proceedings of the 2017 IEEE Conference on Computer Communications Workshops (INFOCOM WKSHPS), Atlanta, GA, USA, 1–4 May 2017; pp. 78–84. [CrossRef]
291. Sohail, M.; Sun, D.; Zhu, Z. Recent developments in intelligent packaging for enhancing food quality and safety. *Crit. Rev. Food Sci. Nutr.* **2018**, *58*, 2650–2662. [CrossRef]
292. Mekala, M.S.; Viswanathan, P. A survey: Smart agriculture IoT with cloud computing. In Proceedings of the International Conference on Microelectronic Devices, Circuits and Systems (ICMDCS), Vellore, India, 10–12 August 2017; pp. 1–7. [CrossRef]

293. Qazi, S.; Khawaja, B.A.; Farooq, Q.U. IoT-equipped and AI-enabled next generation smart agriculture: A critical review, current challenges and future trends. *IEEE Access* **2022**, *10*, 21219–21244. [CrossRef]
294. Ruiz-Garcia, L.; Lunadei, L. The role of RFID in agriculture: Applications, limitations and challenges. *Comput. Electron. Agric.* **2011**, *79*, 42–50. [CrossRef]
295. Farooq, M.; Hussain, A.; Hashim, S.; Yang, L.; Ali, M. Automated irrigation system based on irrigation gates using fuzzy logic. In Proceedings of the International Conference on Internet of Things and Intelligent Applications (ITIA), Zadar, Croatia, 27–29 November 2020; pp. 1–5. [CrossRef]
296. Pacco, H.C. Simulation of temperature control and irrigation time in the production of tulips using fuzzy logic. *Procedia Comput. Sci.* **2022**, *200*, 1–12. [CrossRef]
297. Singh, A.K.; Tariq, T.; Ahmer, M.F.; Sharma, G.; Bokoro, P.N.; Shongwe, T. Intelligent control of irrigation systems using fuzzy logic controller. *Energies* **2022**, *15*, 7199. [CrossRef]
298. Patel, P.; Patel, Y.; Patel, U.; Patel, V.; Patel, N.; Oza, P. Towards automating irrigation: A fuzzy logic-based water irrigation system using IoT and deep learning. *Model. Earth Syst. Environ.* **2022**, *8*, 5235–5250. [CrossRef]
299. Seyedzadeh, A.; Maroufpoor, S.; Maroufpoor, E.; Shiri, J.; Bozorg-Haddad, O.; Gavazi, F. Artificial intelligence approach to estimate discharge of drip tape irrigation based on temperature and pressure. *Agric. Water Manag.* **2020**, *228*, 105905. [CrossRef]
300. Klyushin, D.; Tymoshenko, A. Optimization of drip irrigation systems using artificial intelligence methods for sustainable agriculture and environment. In *Artificial Intelligence for Sustainable Development*; Hassanien, A.E., Bhatnagar, R., Darwish, A., Eds.; Springer: Cham, Switzerland, 2021; pp. 3–17. [CrossRef]
301. Kamyshova, G.; Osipov, A.; Gataullin, S.; Korchagin, S.; Ignar, S.; Gataullin, T.; Terekhova, N.; Suvorov, S. Artificial neural networks and computer vision-based phytoindication systems for variable rate irrigation improving. *IEEE Access* **2022**, *10*, 8577–8589. [CrossRef]
302. Esmail, A.A.; Ibrahim, M.A.; Abdallah, S.M.; Radwan, A.E.; Elsonbaty, H.K.; Elsayed, M.A.; Elnakeib, N.A.; Dawoud, M.S.; El-Ghamry, A.; Fouad, K.M.; et al. Smart irrigation system using IoT and machine learning methods. In *Proceedings of the 5th Novel Intelligent and Leading Emerging Sciences Conference (NILES)*; IEEE: Baghdad, Iraq, 2023; pp. 362–367. [CrossRef]
303. Katimbo, A.; Rudnick, D.R.; Zhang, J.; Ge, Y.; DeJonge, K.C.; Franz, T.E.; Shi, Y.; Liang, W.Z.; Qiao, X.; Heeren, D.M.; et al. Evaluation of artificial intelligence algorithms with sensor data assimilation in estimating crop evapotranspiration and crop water stress index for irrigation water management. *Smart Agric. Technol.* **2023**, *4*, 100176. [CrossRef]
304. Benhmad, T.; Rhaimi, C.B.; Alomari, S.; Aljuhani, L. Design and implementation of an integrated IoT and artificial intelligence system for smart irrigation management. *Int. J. Adv. Soft Comput. Appl.* **2024**, *16*, 197–218. [CrossRef]
305. Kaur, A.; Bhatt, D.P.; Raja, L. Developing a hybrid irrigation system for smart agriculture using IoT sensors and machine learning in Sri Ganganagar, Rajasthan. *J. Sens.* **2024**, 6676907. [CrossRef]
306. Oudah, M.; Al-Naji, A.; AL-Janabi, T.Y.; Namaa, D.S.; Chahl, J. Automatic irrigation system based on computer vision and an artificial intelligence technique using Raspberry Pi. *Automation* **2024**, *5*, 90–105. [CrossRef]
307. Tyagi, S.; Anand, R.; Sabharwal, A.; Reddy, S. Plant recommendation system using smart irrigation integrated with IoT and machine/deep learning. *Commun. Soil Sci. Plant Anal.* **2024**, *55*, 2488–2508. [CrossRef]
308. Singh, N.; Ajaykumar, K.; Dhruw, L.K.; Choudhury, B.U. Optimization of irrigation timing for sprinkler irrigation system using convolutional neural network-based mobile application for sustainable agriculture. *Smart Agric. Technol.* **2023**, *5*, 100305. [CrossRef]
309. Oğuztürk, G.E.; Murat, C.; Yurtseven, M.; Oğuztürk, T. The effects of AI-supported autonomous irrigation systems on water efficiency and plant quality: A case study of Geranium psilostemon Ledeb. *Plants* **2025**, *14*, 770. [CrossRef] [PubMed]
310. Kawai, T.; Mineno, H. Evaluation environment using edge computing for artificial intelligence-based irrigation system. In *Proceedings of the International Conference on Mobility, Sensing and Networking (MSN)*; IEEE: Tokyo, Japan, 2020; pp. 214–219. [CrossRef]
311. Belaud, G.; Mateos, L.; Aliod, R.; Buisson, M.-C.; Faci, E.; Gendre, S.; Ghinassi, G.; Gonzales Perea, R.; Lejars, C.; Maruejols, F.; et al. Irrigation and energy: Issues and challenges. *Irrig. Drain.* **2020**, *69*, 177–185. [CrossRef]
312. International Energy Agency (IEA). *World Energy Outlook*; IEA: Paris, France, 2007.
313. Soto-García, M.; Martin-Gorriz, B.; García-Bastida, P.A.; Alcon, F.; Martínez-Alvarez, V. Energy consumption for crop irrigation in a semiarid climate (south-eastern Spain). *Energy* **2013**, *55*, 1084–1093. [CrossRef]
314. Mo, W.; Zhang, Q.; Mihelcic, J.R.; Hokanson, D.R. Embodied energy comparison of surface water and groundwater supply options. *Water Res.* **2011**, *45*, 5577–5586. [CrossRef]
315. Linn, S.; Ya, Z. Solar/wind/diesel hybrid energy system with battery storage for rural electrification. *Int. J. Sci. Eng. Technol. Res.* **2014**, *3*, 2172–2176.
316. Hartung, H.; Pluschke, L. *The Benefits and Risks of Solar Powered Irrigation—A Global Overview*; FAO: Rome, Italy, 2018.
317. Wazed, S.M.; Hughes, B.R.; O'Connor, D.; Calautit, J.K. Solar driven irrigation systems for remote rural farms. *Energy Procedia* **2017**, *142*, 184–191. [CrossRef]

318. Al-Smairan, M. Application of photovoltaic array for pumping water as an alternative to diesel engines in Jordan Badia, Tall Hassan station: Case study. *Renew. Sustain. Energy Rev.* **2012**, *16*, 4500–4507. [CrossRef]
319. Haffaf, A.; Lakdja, F.; Meziane, R.; Abdeslam, D.O. Study of economic and sustainable energy supply for water irrigation system (WIS). *Sustain. Energy Grids Netw.* **2021**, *25*, 100412. [CrossRef]
320. Scherer, T.T. *Irrigation Water Pumps*; North Dakota State University Extension: Fargo, ND, USA, 2017.
321. Raza, F.; Tamoor, M.; Miran, S.; Arif, W.; Kiren, T.; Amjad, W.; Hussain, M.I.; Lee, G.-H. The socio-economic impact of using photovoltaic (PV) energy for high-efficiency irrigation systems: A case study. *Energies* **2022**, *15*, 1198. [CrossRef]
322. Nikzad, A.; Chahartaghi, M.; Ahmadi, M.H. Technical, economic, and environmental modeling of solar water pump for irrigation of rice in Mazandaran province in Iran: A case study. *J. Clean. Prod.* **2019**, *239*, 118007. [CrossRef]
323. Parvaresh Rizi, A.; Ashrafzadeh, A.; Ramezani, A. A financial comparative study of solar and regular irrigation pumps: Case studies in eastern and southern Iran. *Renew. Energy* **2019**, *138*, 1096–1103. [CrossRef]
324. Mérida García, A.; Gallagher, J.; McNabola, A.; Camacho Poyato, E.; Montesinos Barrios, P.; Rodríguez Díaz, J.A. Comparing the environmental and economic impacts of on- or off-grid solar photovoltaics with traditional energy sources for rural irrigation systems. *Renew. Energy* **2019**, *140*, 895–904. [CrossRef]
325. Khan, Z.A.; Imran, M.; Altamimi, A.; Diemuodeke, O.E.; Abdelatif, A.O. Assessment of wind and solar hybrid energy for agricultural applications in Sudan. *Energies* **2022**, *15*, 5. [CrossRef]
326. Bouzidi, B. Viability of solar or wind for water pumping systems in the Algerian Sahara regions—Case study Adrar. *Renew. Sustain. Energy Rev.* **2011**, *15*, 4436–4442. [CrossRef]
327. Ioannidis, R.; Koutsoyiannis, D. A review of land use, visibility and public perception of renewable energy in the context of landscape impact. *Appl. Energy* **2020**, *276*, 115367. [CrossRef]
328. Canbulat, S.; Balci, K.; Canbulat, O.; Bayram, I.S. Techno-economic analysis of on-site energy storage units to mitigate wind energy curtailment: A case study in Scotland. *Energies* **2021**, *14*, 1691. [CrossRef]
329. Olabi, A.G.; Wilberforce, T.; Elsaid, K.; Salameh, T.; Sayed, E.T.; Husain, K.S.; Abdelkareem, M.A. Selection guidelines for wind energy technologies. *Energies* **2021**, *14*, 3244. [CrossRef]
330. Bertsiou, M.M.; Baltas, E. Power to hydrogen and power to water using wind energy. *Wind* **2022**, *2*, 263–278. [CrossRef]
331. Ghasemi, A. Coordination of pumped-storage unit and irrigation system with intermittent wind generation for intelligent energy management of an agricultural microgrid. *Energy* **2018**, *142*, 1–13. [CrossRef]
332. Campana, P.E.; Li, H.; Yan, J. Techno-economic feasibility of the irrigation system for the grassland and farmland conservation in China: Photovoltaic vs. wind power water pumping. *Energy Convers. Manag.* **2015**, *103*, 311–320. [CrossRef]
333. Dibal, P.Y.; Mustapha, H.B.; Usman, A.S. Processor power and energy consumption estimation techniques in IoT applications: A review. *Internet Things* **2023**, *21*, 100655. [CrossRef]
334. Haj-Amor, Z.; Araya, T.; Kim, D.-G.; Bouri, S.; Lee, J.; Ghiloufi, W.; Yang, Y.; Kang, H.; Jhariya, M.K.; Banerjee, A.; et al. Soil salinity and its associated effects on soil microorganisms, greenhouse gas emissions, crop yield, biodiversity and desertification: A review. *Sci. Total Environ.* **2022**, *843*, 156946. [CrossRef]
335. Libohova, Z.; Seybold, C.A.; Wysocki, D.; Wills, S.; Schoeneberger, P.; Williams, C.; Lindbo, D.; Stott, D.; Owens, P.R. Reevaluating the effects of soil organic matter and other properties on available water-holding capacity using the National Cooperative Soil Survey Characterization Database. *J. Soil Water Conserv.* **2018**, *73*, 411–421. [CrossRef]

Disclaimer/Publisher's Note: The statements, opinions and data contained in all publications are solely those of the individual author(s) and contributor(s) and not of MDPI and/or the editor(s). MDPI and/or the editor(s) disclaim responsibility for any injury to people or property resulting from any ideas, methods, instructions or products referred to in the content.